

CRYOGENIC FLUID MANAGEMENT TECHNOLOGIES FOR SPACE TRANSPORTATION

ZERO G THERMODYNAMIC VENT SYSTEM FINAL REPORT

REPORT NO. SSD 94M0038

CONTRACT NAS8-39202

(NASA-CR-193981) CRYOGENIC FLUID
MANAGEMENT TECHNOLOGIES FOR SPACE
TRANSPORTATION. ZERO G
THERMODYNAMIC VENT SYSTEM Final
Report (Rockwell International
Corp.) 64 p

N94-36806

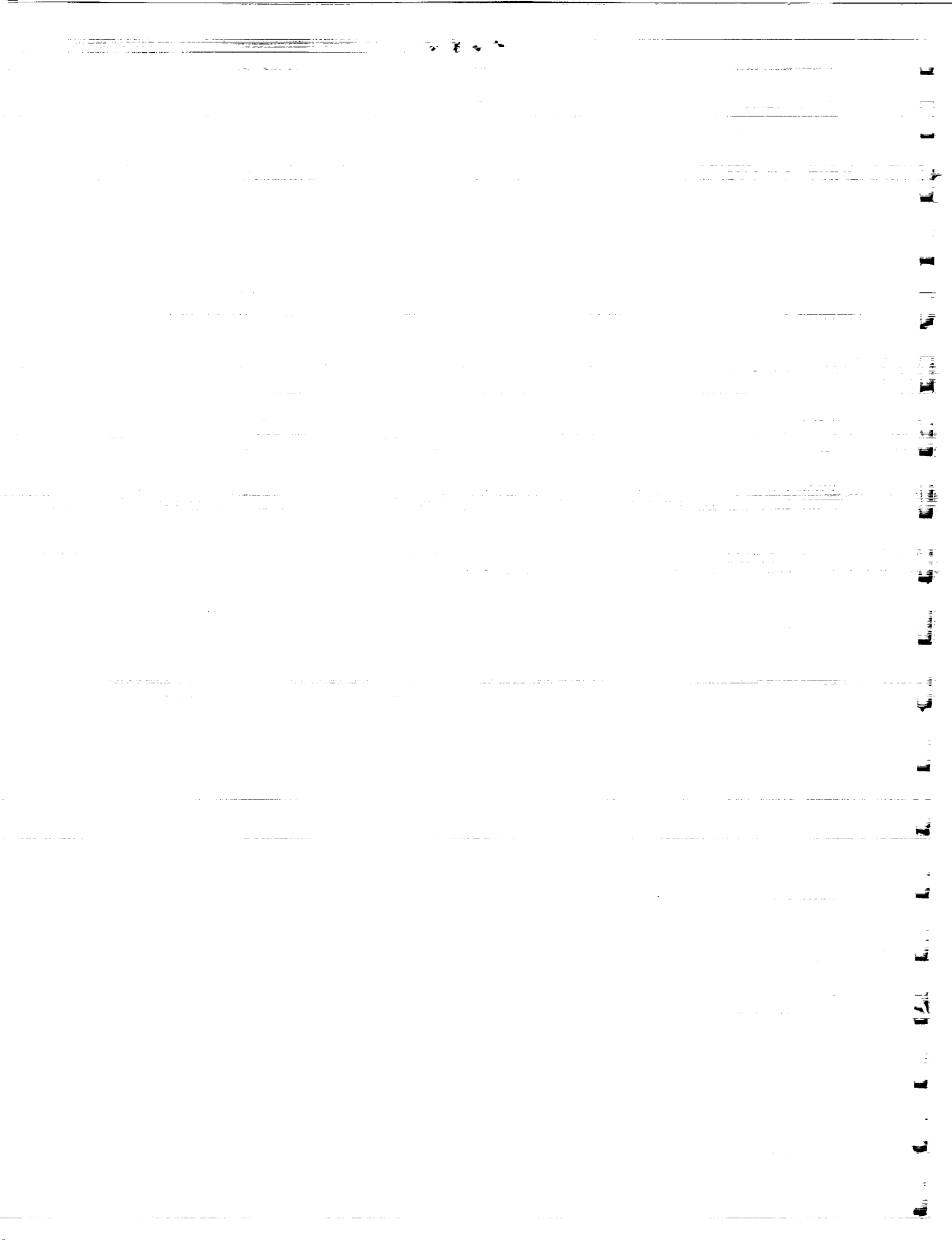
Unclassified

G3/29 0016040

Tibor Lak
MR. TIBOR LAK
TECHNICAL MANAGER

Charles Wood
MR. CHARLES WOOD
PROGRAM MANAGER





CRYOGENIC FLUID MANAGEMENT TECHNOLOGIES FOR SPACE TRANSPORTATION

ZERO G THERMODYNAMIC VENT SYSTEM FINAL REPORT

REPORT NO. SSD 94M0038

CONTRACT NAS8-39202

ZERO G THERMODYNAMIC VENT SYSTEM FINAL REPORT OUTLINE

REPORT NO. SSD94M0038

(DR-4 Contract NAS8-39202)

1.0 INTRODUCTION

2.0 ROCKWELL TVS CONCEPT DEFINITION

3.0 SUBSYSTEM DESIGN DEFINITION

3.1 HEAT EXCHANGER

- 3.1.1 COIL HEAT EXCHANGER (OPTION 1)**
- 3.1.2 SINGLE TUBE HEAT EXCHANGER (OPTION 2)**
- 3.1.3 MULTI-TUBE HEAT EXCHANGER (OPTION 3)**
- 3.1.4 HEAT EXCHANGER TRADE ANALYSIS RESULTS**
- 3.1.5 HEAT EXCHANGER OPERATING PRESSURE DEFINITION**

3.2 SPRAY & RECIRCULATION SYSTEM

3.3 CONTROLLER LOGIC

- 3.3.1 SINGLE PRESSURE CONTROL OF PUMP & VENT VALVE (OPTION 1)**
- 3.3.2 SEPARATE PRESSURE CONTROL FOR PUMP & VENT VALVE (OPTION 2)**
- 3.3.3 USE OF PRESSURE & TEMPERATURE MEASUREMENT TO CONTROL PUMP & VENT VALVE (OPTION 3)**

3.4 TVS INSTRUMENTATION REQUIREMENTS

4.0 HARDWARE SELECTION

4.1 LIQUID HYDROGEN PUMP SELECTION

4.2 VENT VALVE SELECTION

5.0 DETAILED DESIGN LAYOUT OF THE TVS

- 5.1 SPRAY INJECTION/HEAT EXCHANGER ASSEMBLY**
- 5.2 RECIRCULATION & VENT SYSTEM ASSEMBLY**
- 5.3 COMPONENT BOX ASSEMBLY**
- 5.4 SUPPORT RING ASSEMBLY**
- 5.5 TVS STRESS ANALYSIS RESULTS**

ZERO G THERMODYNAMIC VENT SYSTEM FINAL REPORT OUTLINE (Continued)

6.0 SUBSYSTEM TESTING

6.1 LH2 RECIRCULATION PUMP TESTS

6.2 TVS COMPONENT TESTING

7.0 TVS PERFORMANCE CHARACTERISTICS

7.1 HEAT EXCHANGER PERFORMANCE

7.2 TVS VENT VALVE AND RECIRCULATION PUMP OPERATION

8.0 TVS DESIGN GUIDELINES FOR FUTURE VEHICLES

9.0 CONCLUSIONS

10.0 ACKNOWLEDGMENTS

LIST OF FIGURES

Figure 1	Comparison of ground based vs. space based venting systems	Page 7
Figure 2	Schematic of Rockwell TVS concept	Page 7
Figure 3	Program schedule for the zero g TVS contract	Page 8
Figure 4	Comparison of Rockwell TVS concept with typical TVS concepts	Page 8
Figure 5	LH ₂ hold time without venting as a function of heat rate	Page 10
Figure 6	Zero g operation of TVS with or without liquid settling	Page 10
Figure 7	Coil heat exchanger configuration (Option 1)	Page 13
Figure 8	Coil heat exchanger vent line pressure loss sensitivity analysis results	Page 13
Figure 9	Single tube heat exchanger configuration (Option 2)	Page 15
Figure 10	Single tube heat exchanger design sensitivity analysis	Page 15
Figure 11	Heat input to tank due to pumping power (Single Tube)	Page 16
Figure 12	Multi-tube heat exchanger configuration	Page 16
Figure 13	Heat input to LH ₂ tank due to pumping power/frictional loss	Page 18
Figure 14	Multi-tube heat exchanger performance sensitivity to number of tubes	Page 18
Figure 15	Summary of heat exchanger configuration trade study	Page 19
Figure 16	Liquid mass fraction at vent line inlet as a function of liquid vapor pressure and vent line back pressure	Page 20
Figure 17	Heat absorbed through evaporation as a function of liquid vapor pressure and vent line back pressure	Page 20
Figure 18	Heat absorbed by vent flow through sensible heating as a function of liquid vapor pressure and back pressure	Page 21
Figure 19	Total heat absorption potential of vented hydrogen as a function of liquid vapor pressure and back pressure	Page 21
Figure 20	Ullage pressure decay sensitivity to liquid drop diameter	Page 22
Figure 21	Liquid spray injection flowrate as a function of distance from top of spray bar (0.3 lb/sec)	Page 24
Figure 22	Liquid spray injection velocity as a function of distance from top of spray bar (0.3 lb/sec)	Page 24
Figure 23	LeRC ullage pressure collapse test setup	Page 25
Figure 24	LeRC test data for tank ullage pressure	Page 25
Figure 25	LeRC test data for ullage temperature	Page 26
Figure 26	LeRC test data for tank wall temperature	Page 26
Figure 27	LeRC test data for pump flowrate	Page 27
Figure 28	Comparison of predicted ullage pressure and LeRC test result	Page 27
Figure 29	Comparison of predicted and LeRC measured ullage pressure decay rate	Page 28
Figure 30	Comparison of predicted ullage temperature with LeRC test result	Page 28
Figure 31	Zero g thermodynamic vent system option 1 controller logic	Page 30
Figure 32	Option 1 control concept	Page 30
Figure 33	Zero g thermodynamic vent system option 2 controller logic	Page 31
Figure 34	Option 2 control concept	Page 31
Figure 35	Zero g thermodynamic vent system option 3 controller logic	Page 33
Figure 36	Option 3 control concept	Page 33
Figure 37	Summary of controller concept trade study	Page 34
Figure 38	Zero g TVS instrumentation schematic	Page 36
Figure 39	LH ₂ recirculation pump design (Barber-Nichols)	Page 37
Figure 40	LH ₂ recirculation pump predicted and measured performance	Page 38
Figure 41	Hydrogen two-phase flow as a function of valve orifice diameter (20 psia saturated fluid)	Page 40
Figure 42	Hydrogen vent valve design	Page 40

LIST OF FIGURES (Continued)

Figure 43	Vent flowrate as a function of liquid subcooling (20 psi vapor pressure)	Page 41
Figure 44	TVS heat exchanger and spray injection system assembly	Page 41
Figure 45	Solution to compensate for MMC tank line misalignment	Page 42
Figure 46	Vent tube design design to compensate for potential tank interface misalignment	Page 42
Figure 47	Recirculation pump and vent system assembly	Page 43
Figure 48	Component box design	Page 45
Figure 49	Support Ring Assembly	Page 45
Figure 50	Pressure drop through spray injection tubes (Water flow test results)	Page 47
Figure 51	Loss coefficients of spray injection tubes (Water flow test results)	Page 47
Figure 52	Schematic of Rockwell spray injection water flow test	Page 48
Figure 53	Pressure drop in the spray tubes and heat exchanger assembly (Water flow tests)	Page 48
Figure 54	Comparison of predicted and measured spray injection system pressure loss (Water flow test)	Page 49
Figure 55	Schematic of Rockwell spray injection liquid nitrogen flow test	Page 50
Figure 56	Vent tube loss coefficient (Test vs predicted)	Page 50
Figure 57	Flowmeter water flow calibration tests results	Page 52
Figure 58	Schematic of component box test set-up	Page 52
Figure 59	Predicted TVS heat exchanger performance	Page 54
Figure 60	TVS vent flowrate as a function of liquid subcooling	Page 54
Figure 61	Heat absorption potential of vent flow as a function of liquid subcooling	Page 55
Figure 62	Heat exchanger operating pressure (cold side) as a function of liquid subcooling	Page 55
Figure 63	TVS performance simulation at 90 percent liquid quantity (Full scale)	Page 56
Figure 64	TVS performance simulation at 90 percent liquid quantity (Expanded scale)	Page 56
Figure 65	TVS recirculation pump and vent flowrate transient during pressure control at 90 percent liquid quantity	Page 57
Figure 66	TVS performance simulation at 25 percent liquid quantity (Full scale)	Page 57
Figure 67	TVS performance simulation at 25 percent liquid quantity (Expanded scale)	Page 58
Figure 68	TVS recirculation pump and vent flowrate transient during pressure control at 25 percent liquid quantity	Page 58
Figure 69	Time between destratification and venting operation as a function of liquid quantity	Page 60
Figure 70	TVS destratification time (recirc. pump and venting operation) as a function of liquid quantity	Page 60
Figure 71	TVS operation frequency (percent) as a function of liquid quantity	Page 61
Figure 72	TVS design installed in NASA MHTB tank	Page 63

LIST OF TABLES

Table 1	Zero g TVS instrumentation list (Installed on TVS hardware)	Page 36
Table 2	Candidate vent valves for zero g TVS design	Page 38

ZERO G THERMODYNAMIC VENT SYSTEM FINAL REPORT

1.0 Introduction

Long term storage of subcritical cryogens in space must address the problem of thermal stratification in the storage tanks, liquid acquisition devices, and associated feed systems. Due to the absence of gravity induced body forces, thermal stratification in zero g is more severe than commonly experienced in a 1-g environment. If left uncontrolled, the thermal gradients result in excessive tank pressure rise and the formation of undesirable liquid/vapor mixtures within the liquid bulk, liquid acquisition system, and propellant transfer lines. Since external heat leakage cannot be eliminated, a means of minimizing the thermal stratification in the ullage gas, liquid and feed system is required. A subsystem which minimizes the thermal stratification and rejects the environmental heat leakage in an efficient manner is therefore needed for zero-g subcritical cryogenic systems.

In ground based storage systems the ullage gas location is always known (top of the tank) and therefore direct venting of gases as a means of heat rejection is easily accomplished. In contrast, because the ullage location in a zero g environment is not easily predictable, heat rejection through direct gaseous venting is difficult in space (requires liquid settling, or surface tension devices). A means of indirect venting through the use of a thermodynamic vent system (TVS) is therefore required. (See Figure 1). A thermodynamic vent system allows indirect venting of vapor through heat exchange between the vented fluid and the stored fluid. The objective is to ensure that only gas and not liquid is vented, in order to minimize the propellant losses. Consequently, the design of a TVS is a critical enabling technology for future applications such as solar thermal and electric propulsion, single-stage-to orbit vertical landers and upper stages, and any space based operations involving subcritical cryogenics.

To bridge this technology gap NASA MSFC initiated an effort to build, and verify through ground tests a zero g liquid hydrogen TVS. The primary objective of the zero g TVS contract (Contract NAS8-39202) was to design a zero g vent system that is innovative, simple, efficient, lightweight, and can be characterized through 1 g tests. The TVS concept defined by Rockwell International, shown in Figure 2, was selected by NASA for further design evaluation. The 30 month activity which was initiated in November 1991 and concluded on May 1994, is shown in Figure 3 along with the major milestones.

2.0 Rockwell TVS Concept Description

Typically, TVS concepts (Figure 4) only address issues associated with the storage tank stratification and then only the liquid phase is treated. Ullage or feed line destratification issues are not included. Also, the performance of these TVS concepts rely on a good understanding of the complex zero-g fluid mixing and heat transfer phenomenon, and therefore require flight test verifications. A unique TVS concept was identified at Rockwell International (Figure 2) which addresses all aspects of thermal destratification, including liquid bulk, ullage gas, and feed systems. This concept also does not depend on zero-g fluid mixing and heat transfer phenomenon, or requires ullage gas/liquid control, but operates in a self-induced, forced convection environment. Consequently, the system performance characteristics at 1-g can be easily defined and extended to zero-g operation with high confidence, minimizing the need for expensive flight tests.

The zero g TVS concept defined by Rockwell International differs from previously studied TVS concepts in that the tank mixer is replaced with a recirculation pump, and the compact heat exchanger is replaced with a simple heat exchanger that is mounted on a spray injection system.

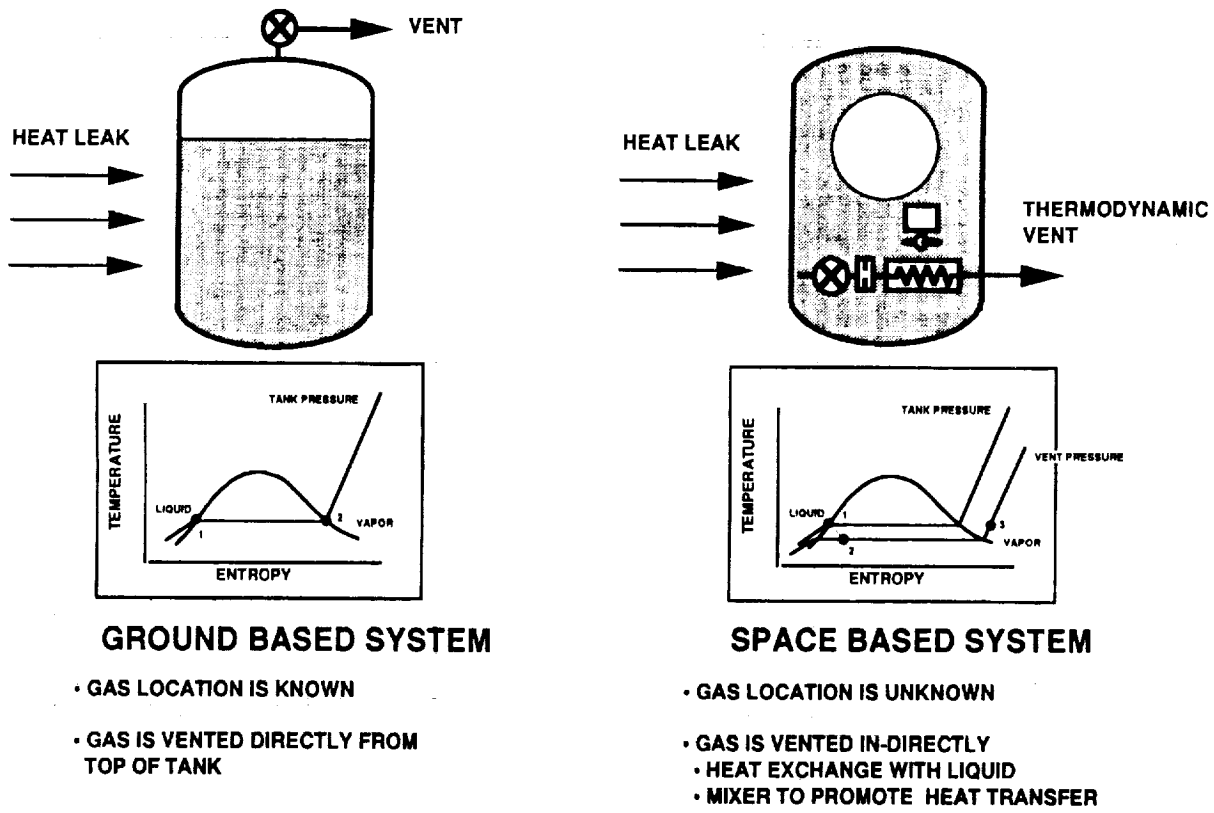


Figure 1 Comparison of ground based vs. space based venting systems

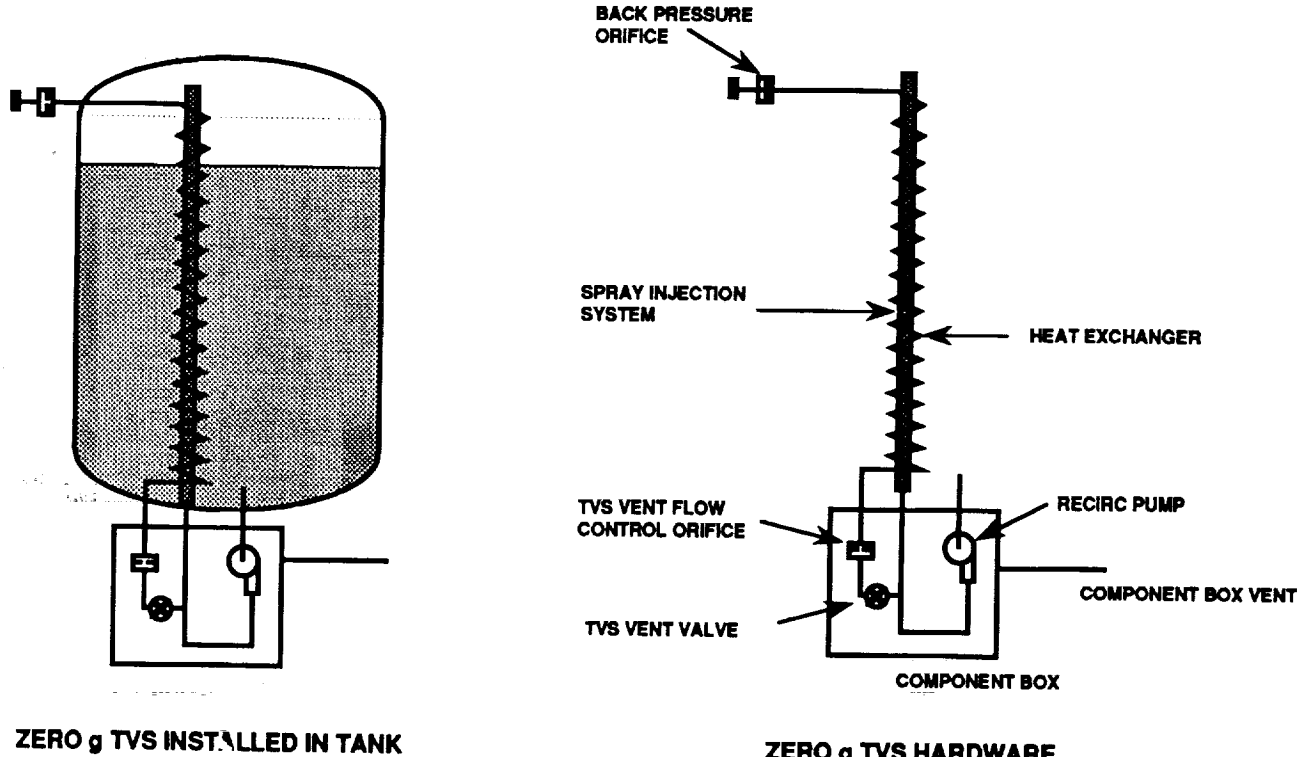


Figure 2 Schematic of Rockwell TVS concept

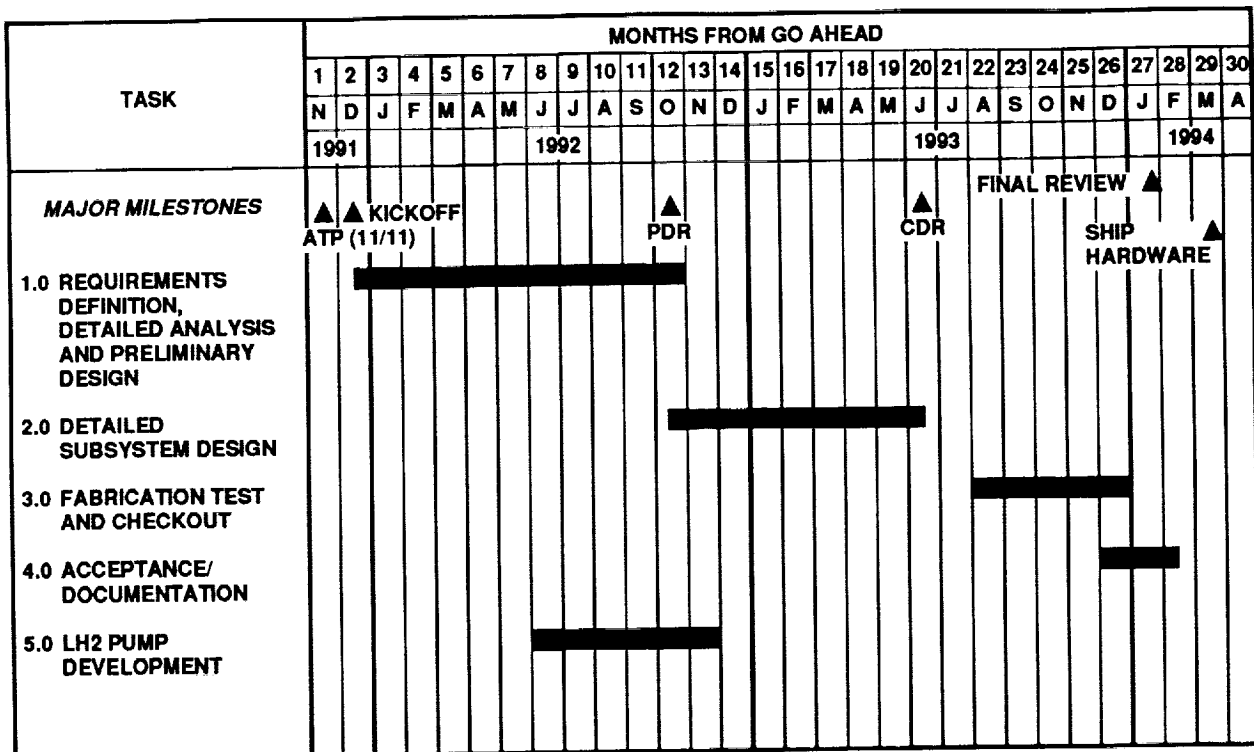


Figure 3 Program schedule for the zero g TVS contract

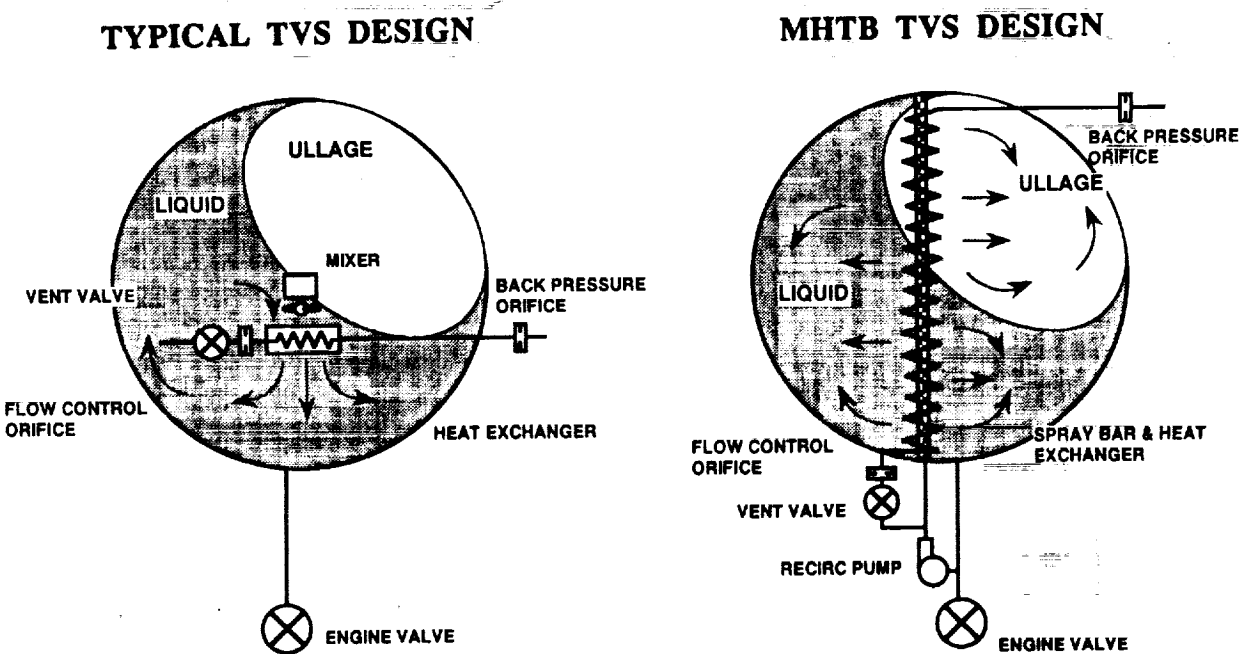


Figure 4 Comparison of Rockwell TVS concept with typical TVS concepts

The function of the recirculation pump and spray injection system is to recirculate the liquid throughout the length of the tank, and thereby destratifying both the ullage gas and liquid bulk regardless of liquid orientation or quantity remaining. For a thermally stratified ullage gas systems in zero g, tank pressure collapse resulting from ullage chill-down and destratification is sometimes sufficient to control the tank pressure level. Consequently, gaseous venting can be avoided or greatly minimized until the maximum allowable liquid temperature level has been reached. Depending on the tank insulation performance, recirculation flow with spray injection may be sufficient to control the tank pressure level for missions lasting several days (Lunar transfer) to weeks. (See Figure 5).

For extended duration missions, heat rejection is accomplished by the opening of the TVS vent valve which allows a small flowrate (~ 2 percent of recirculation flow) to expand to a low pressure thereby producing a low temperature heat sink which is used to absorb heat from the recirculating liquid flow. This heat exchange occurs through forced convection between the vented fluid and the recirculation liquid flow via the spray bar mounted heat exchanger. The heat exchanger is designed such that the vent flow is superheated near the liquid bulk temperature thereby resulting in the maximum heat rejection potential of the vented gas. Since the heat transfer between the vent and recirculation flow is through forced convection (liquid flow to two-phase flow) the heat transfer performance can be characterized through 1-g ground tests. This is in contrast to the previously studied TVS configurations, shown in Figure 4, where the heat transfer can be between liquid/liquid, liquid/gas, gas/liquid, or gas/gas flowrates. Consequently, the heat exchanger and mixer has to be over designed to compensate for the wide range of fluid flowing conditions, or accept the performance losses associated with potential liquid venting. In addition to the simplified forced convection heat transfer mechanism of the Rockwell heat exchanger design, the heat transfer mechanism between the liquid spray droplets and ullage gas is also through self induced forced convection. Consequently, spray droplet mixing and ullage heat transfer characterizations at 1-g ground tests are valid and can be applied for zero-g performance definition. In fact the absence of body forces in zero-g should result in performance improvement compared to 1-g operation.

The Rockwell TVS design also does not require the presence of a liquid acquisition device (LAD) to insure that efficient venting will be accomplished in zero-g. In the event that liquid is not available at the pump inlet, due to adverse liquid orientation (Figure 6) or vapor build-up resulting from local heat leakage, the control logic is designed to open the vent valve when pressure control is required and vapor conditions are detected at the recirculation pump inlet. Ullage pressure control through gaseous venting will therefore be similar to normal 1-g venting operation whenever gas is present at the vent valve inlet.

In addition to satisfying the zero g TVS design objectives, the Rockwell TVS offers additional benefits to the integrated subcritical cryogenic storage and launch system:

- 1) The TVS can also be integrated with the engine bleed/ and recirculation system. Therefore heat rejection from the feed lines, pumps, and engine valves can be accomplished during tank pressure control, ensuring that subcooled liquid is present to support engine start and mainstage operation.
- 2) Because the entire tank fluid is mixed during recirculation operation, thermal conditioning of the liquid within the liquid acquisition device (LAD) capillary screens is accomplished through liquid exchange, minimizing or eliminating the need for additional LAD thermal conditioning subsystems.
- 3) The TVS spray injection system can also be used for zero-g tank chill and no vent fill to assist cryogenic transfer operations.

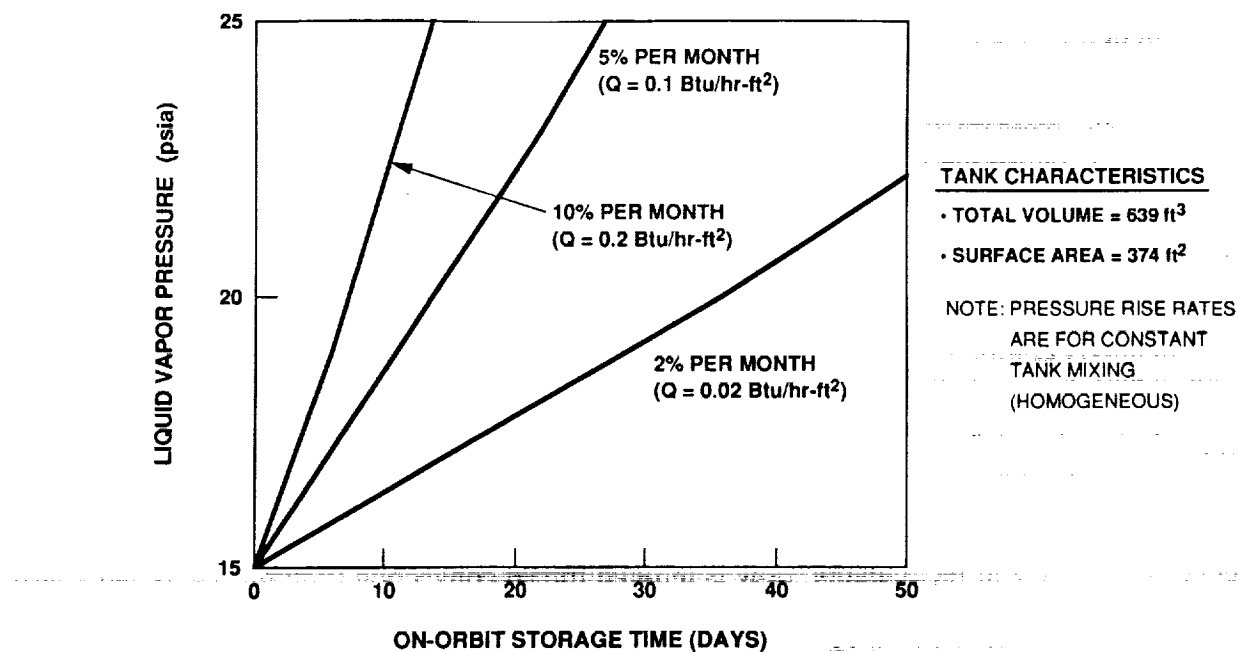
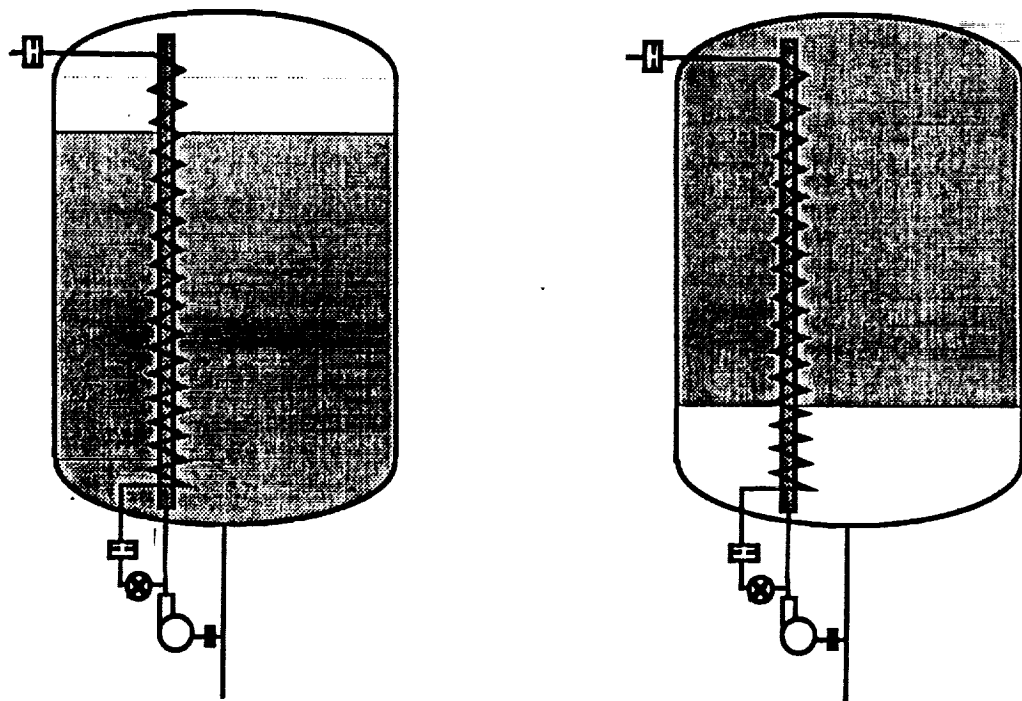


Figure 5 LH₂ hold time without venting as a function of heat rate



VENTING WITH LIQUID AT PUMP INLET

VENTING WITH VAPOR AT PUMP INLET

Figure 6 Zero g operation of TVS with or without liquid settling

- 4) Recirculation pump (with additional valving and lines) can be used for zero g fluid transfer (fill/drain).
- 5) The recirculation pumps may also be integrated for multiple tank vehicle design to reduce system weight and increase system reliability and fault tolerance.
- 6) Can be easily modified to include a zero g emergency venting by adding additional redundant vent valves.
- 7) The in-tank components are minimized with the Rockwell TVS design. Because the recirculation pump is external to the tank, no electrical power penetration of the tank is required for pump or valve operation. This is especially desirable for LO₂ tanks since the presence of an electrical ignition source in oxygen represents a critical failure mode. Also, since the critical components (pump, motor, valve, orifice) are external to the tank, system checkout and ground servicing/replacement is easier. For zero-g operation, component replacement external to the tank may be a significant benefit.

3.0 Subsystem Design Definition

The zero g TVS is designed to operate in the MSFC Multipurpose Hydrogen Test Bed (MHTB) liquid hydrogen tank. The MHTB tank is approximately 10 ft in diameter, and 10 ft high, and is constructed out of 5083 Aluminum. The total capacity of the tank is ~ 2800 lb LH₂ (639.3 cubic feet). The tank is insulated with a combination of spray on foam and multi-layer insulation. Testing will be performed in a large vacuum chamber with electrical heaters to simulate space radiation heat transfer. Tank fluid connections are provided at the top of the tank to allow rejection of the vented gas, and three fluid connections at the bottom of the tank to accommodate the pump inlet, recirculation flow, and heat exchanger (vent flow) inlet line. The TVS components outside the tank (pump, valve, instrumentation) are inclosed in a component box with a vent line to prevent hydrogen contamination of the MSFC vacuum chamber from potential component leakages.

The TVS is required to maintain tank pressure control for a range of tank heat leakage rates (94 Btu/hr to 187 Btu/hr), and liquid level conditions (10% to 95%). The major elements:

- Heat exchanger
- Spray injection and recirculation system,
- Controller
- Instrumentation

were designed to satisfy these operating requirements plus meet the self imposed requirements of design simplicity, low weight, low power consumption, efficient and flexible operation. The following sections will discuss in detail the design approach, trade, and sensitivity analyses that were performed which resulted in the final TVS configuration.

3.1 Heat Exchanger

The heat exchanger is a critical element of the TVS since it is where the heat transfer between the vented fluid and the recirculating liquid flow takes place. The heat exchanger size and flowrate levels must be designed to be capable of rejecting the maximum environmental heat leakage rate and be able to lower the liquid bulk temperature within a reasonable time. The steady state heat leakage rate of the LH₂ tank has been defined by MSFC as 94 Btu/hr minimum, corresponding to a heat flux of 0.25 Btu/hr-sq ft, and 187 Btu/hr maximum, corresponding to a maximum heat flux of 0.50 Btu/hr-sq ft. In order to satisfy this requirement, the heat exchanger design conditions were increased to reject approximately 0.8 Btu/sec (2880 Btu/hr). This self imposed

requirement, which is more than 15 times larger than the maximum heat leakage rate (187 Btu/hr), was chosen in order to reduce the total hours of recirculation pump and vent valve operation, from a nearly continuous operating mode to a more reasonable mission operating time of 5 percent. This increase in the heat exchanger capability also allowed the design to accept growth potential in heat leak and any uncertainties in tank heat leakage level and analysis error. Since the TVS is designed to operate in a cyclic "ON" "OFF" mode, the performance impact is negligible, since the "ON" and "OFF" periods will be self adjusting to compensate for both environmental and internal performance effects. This feature also results in system operating flexibility and robustness.

To define the optimum heat exchanger configuration three candidates were evaluated.

- **Option 1 - Coil Heat Exchanger.** In this option the vent flow tube is wrapped around the spray injection system.
- **Option 2 - Concentric Single Tube Heat Exchanger.** In this design the liquid recirculation flow is inside the inner tube with the vent flow flowing in the space between the inner and outer tube diameter.
- **Option 3 - Multi Tube Heat Exchanger.** Option 3 is similar to Option 2 except the basic concentric tube configuration is repeated to increase the total heat transfer area.

Performance characterization and sensitivity analysis of each of the above concepts were made, and compared to each other in order to select the simplest (design, manufacture, and analysis), lightest, and lowest pressure loss (power consumption, and heat rejection potential) design. Following selection of the best heat exchanger configuration a sensitivity analysis was made to define the optimum system operating pressure in the cold, vent side of the heat exchanger, and the corresponding tank pressure level which resulted in the maximum heat rejection potential of TVS.

3.1.1 Coil Heat Exchanger (Option 1)

The coil heat exchanger, shown in Figure 7, is the simplest heat exchanger configuration. The vent flow is contained in a small diameter tube wrapped around the larger diameter liquid spray bar. Heat is transferred between the low pressure vent flow and the liquid recirculation flow across the contact area between the vent tube and liquid spray bar. The overall heat rejection potential of this concept is low due to the gradual decrease in heat transfer coefficient on the liquid side (hot) resulting from the loss of liquid spray flow from bottom to top of the spray bar. The gradual loss of liquid flow decreases the internal flow regime from highly turbulent (Reynolds Number $> 1.0 \times 10^6$) at the inlet to nearly laminar flow at the top of the spray bar. To compensate for poor heat transfer coefficient the contact area needs to be increased. However, increasing the contact area increases both the vent tube length and vent flow pressure loss. The high pressure loss in the vent line also has the effect of decreasing the amount of liquid available for phase change, and reducing the delta temperature between the vent fluid (cold side) and liquid recirculation flow (hot side). These compounding influences accelerate the increase in vent line length.

A sensitivity analysis was performed to define the relationship between the heat rejection rate and vent line pressure loss. Three different vent tube sizes were evaluated; 0.25", 0.375", and 0.50". The analysis results, shown in Figure 8, indicated that the pressure loss in the vent line increases significantly with respect to total heat rejection rate. As an example, for a heat rejection rate of ~ 0.4 Btu/sec, approximately 60 percent of the spray bar is used to mount the vent line. The total vent line length with a 0.375 inch diameter tube is approximately 100 feet long. The resultant pressure loss is approximately 4 psid. A vent line pressure loss greater than 2 psi does not result in efficient TVS performance. For the coil heat exchanger this pressure loss value is reached at a heat rejection rate of approximately 0.4 to 0.5 Btu/sec.

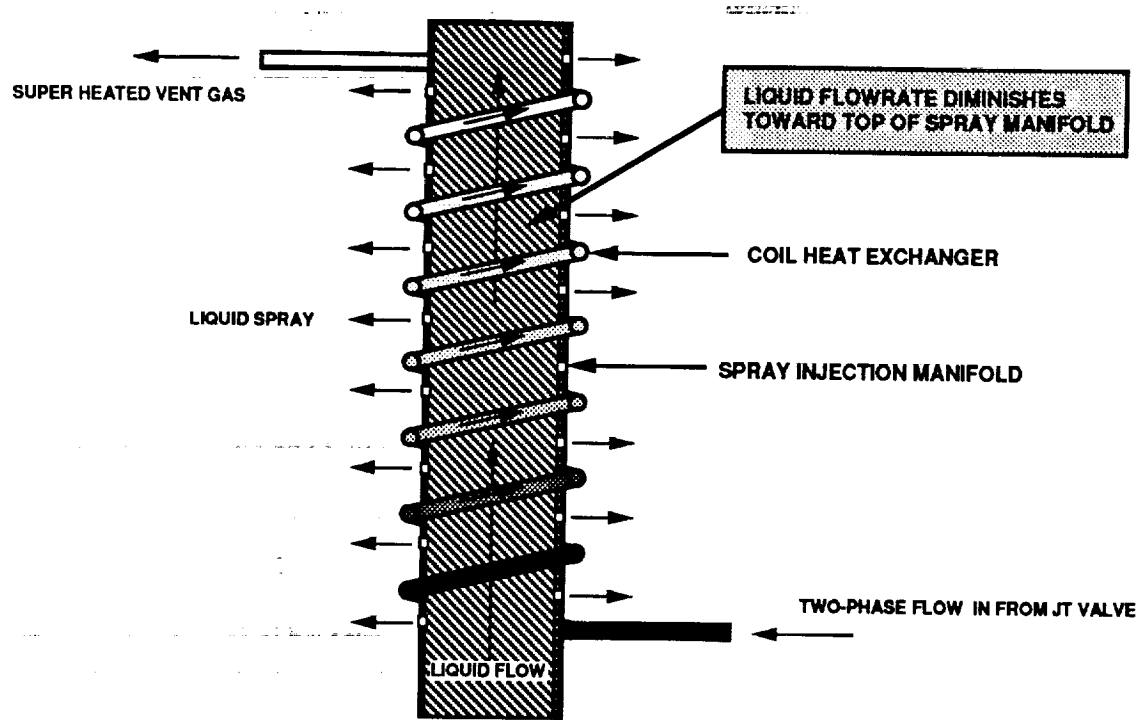


Figure 7 Coil heat exchanger configuration (Option 1)

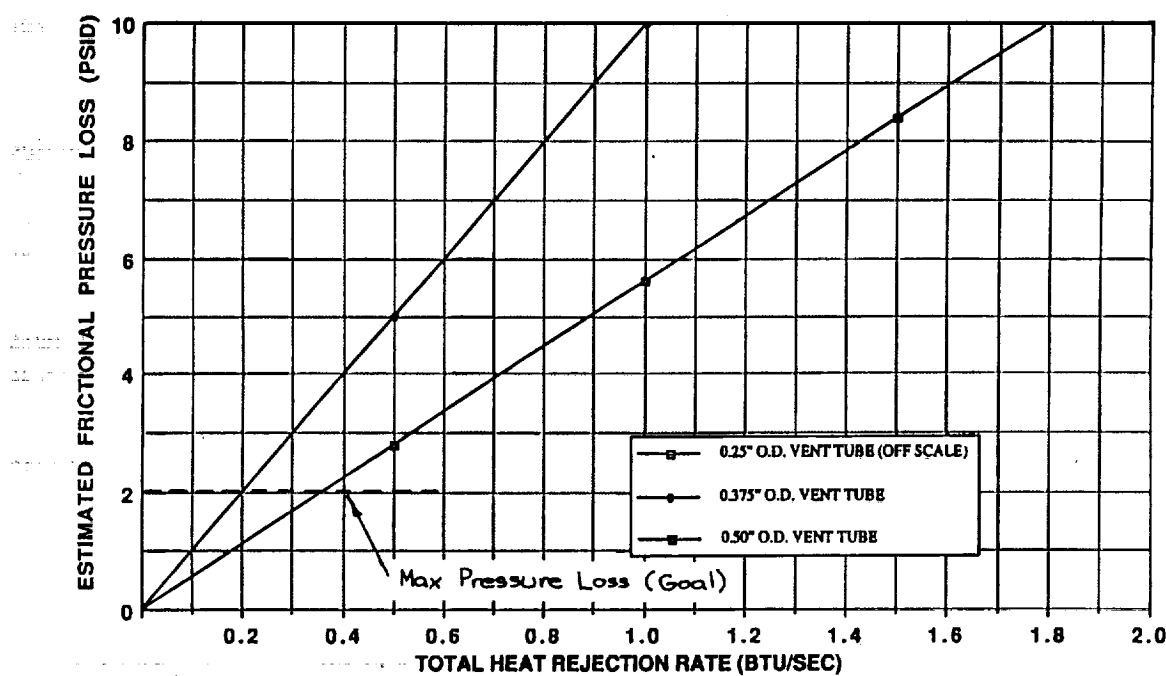


Figure 8 Coil heat exchanger vent line pressure loss sensitivity analysis results

Because the coil heat exchanger design can not satisfy the Rockwell self-imposed heat rejection requirement of 0.8 Btu/sec it was not selected for further evaluation. The coil heat exchanger is also the heaviest due to the long vent line requirement. Potential coil debonding and loss of heat transfer contact area is also a disadvantage which can significantly degrade the heat rejection capability.

3.1.2 Single Tube Heat Exchanger (Option 2)

The single tube heat exchanger, shown in Figure 9, consists of two concentric tubes. The inner tube contains the liquid recirculation flow, while the space between the inner and outer tube contains the overboard vent flow. Because the liquid flowrate is constant throughout the heat exchanger length, the heat transfer coefficient of the liquid side (hot side) is greater than the vent side (cold side), and is no longer the limiting value as compared to the coil heat exchanger design. The heat transfer area is also maximized, because the entire surface area of the inner tube is used to transfer heat between the liquid and the vented two-phase flow. (The heat transfer surface area between the vent fluid and the liquid bulk/ullage gas is also available to transfer heat but was not included in the heat rejection definition since the natural convection heat transfer coefficient within the tank is small, and is dependent on liquid level. However, it is present and represents an additional performance margin that will result in additional heat rejection potential.)

The vent flow (cold side) heat transfer coefficient can also be increased independently by selecting the radial clearance between the inner and outer tube diameter. The selection of this radial clearance is important since it directly effects the Reynolds number, pressure drop, and heat transfer coefficient. A large radial clearance results in low heat transfer coefficient, while a small radial clearance results in high pressure loss. A sensitivity analysis was therefore performed to define the overall heat rejection potential of the single tube heat exchanger design as a function of inner tube diameter, outer tube diameter, and wall thickness. The results, shown in Figure 10, is based on a 0.25 inch difference between the inner tube OD and outer tube OD. It indicates that a 1.5 inch outer tube diameter with 0.058 inch wall, and a 1.25 inch inner tube diameter (OD), (0.035 inch wall) will satisfy the 0.8 BTU/sec heat rejection requirement. The 1.25 inch inner tube diameter also resulted in low frictional pressure loss and recirculation pump power requirement. Figure 11 shows the relationship between inner tube diameter and recirculation pump power requirement, expressed in terms of liquid heating.

In summary, the Single Tube Heat Exchanger design has excellent heat transfer characteristics because the maximum surface area is utilized, and because the vent line pressure loss is small, which results in high liquid quality and low heat sink temperature. Consequently, the heat transfer characteristics of the single tube heat exchanger is superior to the coil heat exchanger design. The heat rejection design goal of 0.8 Btu/sec can therefore be satisfied. Because the diameter on the liquid side (hot side) of the heat exchanger is large the heat transfer area is high while the pressure loss and pumping power requirements are low. Since the liquid and vent mass flowrates are constant, and operates at "constant" pressures, the heat exchanger performance is easy to analyze and therefore will result in a more accurate performance prediction. The debonding concern and loss of contact area is also eliminated and consequently the heat exchanger design is more reliable than the Coil Heat Exchanger. The Single Tube Heat Exchanger is also light weight and easy to manufacture.

3.1.3 Multi Tube Heat Exchnager (Option 3)

The multi tube heat exchanger, shown in Figure 12, is similar to the the single tube heat exchanger design in that the liquid recirculation flow is contained in the inner tube and the vent flow is contained in the outer tube. The liquid and vent flowrates, however, are divided into a number of smaller tubes. The benefit of dividing the flow into smaller tubes is that both the heat

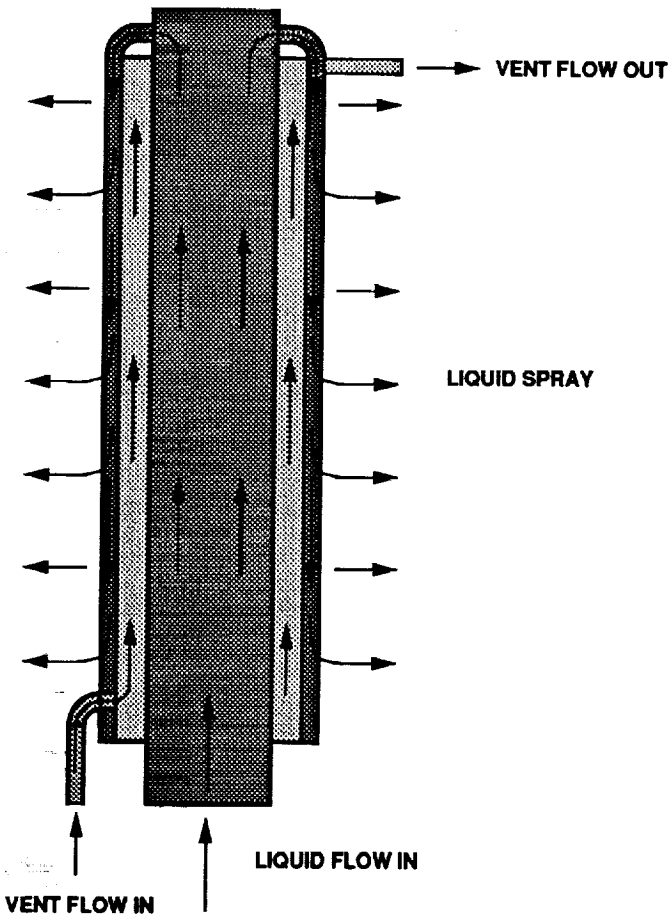


Figure 9 Single tube heat exchanger configuration (Option 2)

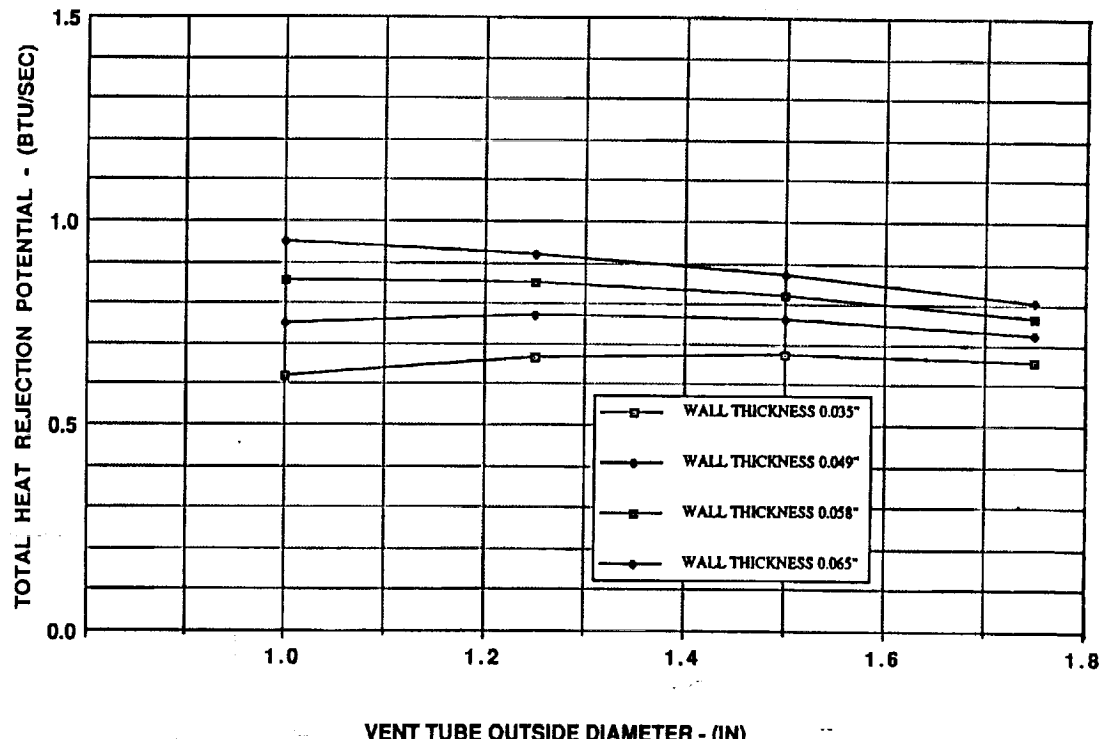


Figure 10 Single tube heat exchanger design sensitivity analysis

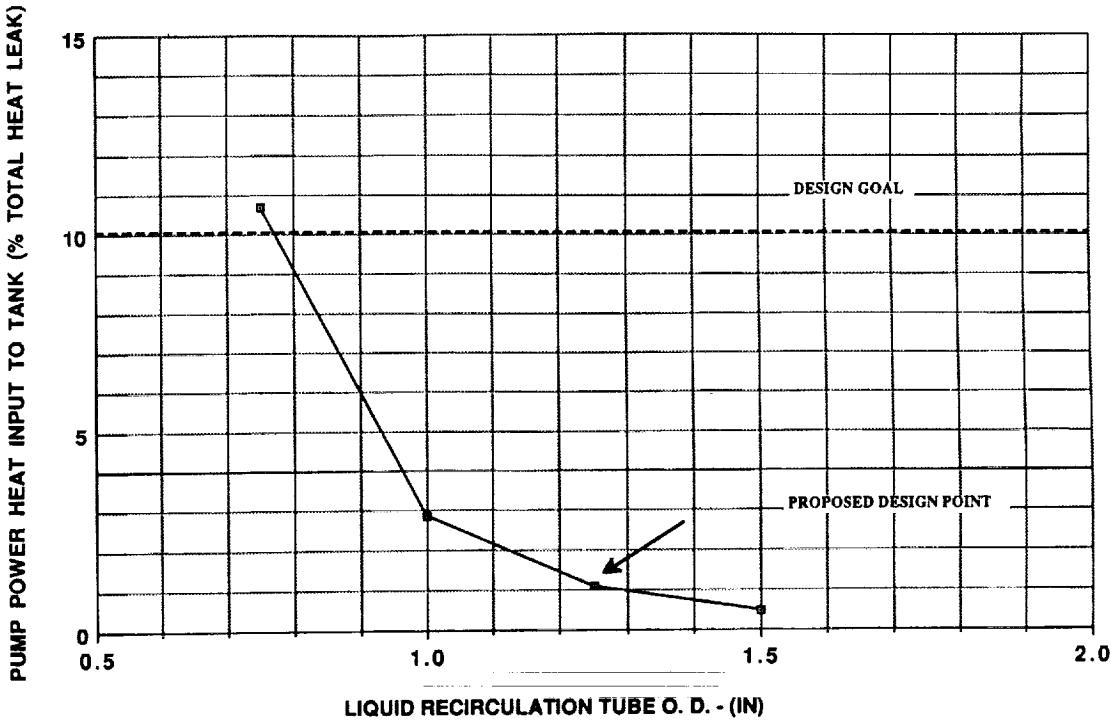


Figure 11 Heat input to tank due to pumping power (Single Tube)

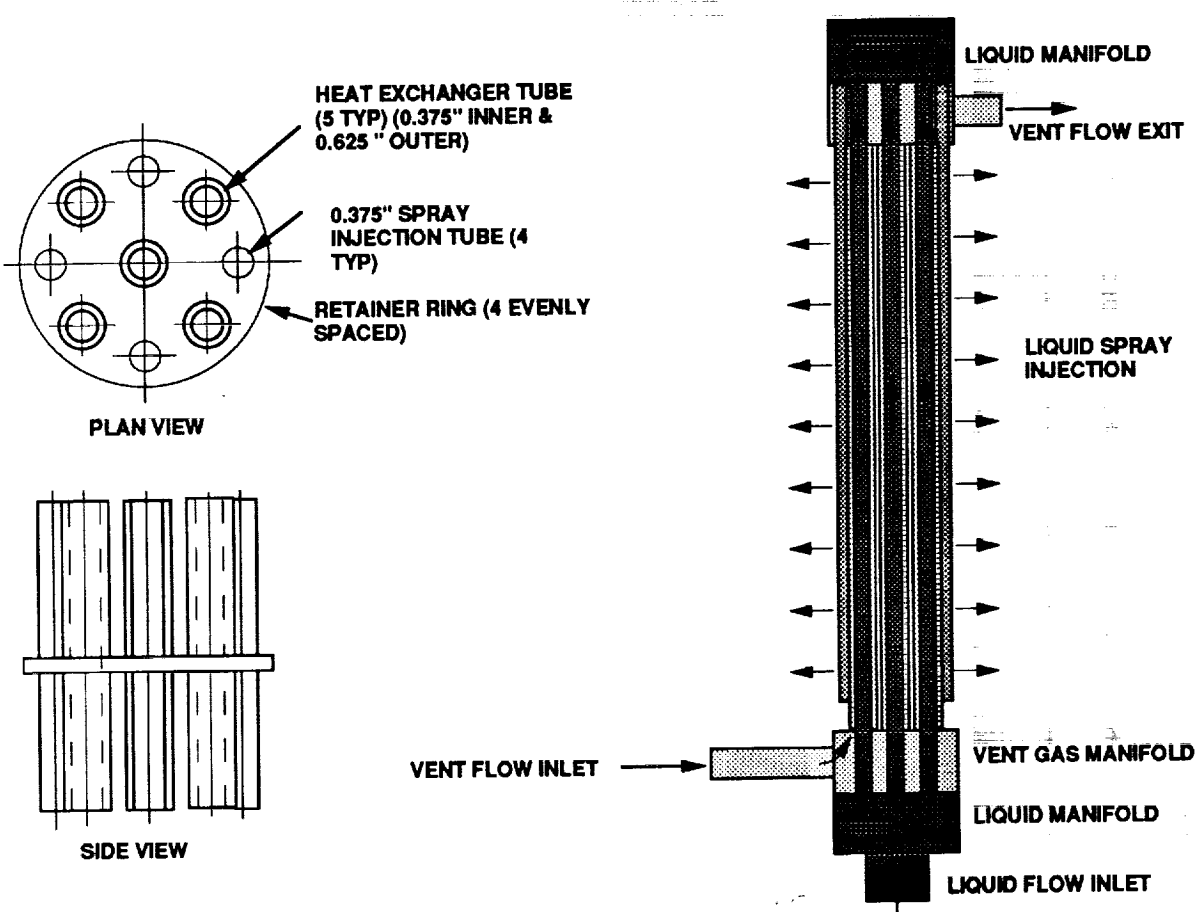


Figure 12 Multi-tube heat exchanger configuration

transfer surface area and the liquid heat transfer coefficient is increased significantly compared to the single tube heat exchanger design.

The pumping power requirement of the multi tube heat exchanger was evaluated to determine the maximum number of tubes required for heat rejection. The sensitivity analysis was based on a 0.375" (O D) tube with minimum wall thickness of 0.022". (Larger liquid tube sizes resulted in large radial clearances on the vent side of the heat exchanger with low heat transfer coefficient. The larger liquid tube sizes were therefore not pursued since it diminished the gain on the liquid side with the loss on the vent side of the flow). The analysis results, shown on Figure 13, indicated that heat exchanger tubes of 5 or more are required to reduce the frictional pressure loss and pump power requirement below an acceptable level (~15 % of total tank heat input).

The heat rejection potential of the multi tube heat exchanger is shown in Figure 14 as a function of number of tubes (0.375 in. OD) and wall thickness. As in the single tube design the radial clearance played a significant role in the overall heat transfer characteristics. The heat transfer performance can be changed by 60 to 70 percent by varying the outer tube wall thickness from a minimum value of 0.022 inches to 0.065 inches. For the 5 tube heat exchanger design, which has acceptable liquid frictional pressure drop, the maximum heat transfer potential is ~ 2.4 Btu/sec. This heat transfer rate is over three times larger than the design goal (0.8 Btu/sec). This is due to the increase in heat transfer area and liquid heat transfer coefficient. The multi tube heat exchanger therefore has the highest heat rejection rate of the three options evaluated. The multi tube heat exchanger, however, is heavier, more complex to manufacture, and has a larger liquid pressure drop than the single tube heat exchanger.

3.1.4 Heat Exchanger Trade Analysis Results

The results of the heat exchanger trade and sensitivity analysis are summarized in Figure 15. The results indicated that the single tube heat exchanger design (Option 2) is superior to the coil heat exchanger and multi tube heat exchanger configurations. The single tube heat exchanger was therefore selected for the TVS design because it is light weight, satisfies the 0.8 BTU/sec heat rejection requirement, is simple to build, and results in low pressure loss and pumping power requirement.

3.1.5 Heat Exchanger Operating Pressure Definition

Definition of the tank operating pressure level and the vent line back pressure are important to the efficient design of a TVS design since it directly influences the venting losses. A trade study was therefore performed to define the optimum TVS operating tank pressure level, and the corresponding vent line back pressure that results in the maximum heat rejection potential of the vented gas. The vent gas heat absorption potential is a combination of heat required to evaporate the two phase vented fluid, and the sensible heat to raise it from the saturated temperature to the superheated level corresponding to the tank liquid bulk temperature.

Lowering the operating pressure of the cold side (vent side) of the heat exchanger has several effects. First the liquid mass fraction decreases due to throttling flow at constant enthalpy. (See Figure 16). Consequently, the quantity of liquid available for vaporization is reduced with lower pressure. Even though the latent heat of vaporization is slightly greater at the lower pressures, the net heat absorbed by boiling is less at lower pressures than at higher pressures as a result of the lower liquid fraction. (See Figure 17).

The second effect in lowering the vent line operating pressure is to reduce the boiling temperature level. The lower boiling temperature increases the amount of sensible heat (The sensible heat is the heat required to raise the gas from the boiling temperature to the liquid bulk temperature). The change in sensible heat is shown in Figure 18 as a function of vent line operating pressure.

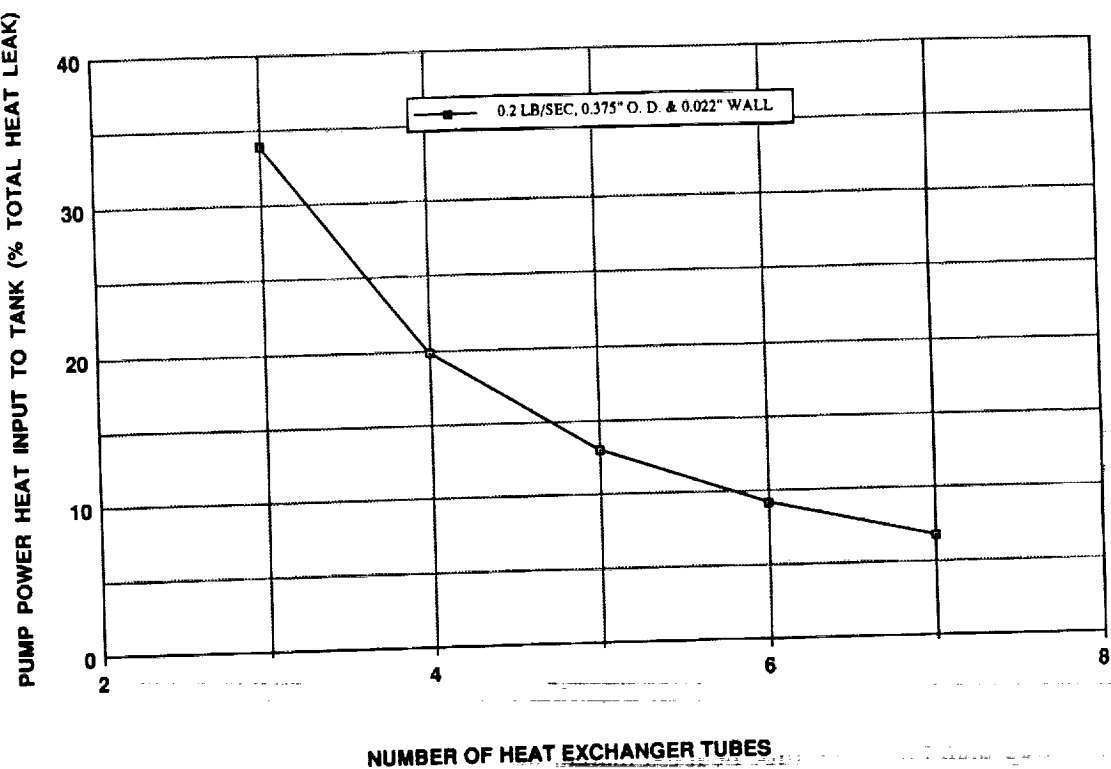


Figure 13 Heat input to LH₂ tank due to pumping power/frictional loss

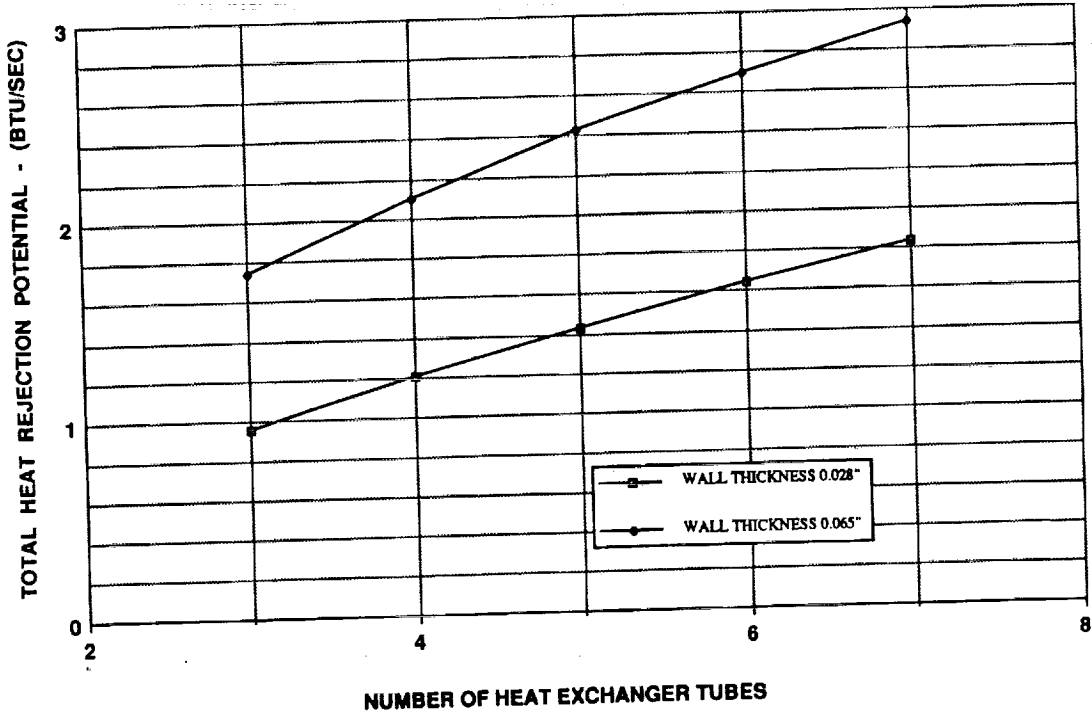


Figure 14 Multi-tube heat exchanger performance sensitivity to number of tubes

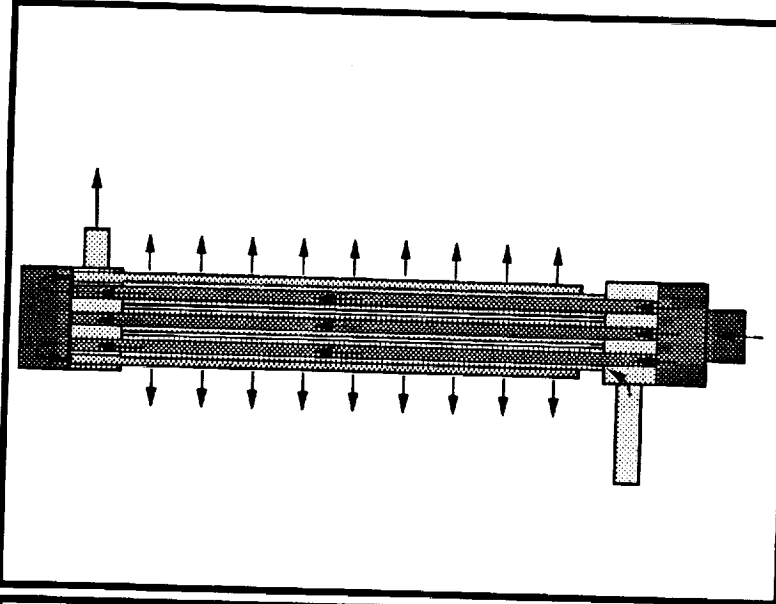
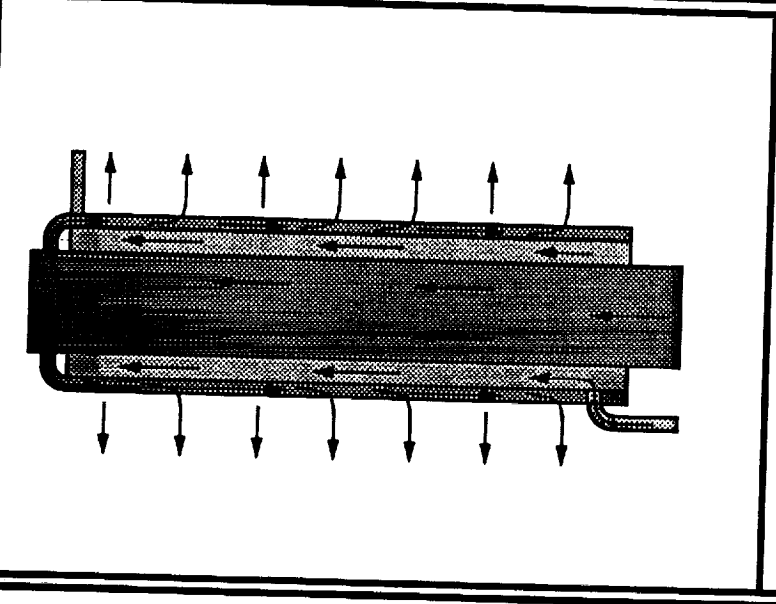
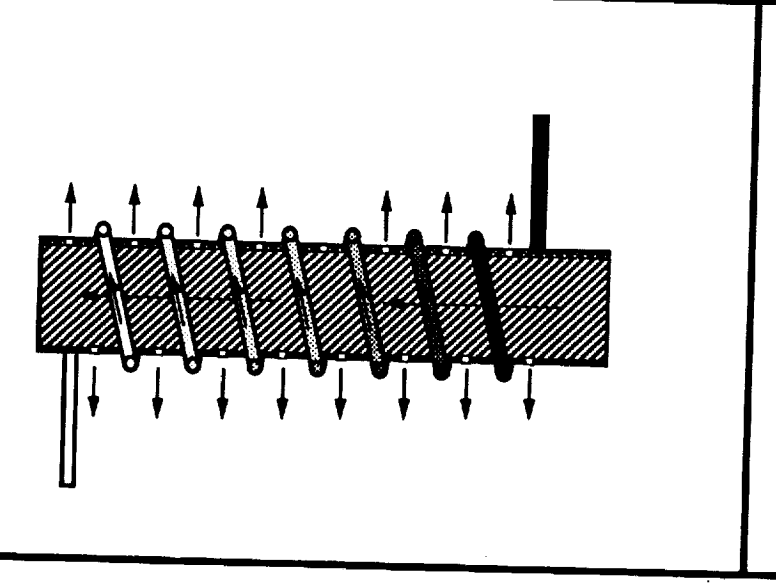
	<p>MULTI-TUBE HEAT EXCHANGER (OPTION 3)</p> <p>ADVANTAGES</p> <ul style="list-style-type: none"> • EXCELLENT HEAT TRANSFER CHARACTERISTICS • EXCEEDS HEAT REJECTION DESIGN GOAL (1 BTU/SEC) <p>DISADVANTAGES</p> <ul style="list-style-type: none"> • HEAVIER THAN SINGLE TUBE HX (OPTION 2) • HIGH PRESSURE LOSS AND PUMPING POWER REQUIREMENT • COMPLEX TO MANUFACTURE <p>NOT RECOMMENDED</p>
	<p>SINGLE TUBE HEAT EXCHANGER (OPTION 2)</p> <p>ADVANTAGES</p> <ul style="list-style-type: none"> • EXCELLENT HEAT TRANSFER CHARACTERISTICS • GOOD HEAT REJECTION POTENTIAL (~1 BTU/SEC) • LOW PRESSURE LOSS & PUMPING POWER REQUIREMENT • LIGHT WEIGHT <p>DISADVANTAGES</p> <ul style="list-style-type: none"> • MORE COMPLEX TO BUILD <p>RECOMMENDED OPTION</p>
	<p>COIL HEAT EXCHANGER (OPTION 1)</p> <p>ADVANTAGE</p> <ul style="list-style-type: none"> • SIMPLE DESIGN <p>DISADVANTAGES</p> <ul style="list-style-type: none"> • LIMITED HEAT REJECTION (<0.5 BTU/SEC) • INEFFICIENT HEAT TRANSFER CHARACTERISTICS (LOSS OF CONTACT AREA) • HEAVIEST • LARGE VENT FLOW PRESSURE DROP <p>NOT RECOMMENDED</p>

Figure 15 Summary of heat exchanger configuration trade study

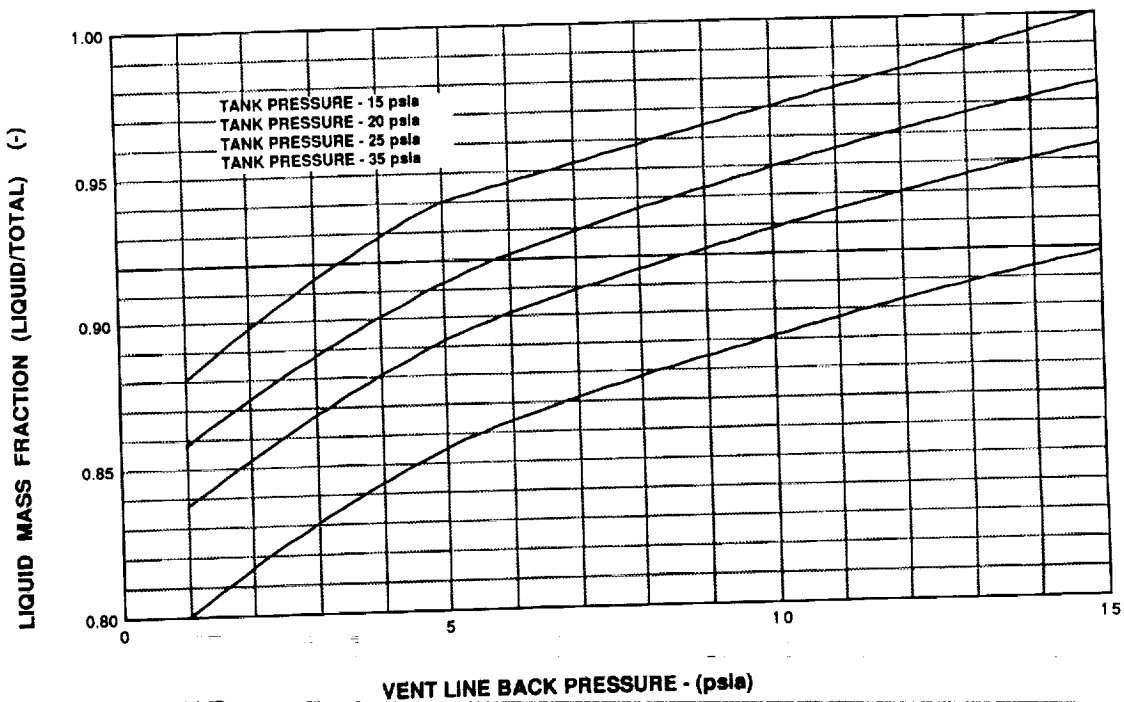


Figure 16 Liquid mass fraction at vent line inlet as a function of liquid vapor pressure and vent line back pressure

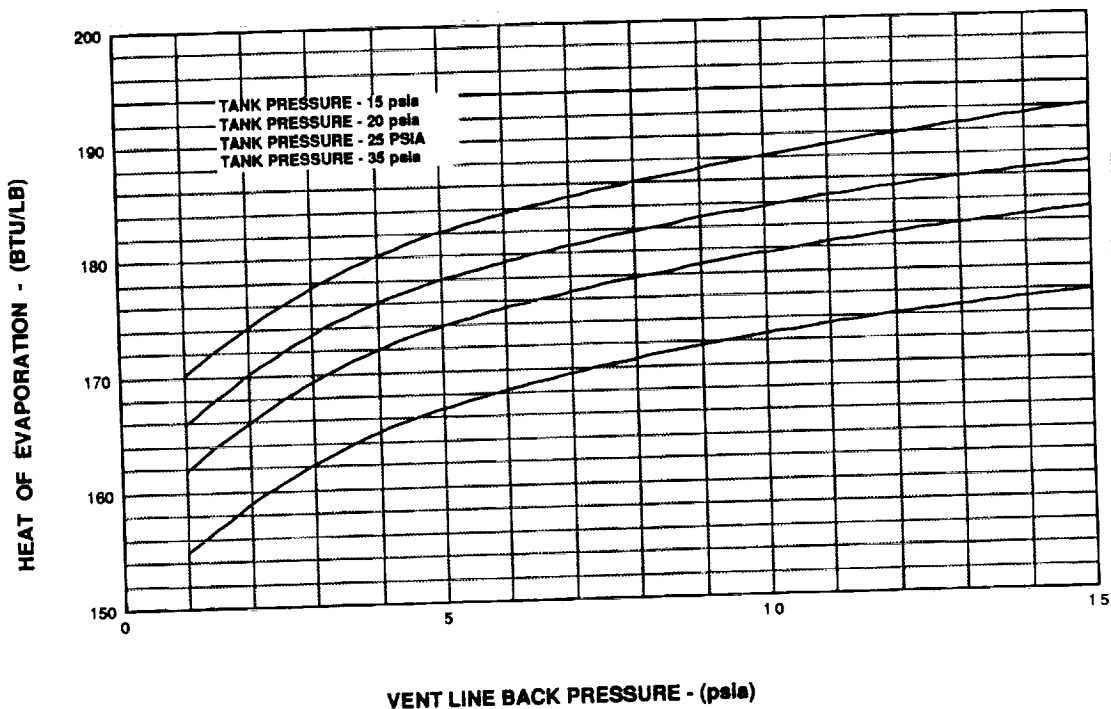


Figure 17 Heat absorbed through evaporation as a function of liquid vapor pressure and vent line back pressure

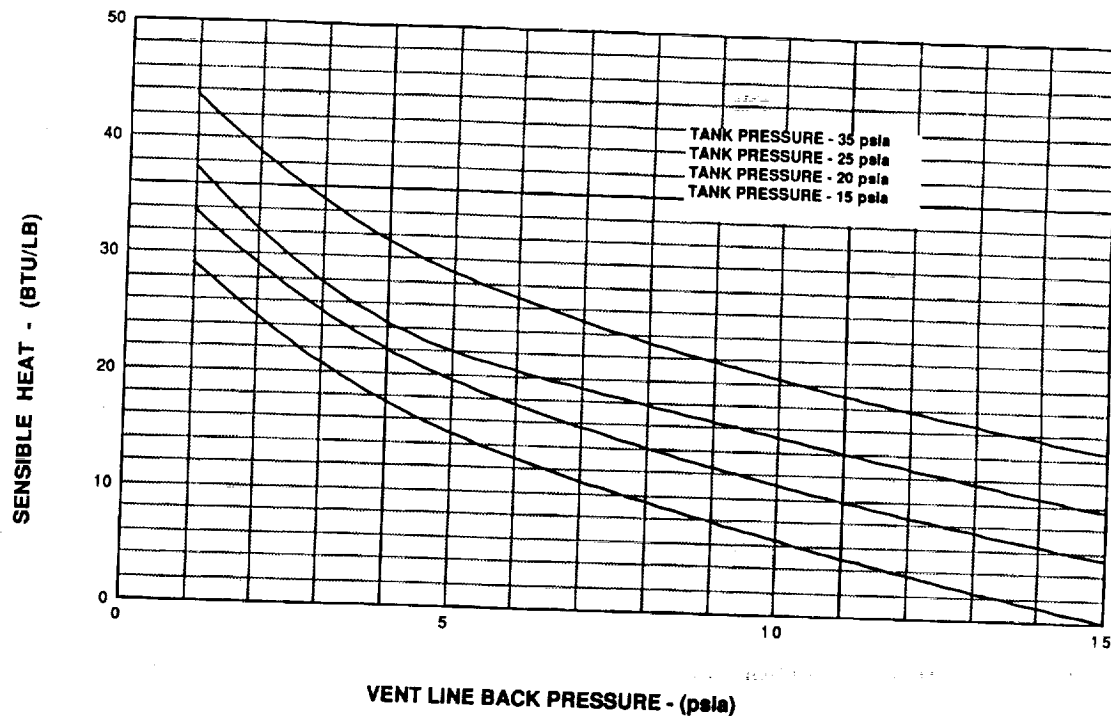


Figure 18 Heat absorbed by vent flow through sensible heating as a function of liquid vapor pressure and back pressure

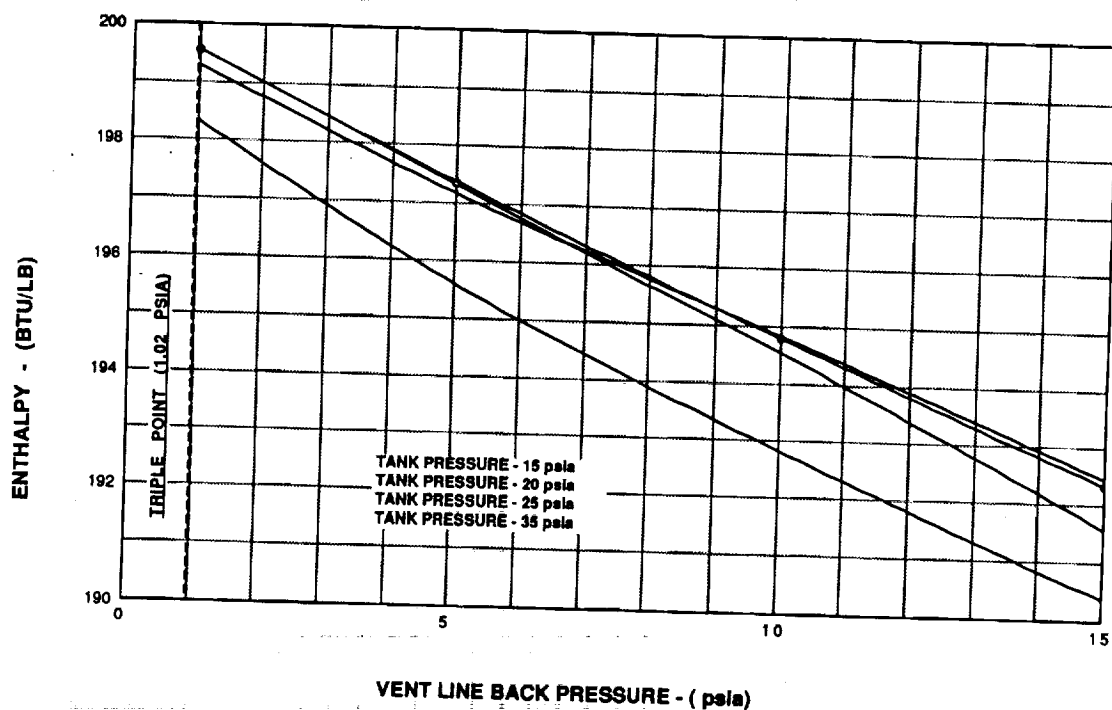


Figure 19 Total heat absorption potential of vented hydrogen as a function of liquid vapor pressure and back pressure

Although it is smaller than the heat absorbed due to evaporation, it represents a significant amount of heat capacity.

While the evaporation heat capacity decreases with lower operating pressure, the amount of sensible heat increases with lower operating pressure. The net effect of the two heat capacities is shown in Figure 19. As can be seen the total heat absorption potential of the vented fluid increases with decreasing pressure level. The lower the vent line pressure the higher the total heat absorption potential of the vent flow. Although the maximum heat absorption potential of hydrogen is at the triple point (1.02 psia), a higher pressure level of 3 psia was selected as the design point.

The tank operating pressure, although significantly less sensitive, also effects the TVS heat rejection potential. The total heat absorption potential at 3 psia back pressure gradually increases from 15 psia (ambient pressure) to a maximum value near 20 psia. (See Figure 19). Consequently, the 20 psia tank pressure level was selected where heat rejection through venting is initiated. The 20 psia pressure level also allows a significant amount of heat to be absorbed by the liquid bulk without venting. Depending on the insulation efficiency, missions with operating durations from days to a couple of weeks can be satisfied by absorbing the environmental heat in the liquid/tank mass with no venting losses.

3.2 Spray & Recirculation System

The purpose of the spray injection system is to provide uniform liquid flow into the ullage and liquid bulk for thermal destratification through forced convection heat transfer. Ullage pressure collapse and condensation through mixing is the primary heat transfer mode in the ullage during TVS operation. The liquid spray velocity therefore needs to be sufficient in order to promote good droplet atomization and heat transfer. High injection velocity, however, results in increased pressure loss which requires high recirculation pump discharge pressure, and increased pump power and liquid bulk heating. Because the high discharge velocity and low pump power are two opposing requirements, a sensitivity analysis was performed to define an acceptable spray injection design.

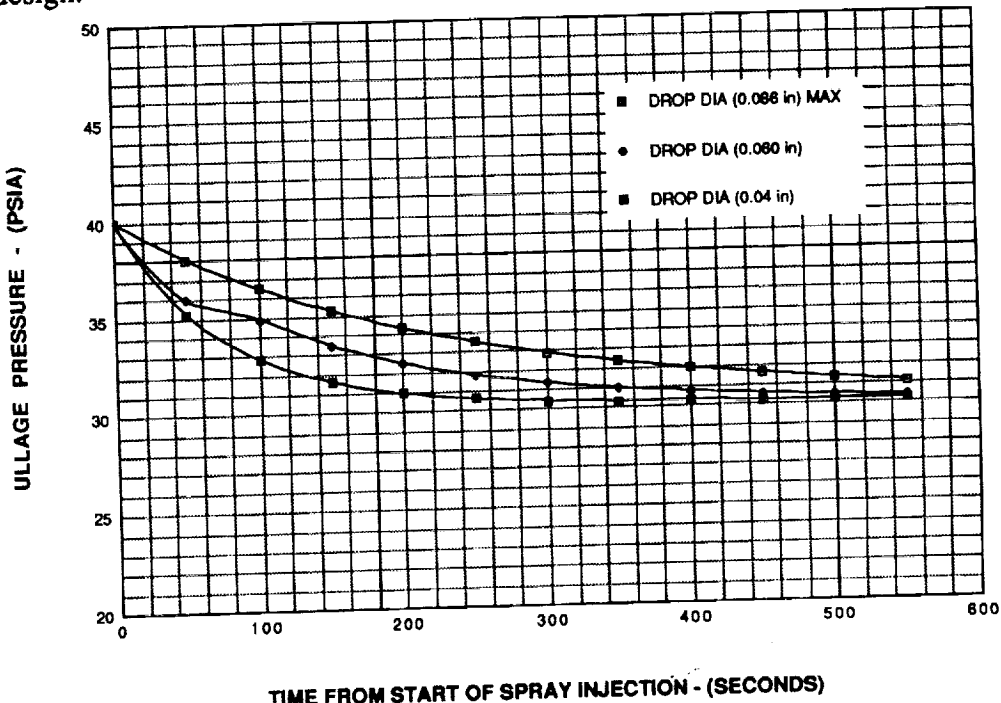


Figure 20 Ullage pressure decay sensitivity to liquid drop diameter

3.2.1 Spray Injection Orifice Sizing

The spray injection configuration for Zero g TVS is dictated by the heat exchanger design selection (concentric tube heat exchanger). It consists of four 0.50" tubes manifolded to the heat exchanger outlet and equally spaced to give uniform spray injection into the tank in four directions, and along the length of the tank. To define an acceptable orifices size an ullage pressure decay sensitivity analysis was performed. In the heat transfer estimate the liquid droplets were assumed to be equal to the orifice diameter. (This approximation is nearly correct for low pressure drop, and low Reynolds number jets and was subsequently verified by spray injection tests performed at NASA Lewis Research). The number of droplets and total droplet surface area was calculated for the liquid spray injection flowrate. The analysis results, simulating an empty thermally stratified tank, indicates that ullage pressure decay increases with smaller liquid droplets, and orifice size. (See Figure 20). To further narrow the orifice size selection the orifice diameter which results in nearly uniform mass flowrate along the length of the spray tube was defined. An orifice diameter of 0.0670 inches (standard 51 drill) resulted in nearly uniform spray injection flow at 50 percent liquid level (design point). The spray injection flow analysis results are presented in Figure 21 for the full tank, 50 percent level, and empty tank (10 percent) at 1 g. As can be seen the mass flowrates are relatively constant for the range of liquid levels. The differences are due to the 1 g hydrostatic pressure effects. For the 1 g tests the injection flowrate gradient is sensitive to the liquid level, while in zero g the spray injection flowrate will be uniform due to the absence of hydrostatic pressure. The spray injection velocity gradient corresponding to the mass flowrates of Figure 21, are shown in Figure 22. These injection velocities are considered to be significant and will penetrate the ullage volume as have been verified by water flow spray injection tests at Rockwell Downey.

3.2.2 LH2 Spray Injection Test (Lewis Research)

Liquid hydrogen spray injection tests were performed at the Lewis Research Center (LeRC) to verify the analytical model and assumptions that were used in defining the liquid spray injection heat transfer and resultant ullage pressure collapse effects. A schematic of the LeRC test configuration is shown in Figure 23. A spray bar segment of 25 inches was simulated due to the limitations of the vacuum jacketed dewar. The spray orifices (0.055 inch, standard drill size of 54) were spaced 2.5 inches apart throughout the length of the spray bar in four directions. The flowrate level was scaled based on the total number of orifices to simulate the spray injection velocity of the full size TVS design. A turbine type flowmeter was used as a pump to recirculate the flow from the tank bottom to the spray bar. Because of the performance limitation of the recirculation pump, only 3 GPM, instead of the 5 GPM desired liquid flowrate level could be achieved. In addition to the low flowrate level, the duration of the steady state (~3 GPM) recirculation flowrate was limited to 20 seconds. Figures 24 through 27 present the measured tank pressure, ullage temperature, wall temperature and spray injection flowrate data of a typical spray injection test. Even though the recirculation flowrate was lower than desired, and the tests were limited in duration, the LeRC tests provided valuable data in defining the spray injection heat transfer characteristics. The results allowed verification of the original analytical model with minor refinement. A comparison of the measured ullage pressure, pressure decay rate, and temperature decay with the analytical model prediction is shown in Figures 28, 29, and 30, respectively for the 20 second steady state flow duration. The good correlation between the analytical prediction and test data indicates that the spray injection design parameters are acceptable and will provide good tank pressure control during MHTB TVS testing.

3.3 Controller Logic

A controller is required to operate the TVS in order to maintain the tank pressure at an acceptable level. The function of the controller is to activate the recirculation pump, to initiate liquid spray injection and destratification, and also to reject heat through gaseous venting. A trade analysis was

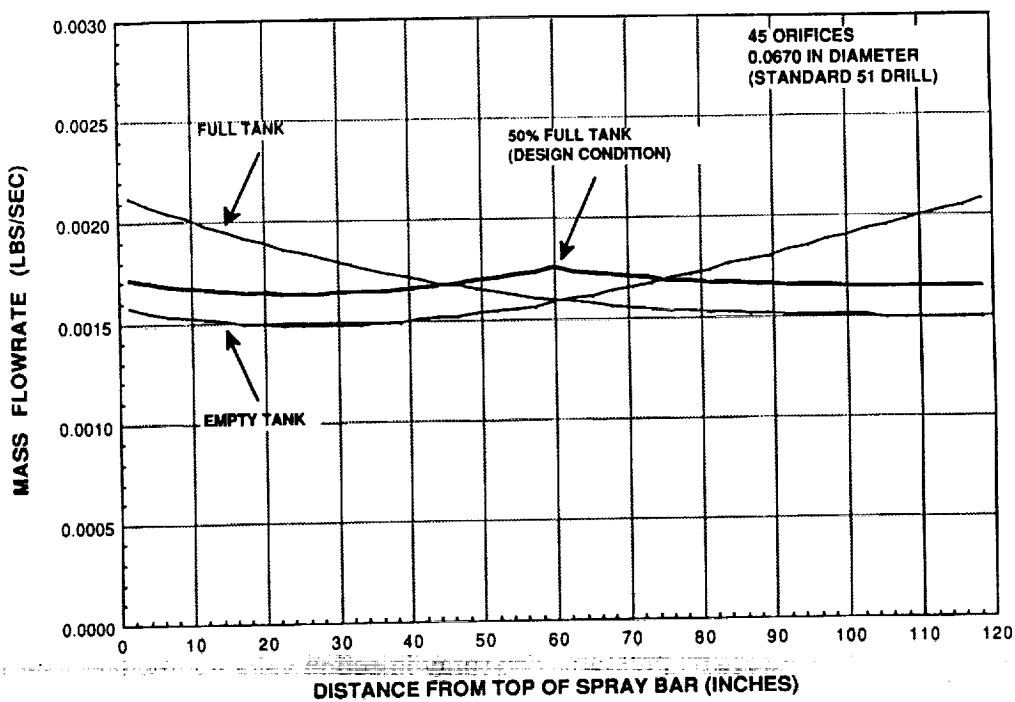


Figure 21 Liquid spray injection flowrate as a function of distance from top of spray bar (0.3 lb/sec)

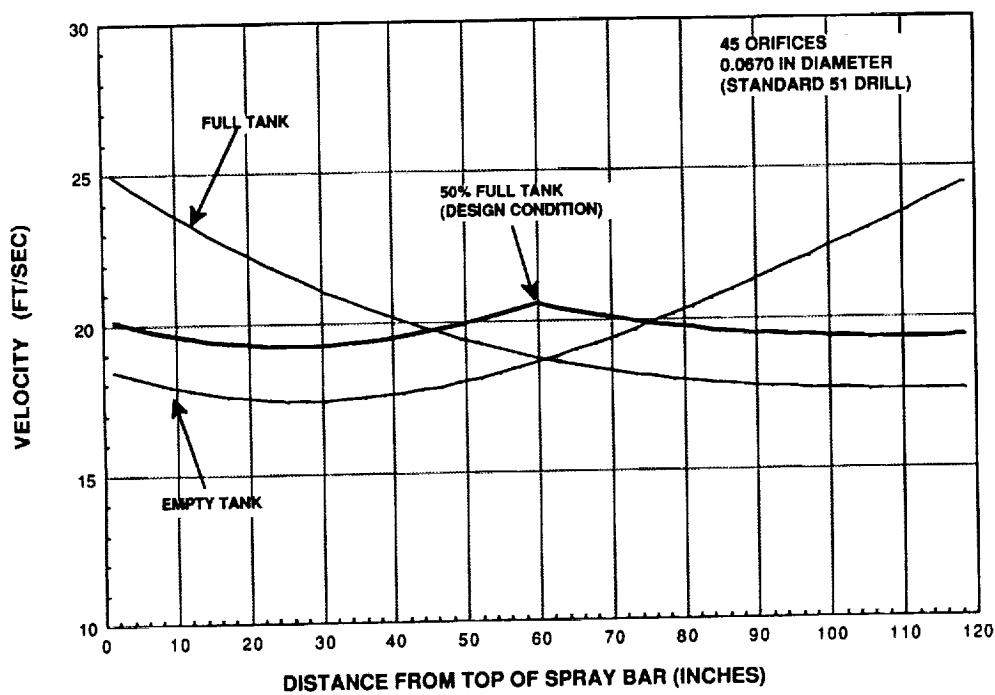


Figure 22 Liquid spray injection velocity as a function of distance from top of spray bar (0.3 lb/sec)

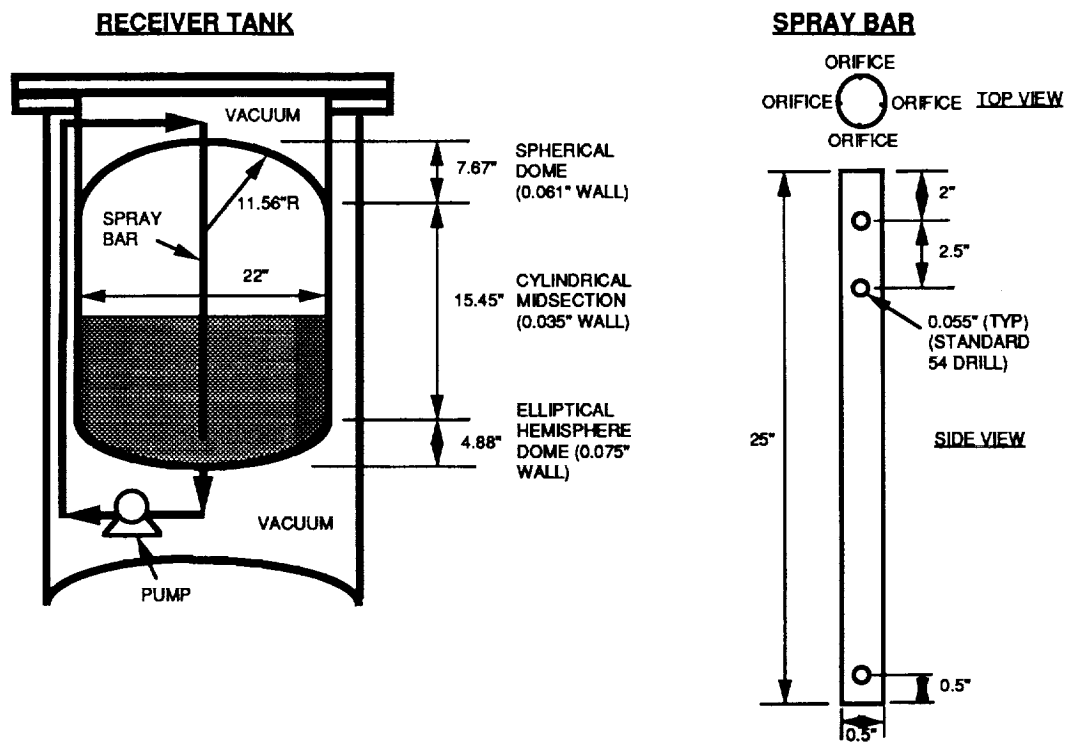


Figure 23 LeRC ullage pressure collapse test setup

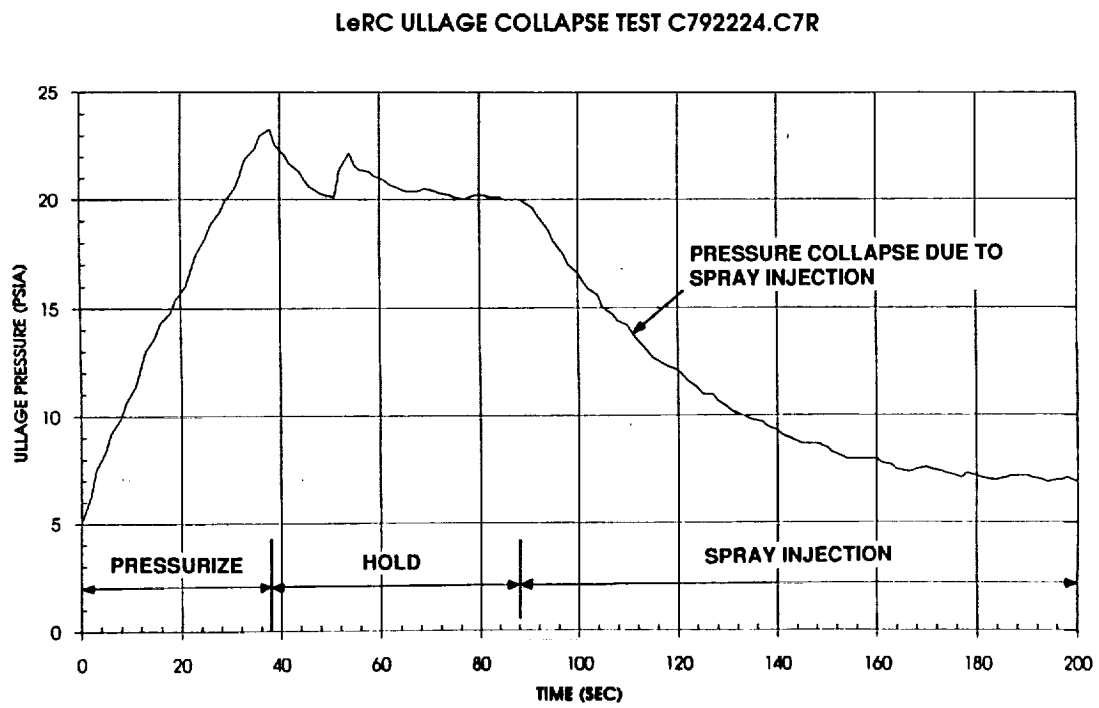


Figure 24 LeRC test data for tank ullage pressure

LeRC ULLAGE COLLAPSE TEST C792224.C7R

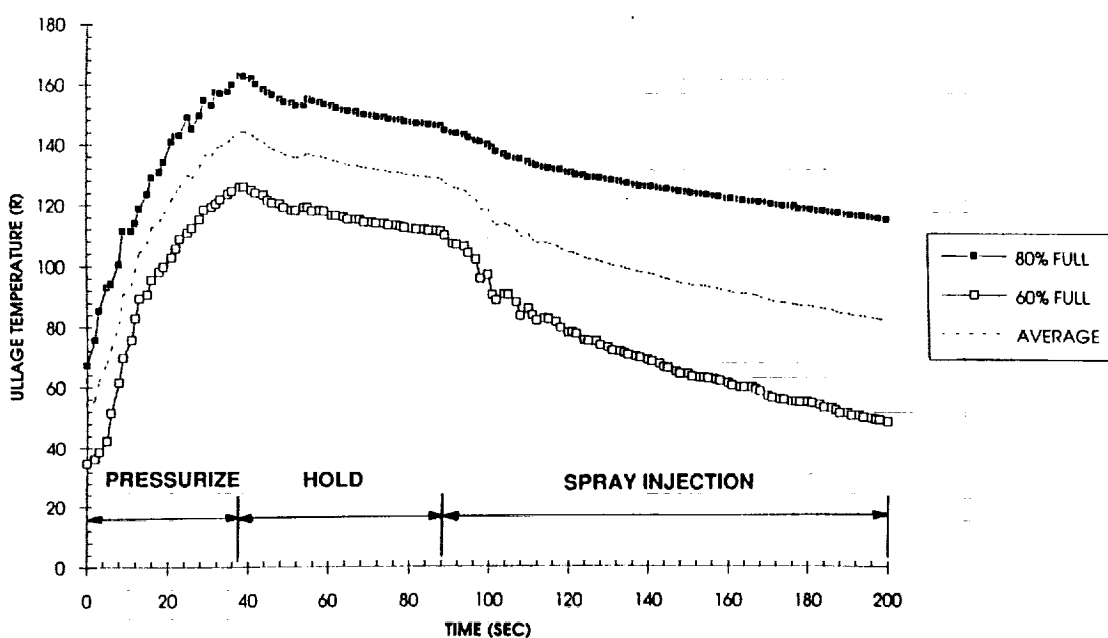


Figure 25 LeRC test data for ullage temperature

LeRC ULLAGE COLLAPSE TEST C792224.C7R

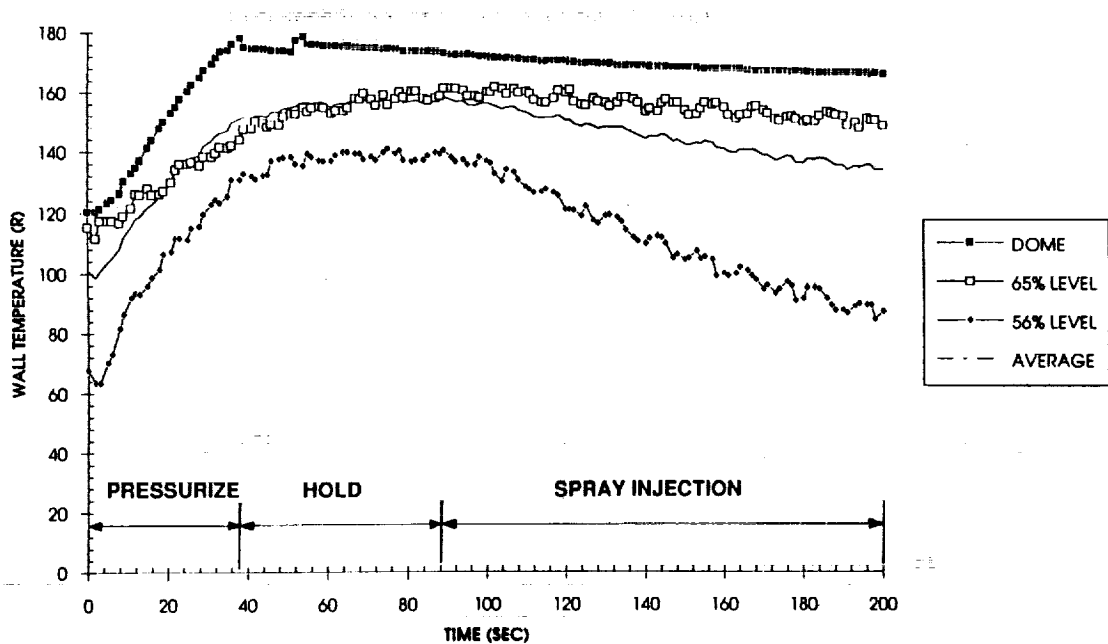


Figure 26 LeRC test data for tank wall temperature

LeRC ULLAGE COLLAPSE TEST C792224.C7R

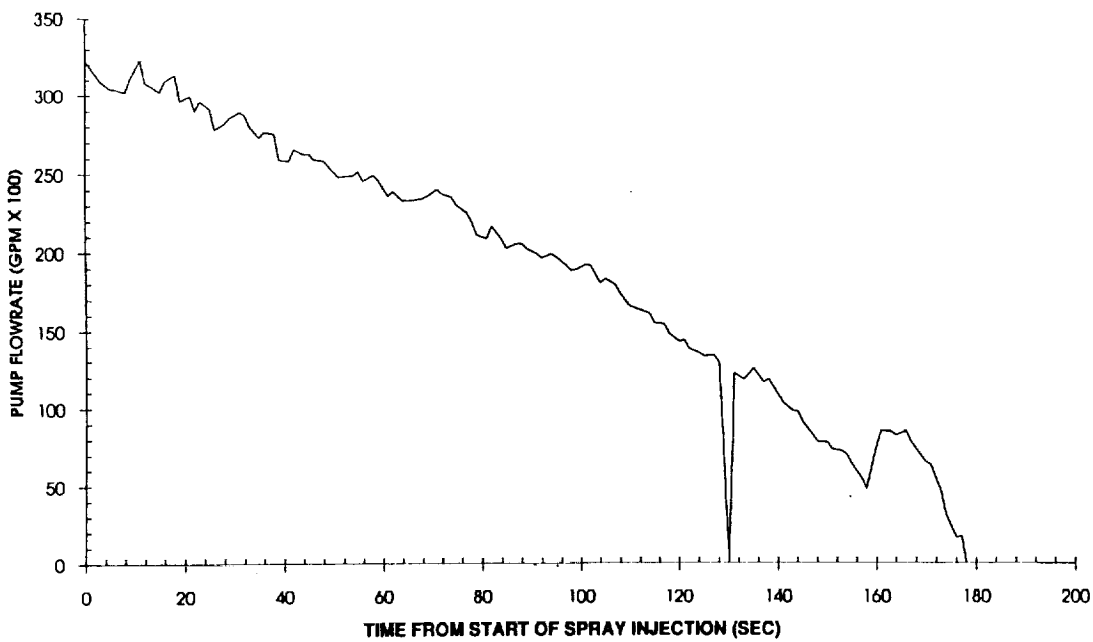


Figure 27 LeRC test data for pump flowrate

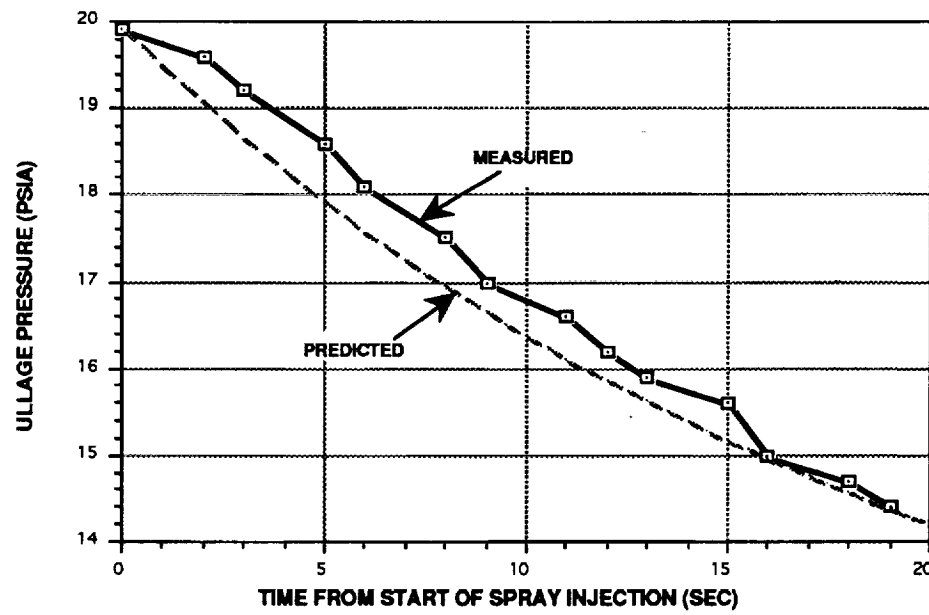


Figure 28 Comparison of predicted ullage pressure and LeRC test result

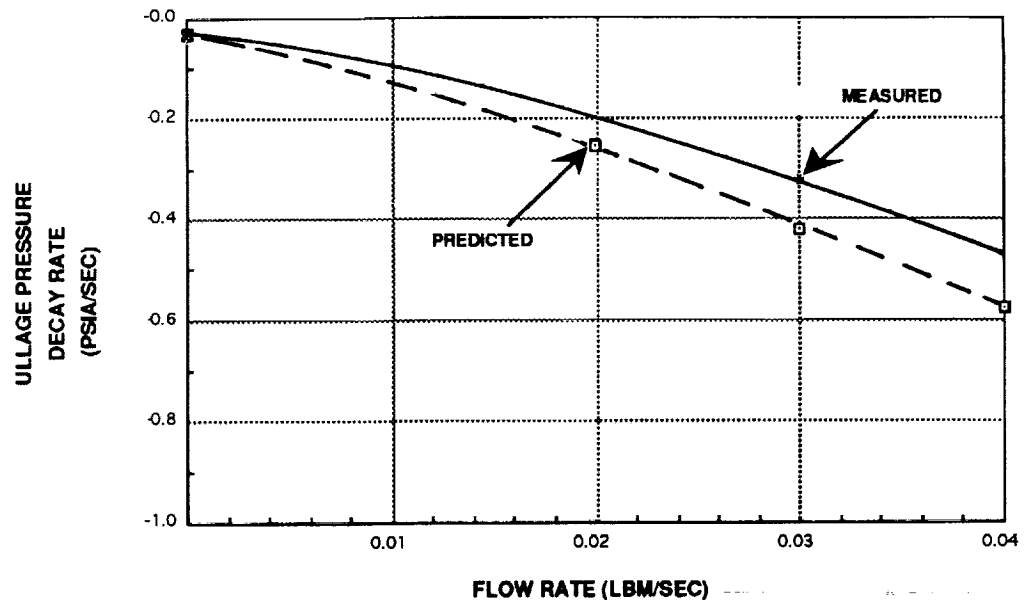


Figure 29 Comparison of predicted and LeRC measured ullage pressure decay rate

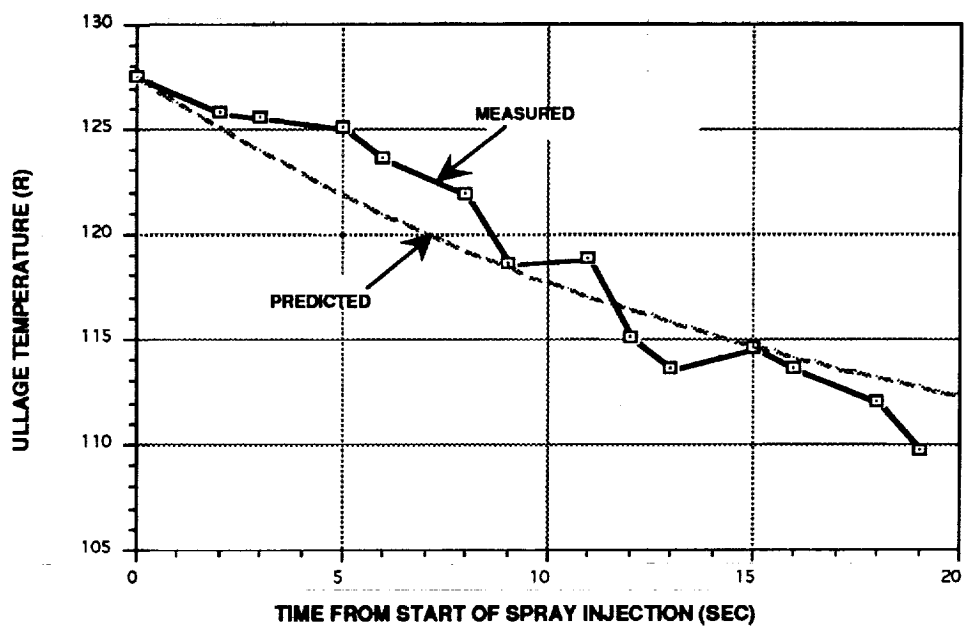


Figure 30 Comparison of predicted ullage temperature with LeRC test result

therefore performed to define the best controller logic which is simple, flexible, and results in efficient venting operation.

3.3.1 Single Pressure Control of Pump & Vent Valve (Option 1)

The recirculation pump and vent valve are operated simultaneously in Option 1 whenever the maximum tank pressure level (P_{max}) is reached. The recirculation pump is powered and the vent valve is opened until the ullage pressure level decays below the minimum control band pressure level (P_{min}). The simultaneous operation of the recirculation pump and vent valve results in ullage pressure collapse, due to liquid spray injection, and liquid bulk temperature cooling due to heat rejection through the vent valve.

The Option 1 control logic, shown in Figure 31, is the simplest since only one tank measured parameter is used. Tank pressure measurement activates both the recirculation pump and the vent valve. Operation of the vent valve in unison with the recirculation pump ensures that the recirculation pump is primed at all times and minimizes the potential of recirculation pump operation with gas internal to the pump. The disadvantage of Option 1 is that venting is always initiated even when tank pressure control could be accomplished with only liquid spray injection. (See Figure 32). Consequently the vented mass penalty is the highest with this control logic. Also, because liquid bulk cooling always exists whenever the TVS system is activated it is possible that the liquid bulk temperature could be significantly subcooled below the desired liquid temperature level. This Option, although simple, yet is inefficient and could result in unacceptable low liquid temperature. This option was therefore not selected.

3.3.2 Separate Pressure Control For Pump & Vent Valve (Option 2)

In order to minimize the venting losses and improve the system performance of Option 1, the recirculation pump and vent valve need to be operated independently. Figure 33 shows the Option 2 control logic. Option 2 uses separate control logic to activate the recirculation pump and vent valve. The pump control logic is identical to Option 1 in that the recirculation pump is controlled by ullage pressure between maximum (P_{max1}) and minimum pressure (P_{min}). This allows heat rejection from the ullage gas into the liquid bulk through mixing and without venting. This mode of operation can be sustained until the liquid vapor pressure exceeds the maximum pressure level (P_{max1}). The vent valve consequently must be opened to reject the heat stored in the liquid bulk and tank mass. The vent valve is opened only after the pressure level reaches P_{max2} and remains open until the tank pressure (and liquid vapor pressure) decreases to the lower control limit (P_{min}). Figure 34 shows the pump and vent valve operation resulting from Option 2 control logic.

Option 2 control logic is simple but slightly more complex than Option 1. Only the tank ullage pressure measurement is required for pump and vent valve control with different actuation set points. The primary disadvantage of this control logic is that once the liquid vapor pressure exceeds the minimum control band pressure level (P_{min}), liquid spray injection into the ullage can no longer lower the ullage pressure back to the minimum control level where the pump is turned off since the liquid vapor pressure is higher than the minimum control pressure level. Consequently, the recirculation pump continues to operate, heating the liquid bulk until the liquid vapor pressure slowly reaches the maximum pressure (P_{max2}) where the vent valve is opened. (See Figure 34). This continuous pump operation can last from approximately 1.7 hours at low liquid level (10%) to 16 hours at maximum liquid level. In addition to operating the recirculation pump for these extended durations, the heat that is added by the pump to the liquid bulk also has to be removed through venting. This delta vent loss represents a significant performance penalty to Option 2. A preliminary estimate indicates that the performance degradation is on the order of 40% increase in venting requirement over the recommended option (Option 3).

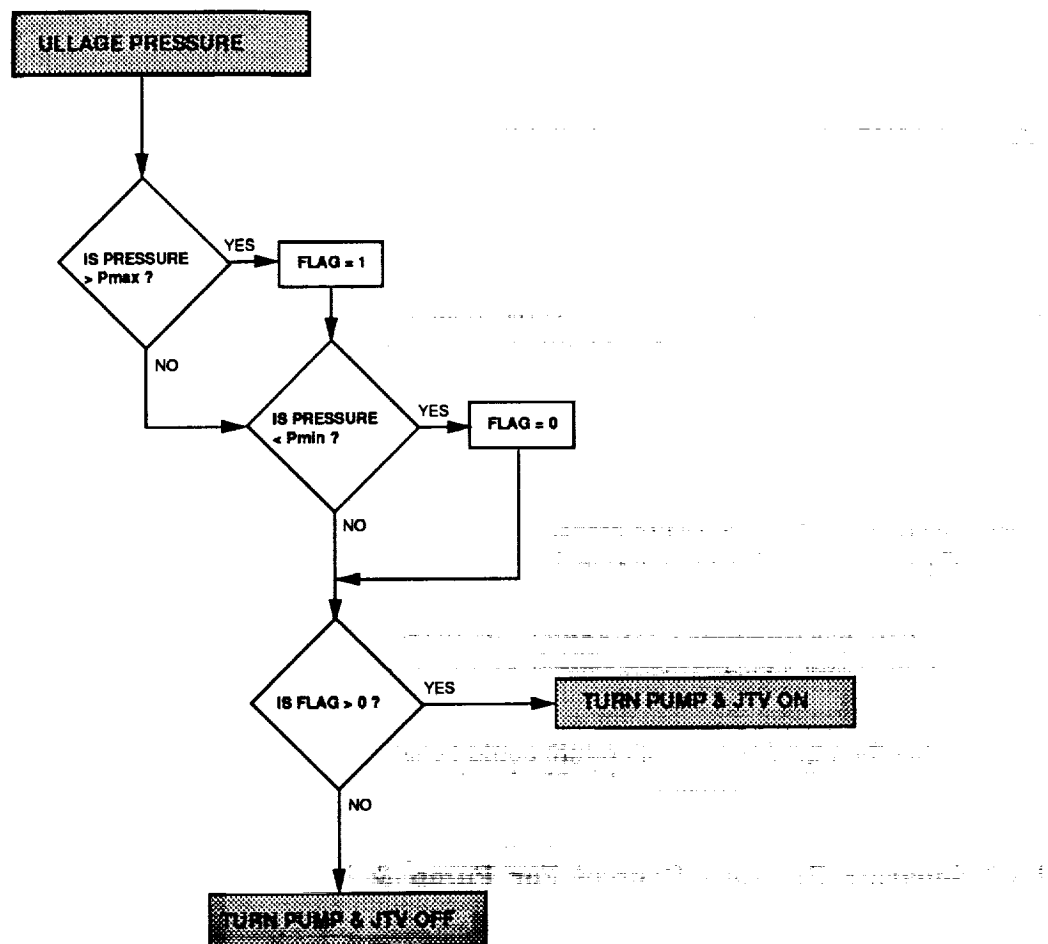


Figure 31 Zero g thermodynamic vent system option 1 controller logic

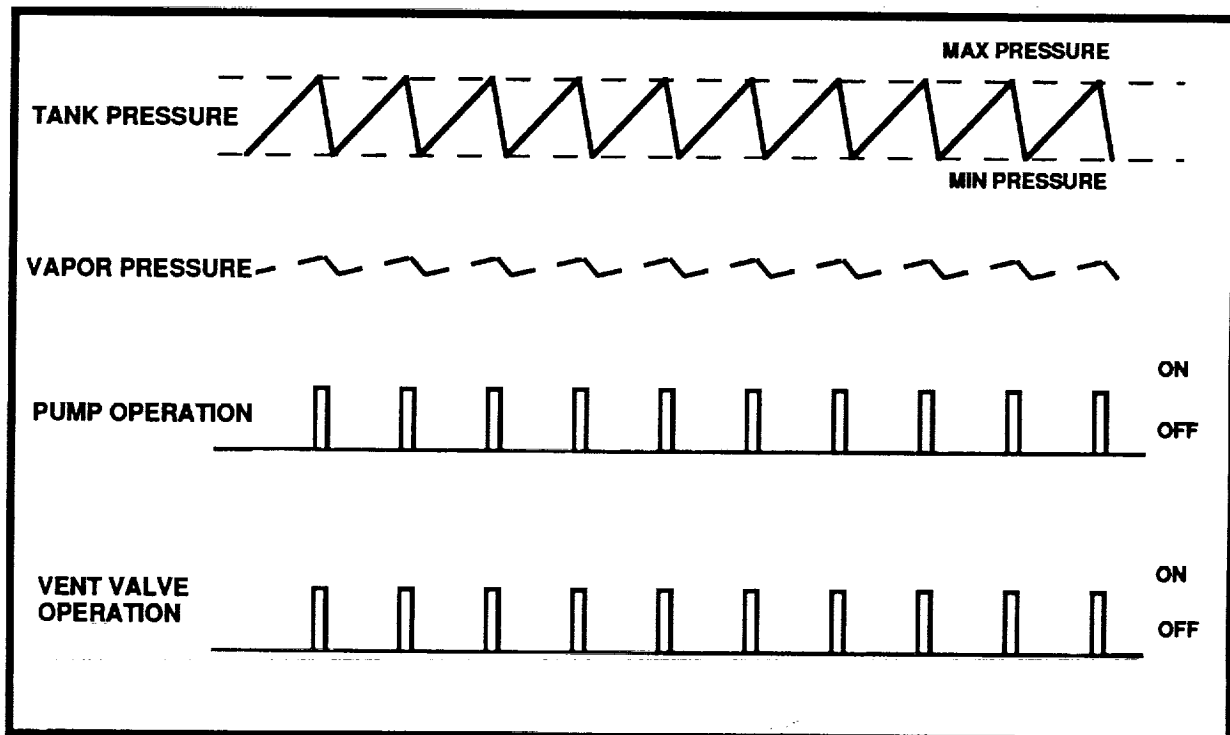


Figure 32 Option 1 control concept

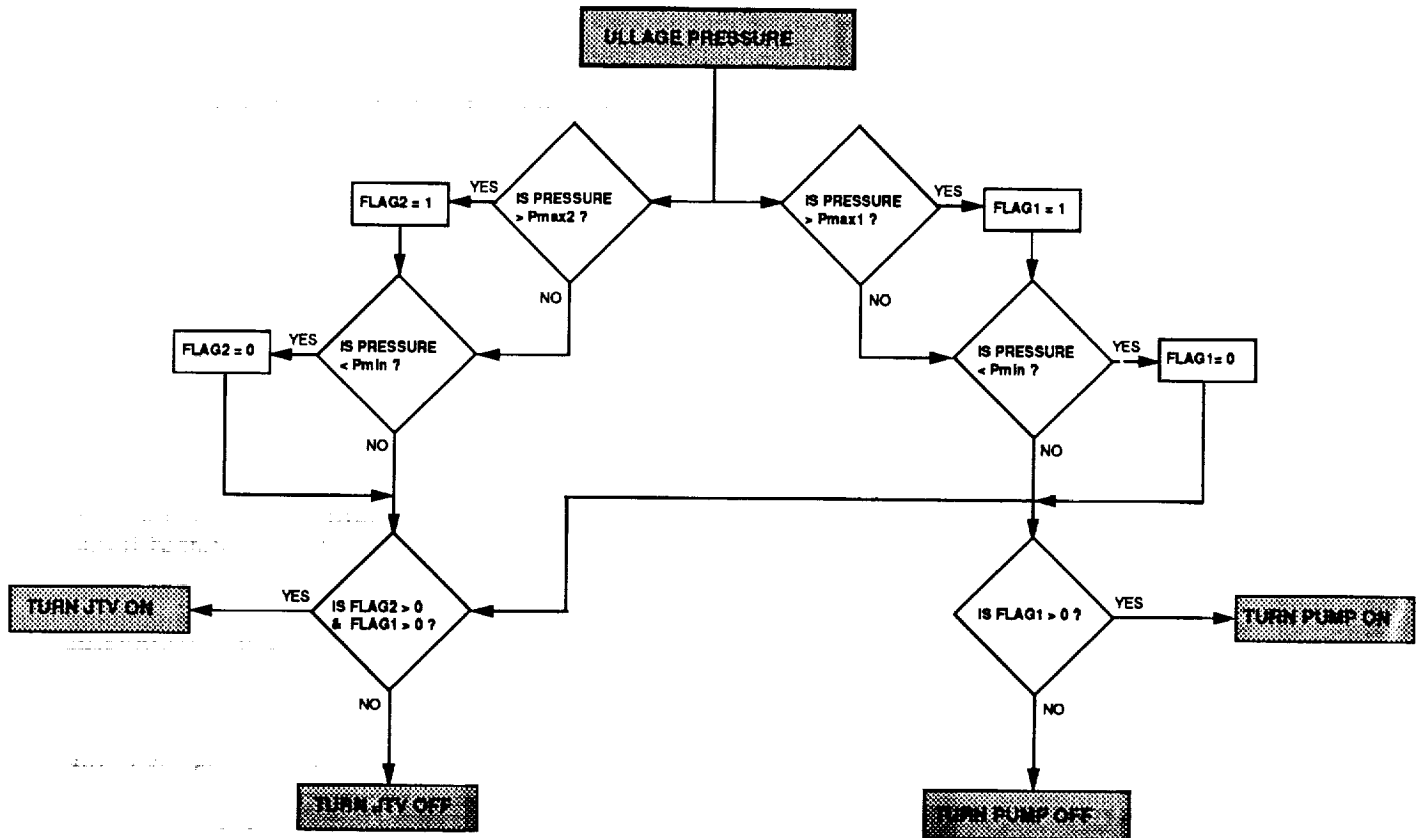


Figure 33 Zero g thermodynamic vent system option 2 controller logic

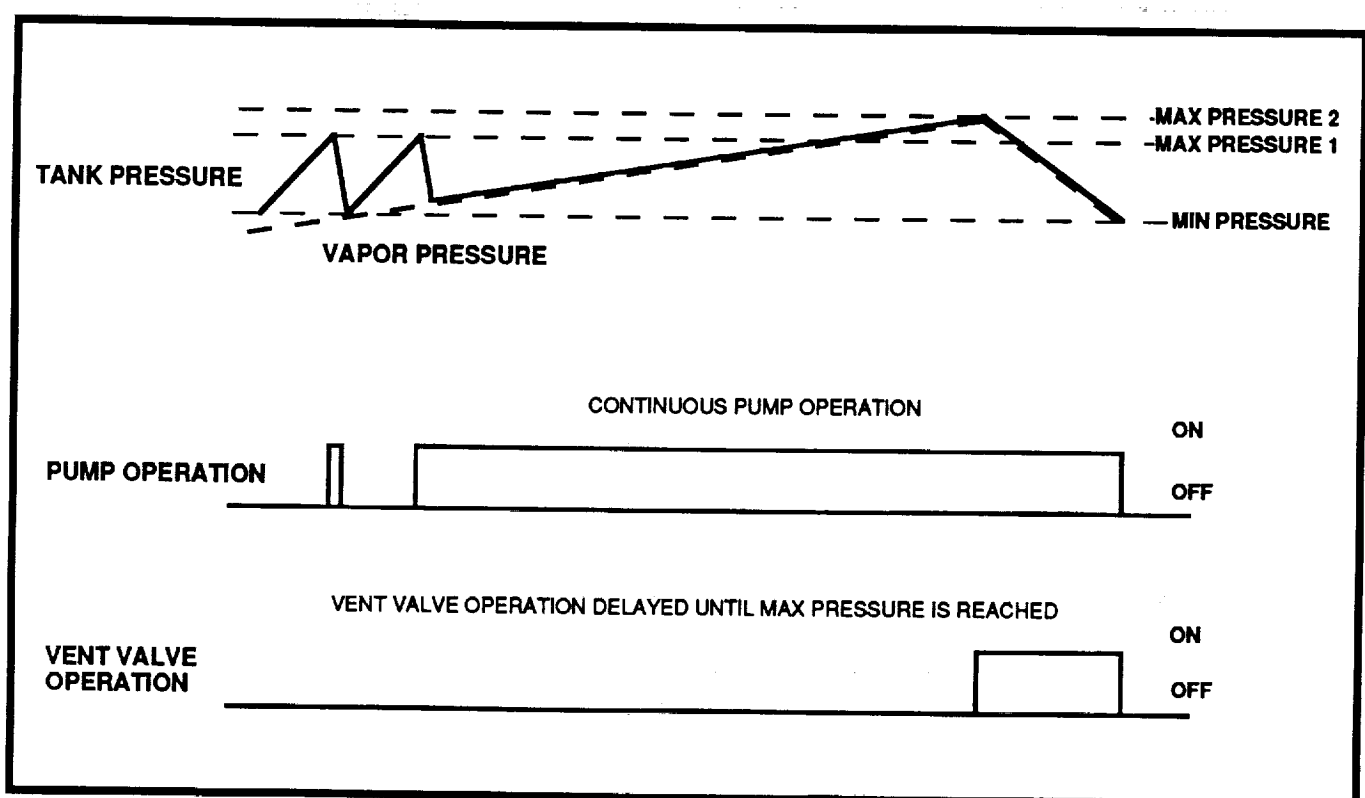


Figure 34 Option 2 control concept

3.3.3 Use Of Pressure & Temperature Measurement To Control Pump & Vent Valve (Option 3)

In order to minimize the vent valve operation and venting losses the recirculation pump and vent valve are operated through separate logic paths, as shown in Figure 35. Since the tank pressure measurement cannot be used by itself to efficiently control both the pump and vent valve, as discussed above, a liquid temperature measurement is used in addition to the tank ullage pressure measurement in Option 3. The recirculation pump is still controlled by the tank pressure transducer. The pump is turned "ON" when the tank pressure reaches the maximum pressure limit, and turned "OFF" when the tank pressure drops below the minimum pressure limit. The vent valve is controlled by inputs from both the tank pressure and pump inlet temperature measurements. The pump temperature data is used to define the liquid vapor pressure. (A third order equation is provided that can be used to calculate the vapor pressure from the temperature measurement. The error is less than 0.1 psi.). The calculated vapor pressure is then compared to the measured tank pressure to determine the fluid state at the pump inlet. If the calculated liquid vapor pressure is greater than the measured tank ullage pressure, then vapor is present at the pump inlet. Therefore, the vent valve will be opened to reject the vapor if the recirculation pump is already operating. This vent valve control mode results in venting only when the pump contains vapor, or when the liquid vapor pressure is at the maximum allowable level (P_{min}). Figure 36 presents the expected pump and vent valve operating histories.

Because the venting cycles are minimized with Option 3, tank pressure control through recirculation may result initially from days to weeks (depending on insulation performance) with potentially no venting losses. Also, because the pump is purged if vapor is present, no LAD is required to insure efficient TVS operation.

The slight disadvantage of Option 3 is that both a temperature and pressure measurement are required, and a computation has to be performed to convert the liquid temperature to a vapor pressure. The performance benefit of Option 3 controller logic (flexibility, and minimum venting losses) more than outweigh the additional controller complexity. Therefore, Option 3 was selected as the baseline TVS controller logic configuration. (The advantages and disadvantages of the three controller options are summarized in Figure 37).

3.4 TVS Instrumentation Requirements

The purpose of the TVS instrumentation is to provide input to the controller, and to define the TVS performance characteristics. The TVS instrumentation list that will be installed on the TVS hardware is presented in Table 1. (Other instrumentation that will be added by MSFC on the component box, LH₂ storage tank, downstream of the back pressure orifice, vacuum chamber, etc.. are not included). The instrumentation and location on the TVS is presented in Figure 38. Based on the controller logic (Option 3) discussed above, the controller input requires a tank ullage pressure measurement and a liquid temperature measurement. Two tank pressure measurements will be provided by MSFC for redundancy. The temperature measurement to activate the vent valve will include the pump inlet temperature measurement (primary), pump discharge (secondary) and tank bulk liquid temperature (back-up).

The TVS performance characterization includes definition of the vent flowrate, heat exchanger performance, and recirculation spray injection flowrate. The vent flowrate is determined from choke flow calculations based on the calibrated back pressure orifice CdA, inlet pressure, and temperature measurement. One pressure transducer is furnished upstream of the back pressure orifice, while there are three temperatures provided; two upstream and one downstream of the back pressure orifice. The additional temperature measurements are for redundancy and also used to define the heat exchanger performance.

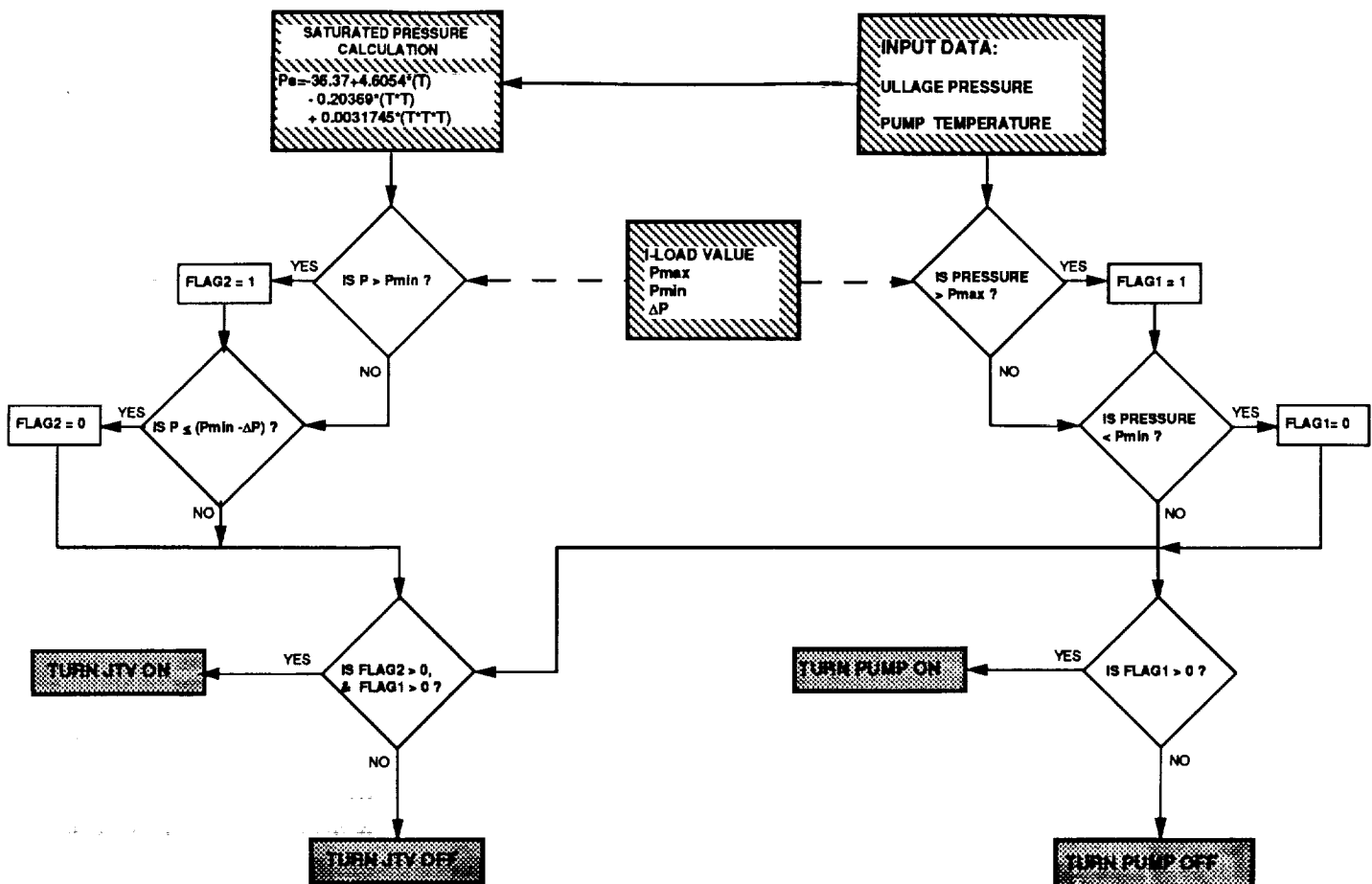


Figure 35 Zero g thermodynamic vent system option 3 controller logic

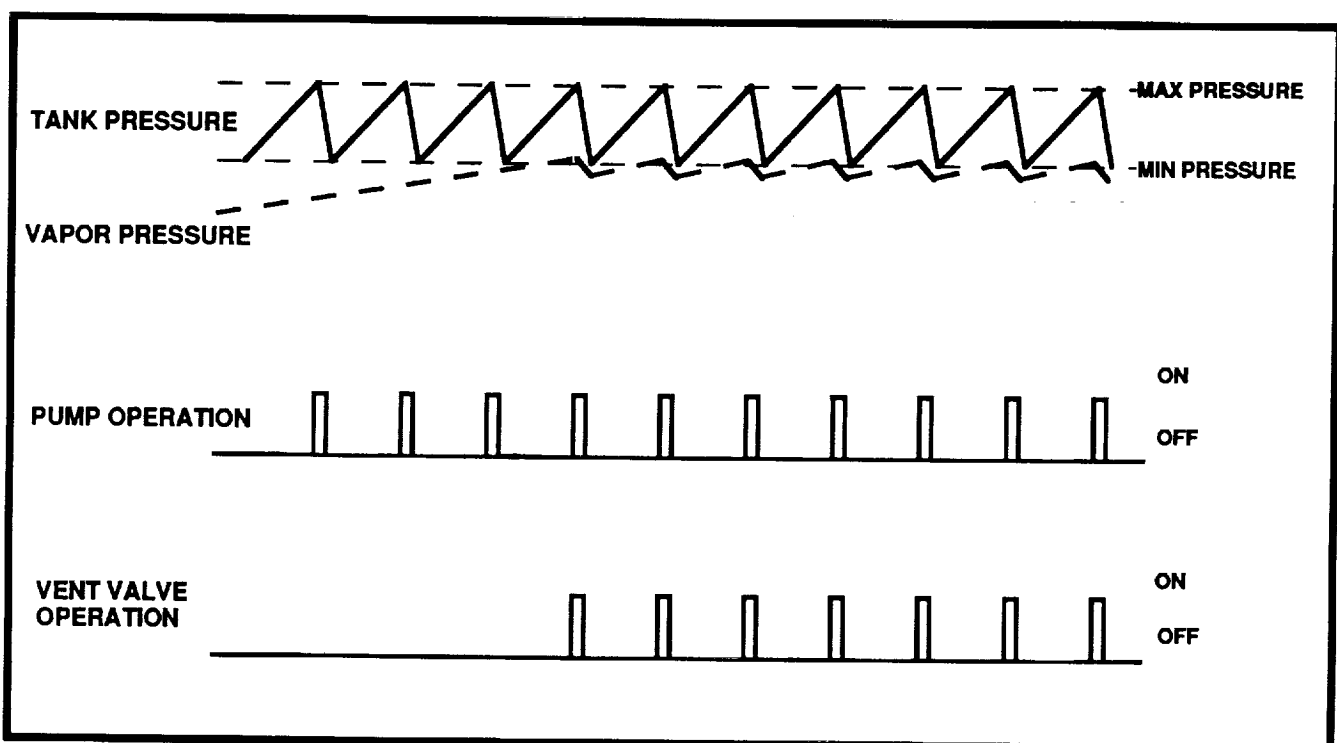
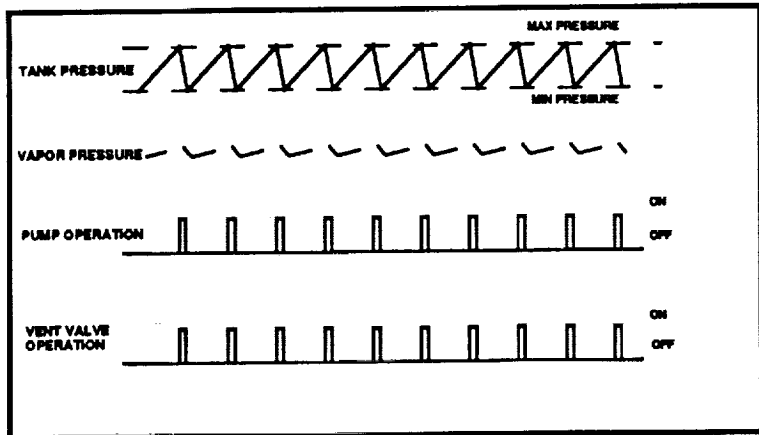


Figure 36 Option 3 control concept



OPTION 1 CONTROL CONCEPT

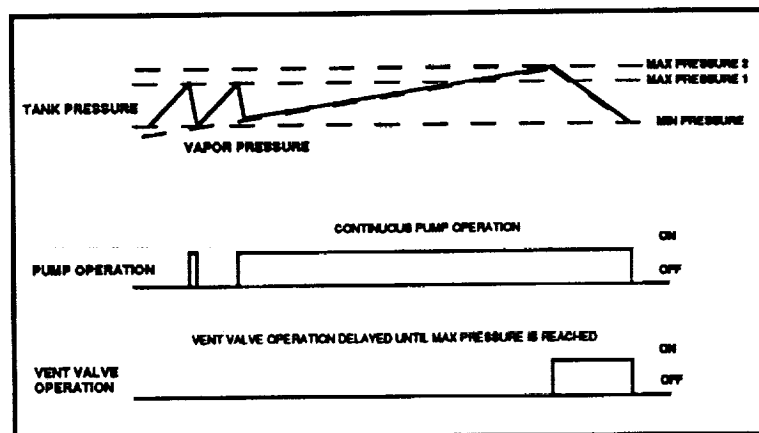
ADVANTAGES

- SIMPLE LOGIC
- PUMP IS PRIMED DURING PUMP OPERATION
- NO LAD REQUIRED FOR PRESSURE CONTROL

DISADVANTAGES

- INEFFICIENT TV8 VENTING OPERATION (HIGH VENTING LOSSES)
- LOSS OF LIQUID TEMPERATURE CONTROL (LOW TEMPERATURE)

NOT RECOMMENDED



OPTION 2 CONTROL CONCEPT

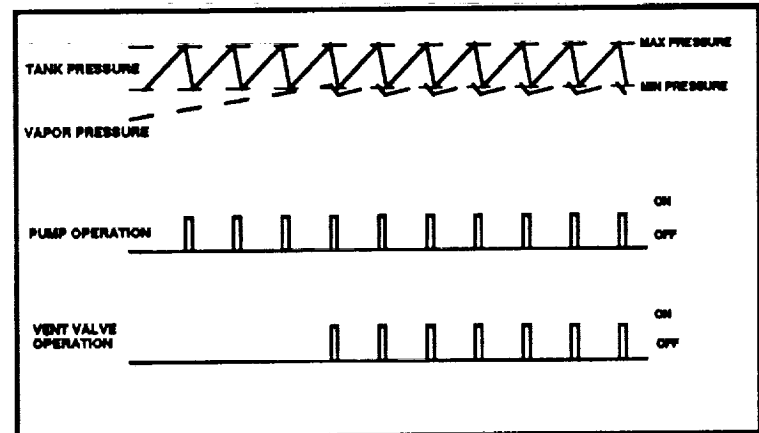
ADVANTAGES

- SIMPLE (RELATIVELY MORE COMPLEX THAN OPTION 1 LOGIC)
- PUMP CAN BE OPERATED SEPARATELY FROM VENT VALVE

DISADVANTAGES

- LONG RECIRC PUMP OPERATION (PUMP LIFE & LIQUID HEATING ISSUES)
- LAD REQUIRED (INABILITY TO DESTRAFFY ULLAGE GAS IF BUBBLE IS PRESENT AT PUMP INLET)

NOT RECOMMENDED



OPTION 3 CONTROL CONCEPT

ADVANTAGES

- PUMP CAN BE OPERATED SEPARATELY FROM VENT VALVE (MINIMIZES VENTING CYCLES)
- POTENTIALLY NO VENTING REQUIRED FOR SHORT DURATION MISSIONS
- NO LAD REQUIRED FOR PRESSURE CONTROL
- BEST PERFORMANCE (MINIMUM VENTING LOSSES)

DISADVANTAGES

- MORE COMPLEX THAN OPTION 1 OR 2 LOGIC
- REQUIRES TEMPERATURE MEASUREMENT

RECOMMENDED OPTION

Figure 37 Summary of controller concept trade study

The heat exchanger performance estimate is based on the vent flow calculation, discussed above, along with the temperatures measurements at the inlet and outlet of the vent side of the heat exchanger. The heat exchanger inlet temperature, along with the pump discharge, and vent valve inlet pressure, are used to define the heat exchanger inlet fluid two-phase quality, and total enthalpy. The change in inlet to outlet enthalpy times the vent flowrate level will be used to define the heat exchanger performance and the total heat rejection rate from the storage tank.

To define the spray injection flowrate a turbine flowmeter has been provided at the inlet to the heat exchanger. The flowmeter has been calibrated at Rockwell Downey with the inlet and outlet line simulated to increase measurement accuracy. The recirculation flowrate can also be estimated indirectly using the pump speed indication and pump delta pressure measurement. The spray injection temperature exiting the heat exchanger is measured through the use of two silicone diode transducers located at the inlet to the 4 spray tubes. This temperature measurement can be used in the tank thermodynamic reconstruction analysis to update the liquid spray heat transfer characteristics.

Temperature and pressure measurement inside the component box are also available to record the environment, and to detect potential component leakages. The complete Zero g TVS instrumentation list is summarized in Table 1, including measurement type, range, accuracy, and number of pins required to access the data.

4.0 Hardware Selection

Following definition of hardware design requirements a search of available components from existing NASA and industry inventories was made. The objective of this search was to minimize the total cost and schedule associated with designing the TVS hardware. Three areas were investigated; liquid hydrogen compatible recirculation pump, vent valve, and instrumentation.

4.1 Liquid Hydrogen Pump Selection

The recirculation pump design requirement identified in the design definition resulted in a 0.3 lb/sec (30 GPM) nominal flowrate, with a pressure rise between 0.4 psid to 0.6 psid (full and empty tank). Because the TVS must operate with saturated liquid the minimum net positive suction pressure (NPSP) requirement is zero psi. After extensive search of the Rockwell, and NASA inventories, and consulting with industry (total of 13 companies across the country were contacted) it was determined that no off-the-shelf liquid hydrogen pump was available per the TVS specifications. Consequently, a pump procurement process was initiated. Only two companies responded with a technical proposal, Allied-Signal Aerospace (Airesearch) company in Torrance California , and Barber Nichols Inc. located in Arvada, Colorado. The Barber Nichols Inc proposal was selected. Pump contract was awarded in June 1993, with hardware delivered in November of 1993, or in approximately 6 months. The liquid hydrogen pump design, shown in Figure 39, is based on a previous design by Barber Nichols used to pump slush hydrogen. The performance characteristics of the centrifugal pump is shown in Figure 40, and compared to the predicted value. The electric motor which powers the pump, via a variable frequency drive (VFD), is submerged and cooled with liquid hydrogen. The power requirement of the pump ranges from 20 watt at minimum flow (20 GPM) to 70 watt at maximum flow (40 GPM).

4.2 Vent Valve Selection

A number of valves were identified in the NASA inventory that are liquid hydrogen compatible. The list of potential candidates are summarized in Table 2. To determine the feasibility of these units a two-phase flow and pressure drop analysis was performed to determine the flow capacity of the valves. Figure 41 summarizes the flow capacity of the individual valves. Although all of the valves satisfied the design goal flowrate of 0.005 lb/sec at 20 psia inlet pressure, valve MC284-

ID	DESCRIPTION	INSTRUMENT	RANGE	ACCURACY	NO. PINS
TV1A	TEMP UPSTREAM OF BACK PRESSURE ORIFICE	SILICON DIODE PROBE	25 - 50 R	+/- 0.5 R	4 (DC)
TV1B	TEMP UPSTREAM OF BACK PRESSURE ORIFICE	SILICON DIODE PROBE	25 - 50 R	+/- 0.5 R	4 (DC)
PV1A	PRESS UPSTREAM OF BACK PRESSURE ORIFICE	KELLER PSI TRANSDUCER	0 - 10 PSIA	+/- 0.1 PSIA	4 (DC)
TP1A	TEMP PUMP INLET	TYPE "E" THERMO COUPLE	25 - 50 R	+/- 0.5 R	2 (TC)
TP2A	TEMP PUMP DISCHARGE	TYPE "E" THERMO COUPLE	25 - 50 R	+/- 0.5 R	2 (TC)
TJT1A	TEMP AT FLOW CONTROL ORIFICE INLET	TYPE "E" THERMO COUPLE	25 - 50 R	+/- 0.5 R	2 (TC)
TJT2B	TEMP AT FLOW CONTROL ORIFICE OUTLET	TYPE "E" THERMO COUPLE	25 - 50 R	+/- 0.5 R	2 (TC)
TJT2A	TEMP AT FLOW CONTROL ORIFICE OUTLET	TYPE "E" THERMO COUPLE	25 - 50 R	+/- 0.5 R	2 (TC)
PP1A	PRESS PUMP INLET	KELLER PSI TRANSDUCER	0 - 50 PSIA	+/- 0.5 PSIA	4 (DC)
DPP	DELTA PRESS OF PUMP	KELLER PSI TRANSDUCER	0 - 5 PSIA	+/- 0.1 PSIA	4 (DC)
PJT1A	PRESS AT FLOW CONTROL ORIFICE INLET	KELLER PSI TRANSDUCER	0 - 50 PSIA	+/- 0.5 PSIA	4 (DC)
PJT2A	PRESS AT FLOW CONTROL ORIFICE OUTLET	KELLER PSI TRANSDUCER	0 - 50 PSIA	+/- 0.5 PSIA	4 (DC)
PS1A	PRESS SPRAY INJECTION INLET	KELLER PSI TRANSDUCER	0 - 50 PSIA	+/- 0.5 PSIA	4 (DC)
TS1A	TEMP SPRAY INJECTION TUBE	SILICON DIODE PROBE	25 - 50 R	+/- 0.5 R	4 (DC)
TS1B	TEMP SPRAY INJECTION TUBE	SILICON DIODE PROBE	25 - 50 R	+/- 0.5 R	4 (DC)
MIXFM	RECIRCULATION FLOW RATE	TURBINE FLOWMETER	15 - 150 GPM	CAL. CURVE	2 (DC)

(NOTE: INSTRUMENTATION ON COMPONENT BOX, DOWNSTREAM OF BACK PRESSURE ORIFICE,
VACUUM CHAMBER, FACILITY, ETC... NOT INCLUDED)

Table 1 Zero g TVS instrumentation list (Installed on TVS hardware)

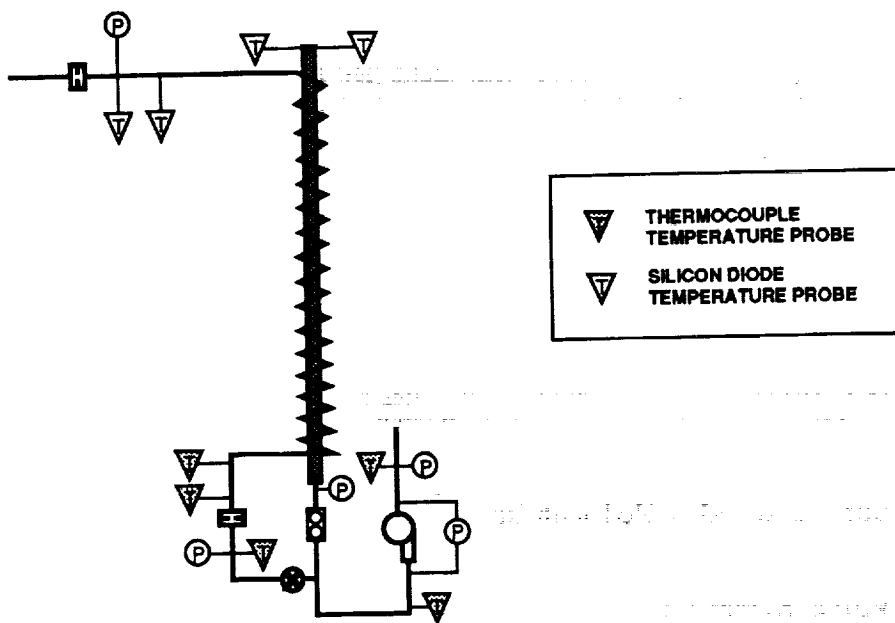


Figure 38 Zero g TVS instrumentation schematic

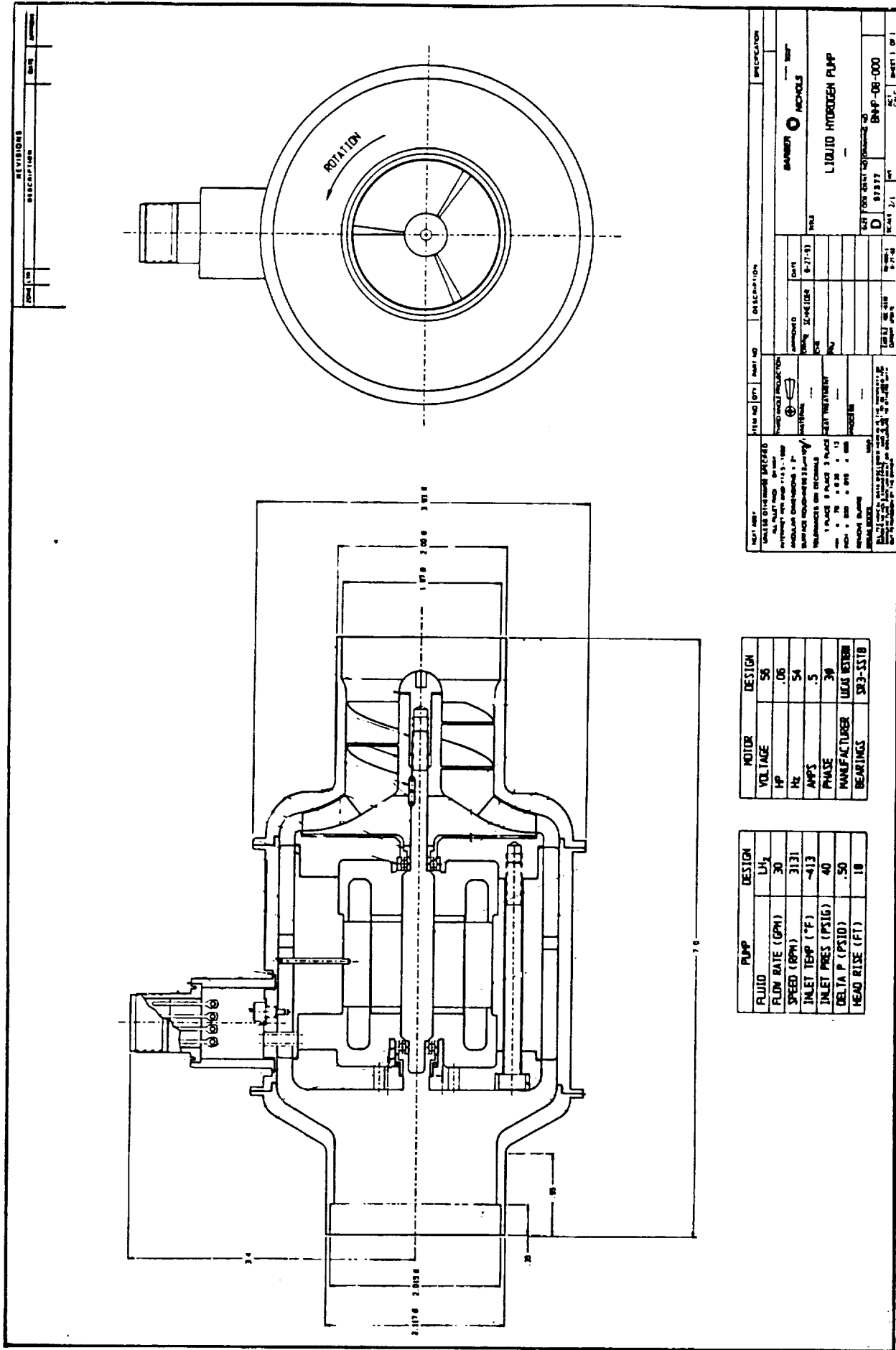


Figure 39 LH₂ recirculation pump design (Barber-Nichols)

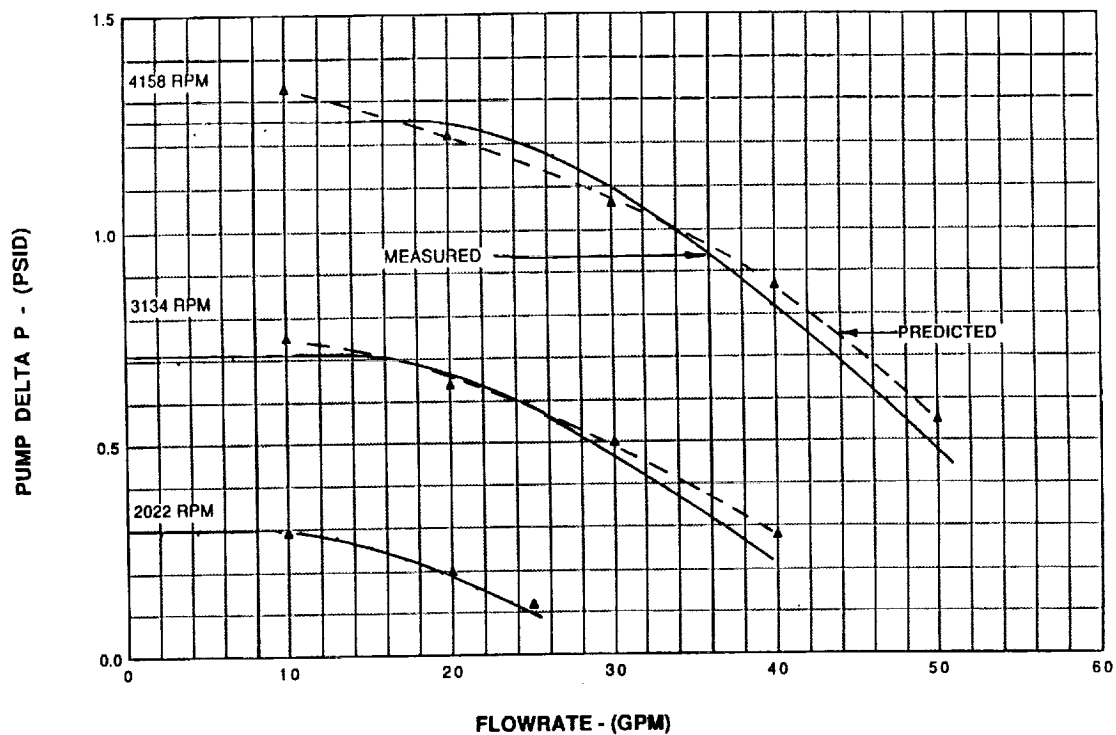


Figure 40 LH2 recirculation pump predicted and measured performance

RI P/N	PRESSURE LOSS* DELTA P (PSID)	FLOW (LB/HR)	ORIFICE DIA (INCHES)	MAX. FLOW ** FLOW (LB/SEC)	COMMENTS
MC284-0429-4102	7	10	0.077	0.0047	0.038 PRSD O2 unidirectional valve Status of valve unknown. Potential refurbishment required. Recommended for TVS spare.
MC284-0429-4110	7	20	0.102	0.0083	0.038 Used in Shuttle PRSD O2 manifold. Extensive refurbishment required.
MC284-0429-4210	3.5	20	0.125	0.0125	0.038 Used in Shuttle PRSD H2 manifold. Status of valve unknown. Potential refurbishment required.
MC284-0429-4220	4	10	0.077	0.0047	0.038 Used in Shuttle Fuel Cell H2 system. Valve condition is good. No refurbishment required. Available for TVS use. NASA approval gained. Recommended for TVS use.

(*): Pressure loss with GN2 at 100 psia inlet & 70 degrees temperature
(**): Inlet condition at 20 psia saturated pressure and temperature.

Table 2 Candidate vent valves for zero g TVS design

0429-4220 (part number 74405-4220, serial number 097906-CRP-0020) was selected because the valve is in good working condition, does not require refurbishing, and resulted in nearly the design flowrate level, without the use of additional downstream orifices. The valve design is presented in Figure 42 is a bi directional electrically actuated solenoid valve. This valve design is currently used in the Space Shuttle supercritical hydrogen power reactant storage distribution (PRSD) system. Consequently, the operating life of this valve is a minimum of 20,000 hours (~ 2 years, and 3 months), which is well in excess of the TVS requirement. The power consumption of this valve is less than 160 watt at 32 VDC. The operating pressure is between 0.01 and 320 psig. The minimum internal flow area is dictated by an internal orifice diameter of 0.077 inches. The vent flow characteristics based on this internal orifice has been defined and is shown in Figure 43, as a function of liquid hydrogen subcooling.

Permission to use the PRSD valve for TVS testing has been attained from NASA. The valve has been cleaned to level 100 on 10/23/91. Acceptance test data and specification has been forwarded to NASA MSFC as part of the Critical Design Review.

5.0 Detailed Design Layout of the TVS

At the completion of performance design definition and hardware selection a detailed design layout of the TVS hardware was made. The design drawings generated were used to manufacture and assemble the TVS elements. The assembly and installation drawings were generated on the Rockwell Anvil 5k CAD system. A total of 28 drawings were generated. The TVS design can be divided into four major assemblies:

- Spray injection/heat exchanger assembly
- Recirculation/vent component assembly
- Component box
- Support ring assembly

5.1 Spray injection/heat exchanger assembly

The function of the spray injection and heat exchanger assembly is to inject the recirculation flow uniformly into the tank ullage and liquid, and to transfer heat from the recirculation flow to the vent flowrate. The assembly, shown in Figure 44, consists of two concentric tubes made of stainless steel material. The outer diameter tube is 1.5 inches OD, with a 0.035 inch wall, while the inner tube is a 1.25 inch OD with a 0.035 inch wall thickness. The overall length of the assembly is 105 inches. The heat transfer area between the liquid flow and the vent flow is 2.9 square feet. The heat transfer area between the vent flow and the tank fluid is 3.1 square feet. Therefore the total area available for the vent flow is ~ 6 square feet.

The axial spray injection design consists of four 0.5 inch tubes manifolded together at the heat exchanger outlet. Each tube contains 43 orifices equally spaced ~ 2.4 inches apart and allow spray injection in four direction. In addition to the orifices in the spray tubes, there are a total of 8 orifices (2 per axis) above the heat exchanger outlet. These 8 orifices were added to increase the degree of ullage gas injection for high liquid levels.

Because the tank supplied 1.25 inch line interface was installed at a 2 degree angle from the vertical, the Rockwell furnished interface flange was modified to off-set the tank line misalignment. Figure 45 presents the modified TVS interface flange. Provision to accept potential misalignment in the 0.5 inch vent line was also provided. The design includes a 2.5 inch loop, shown in Figure 46, to allow correction and alignment during hardware installation.

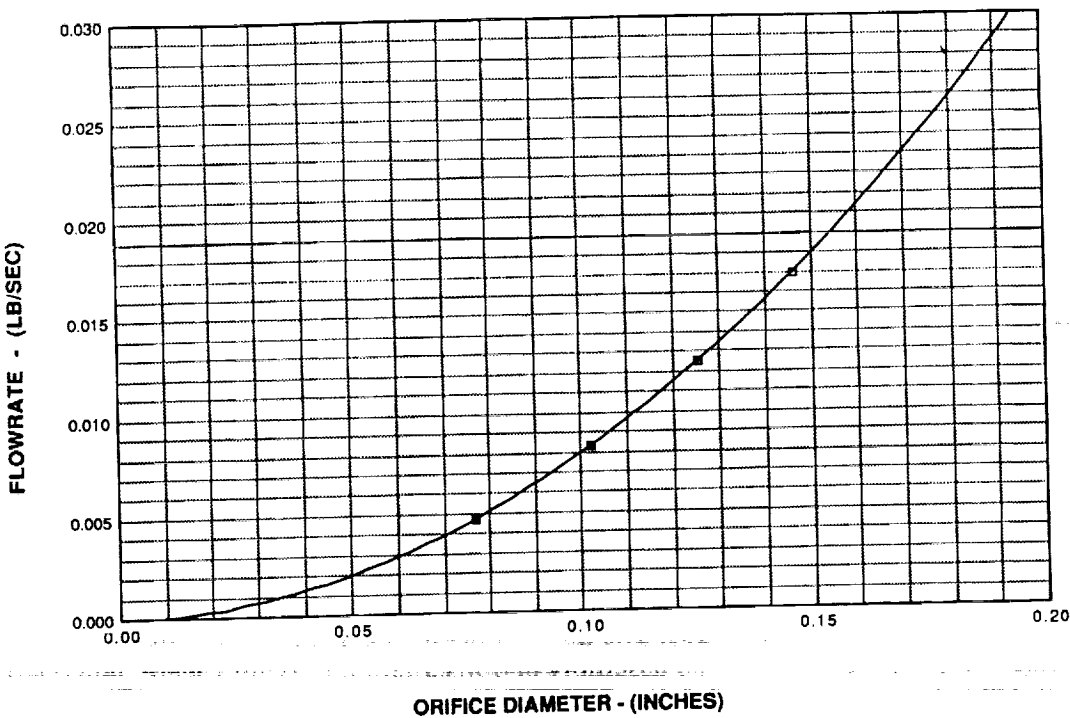


Figure 41 Hydrogen two-phase flow as a function of valve orifice diameter
(20 psia saturated fluid)

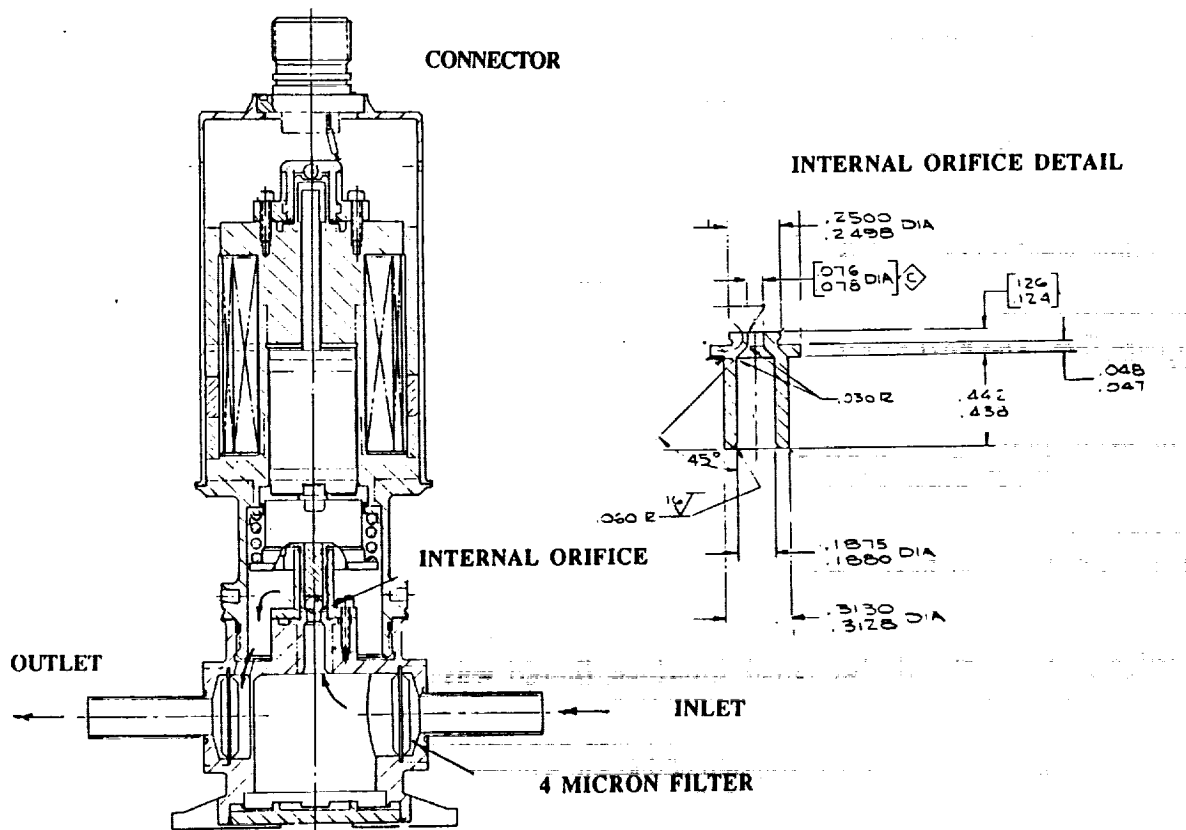


Figure 42 Hydrogen vent valve design

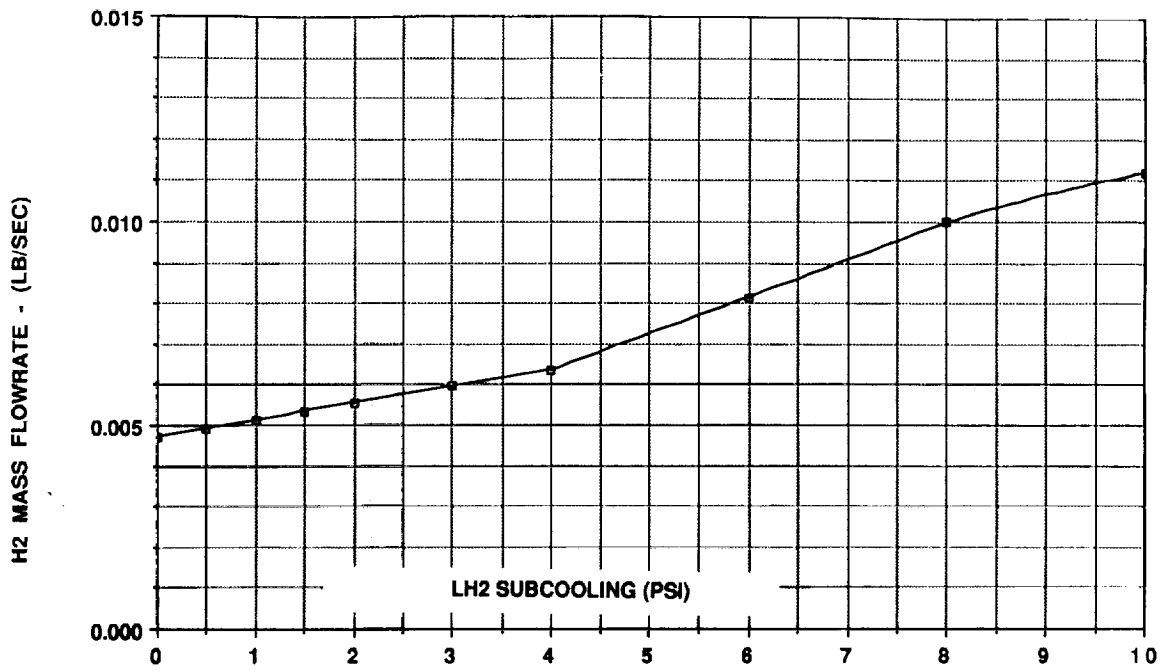


Figure 43 Vent flowrate as a function of liquid subcooling (20 psi vapor pressure)

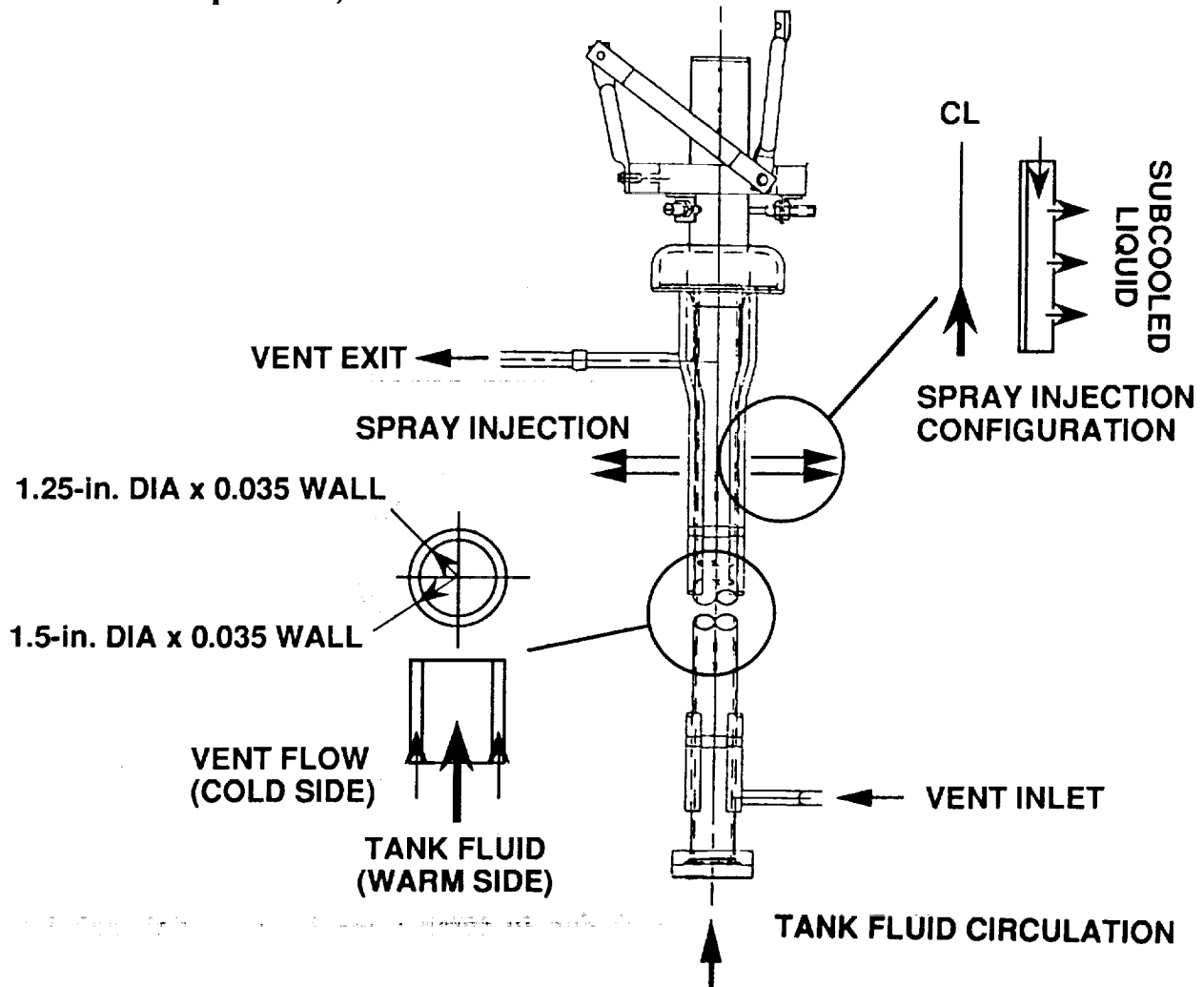


Figure 44 TVS heat exchanger and spray injection system assembly

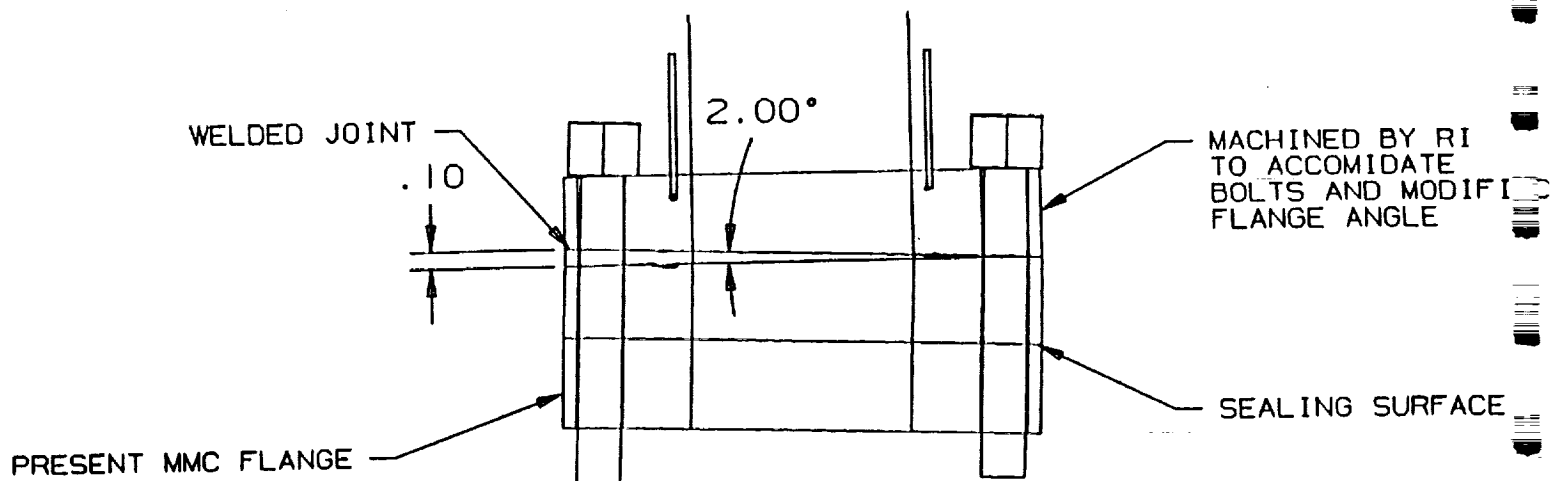


Figure 45 Solution to compensate for MMC tank line misalignment

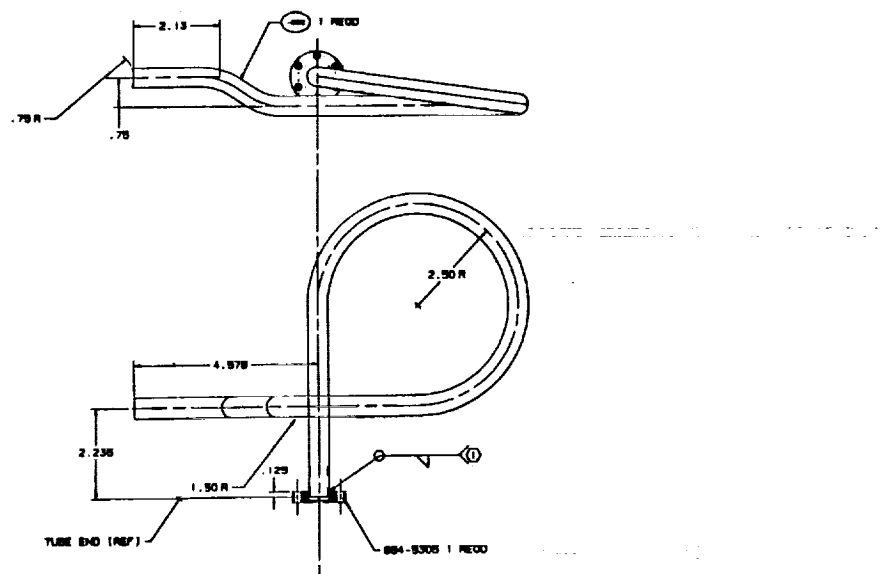


Figure 46 Vent tube design design to compensate for potential tank interface misalignment

5.2 Recirculation & Vent System Assembly

The recirculation and vent system assembly, shown in Figure 47, contains the active components of the TVS design; recirc. pump, vent valve, and turbine flowmeter. As in the spray/heat exchanger assembly, provisions are made for potential misalignment between the tank supplied interface and the TVS lines. The line segments will be trimmed by MSFC to correct for any misalignment. Also provision has been made to add a bellows segment in the 2 inch line downstream of the recirculation pump. A large bend is also provided in the 0.5 inch vent line to correct for tank and TVS vent line alignment.

The present line configuration was a result of the limited space that is available between the tank bottom and the vacuum chamber solar heating panels. The line routing, and diameters were defined to minimize the total recirculation system pressure losses and resultant pump power consumption. Consideration was also made to eliminate potential vapor accumulation in the recirculation pump and line. Consequently, the recirculation pump inlet was raised as close as possible to the tank outlet line.

Instrumentation ports are provided for 5 pressure transducers and 5 thermocouples. Thermocouples were selected over the silicone diode transducers because they are less susceptible to potential magnetic flux generated by the electric motor.

Provisions for a flow reducing orifice, downstream of the vent valve is also provided in support of future sensitivity testing.

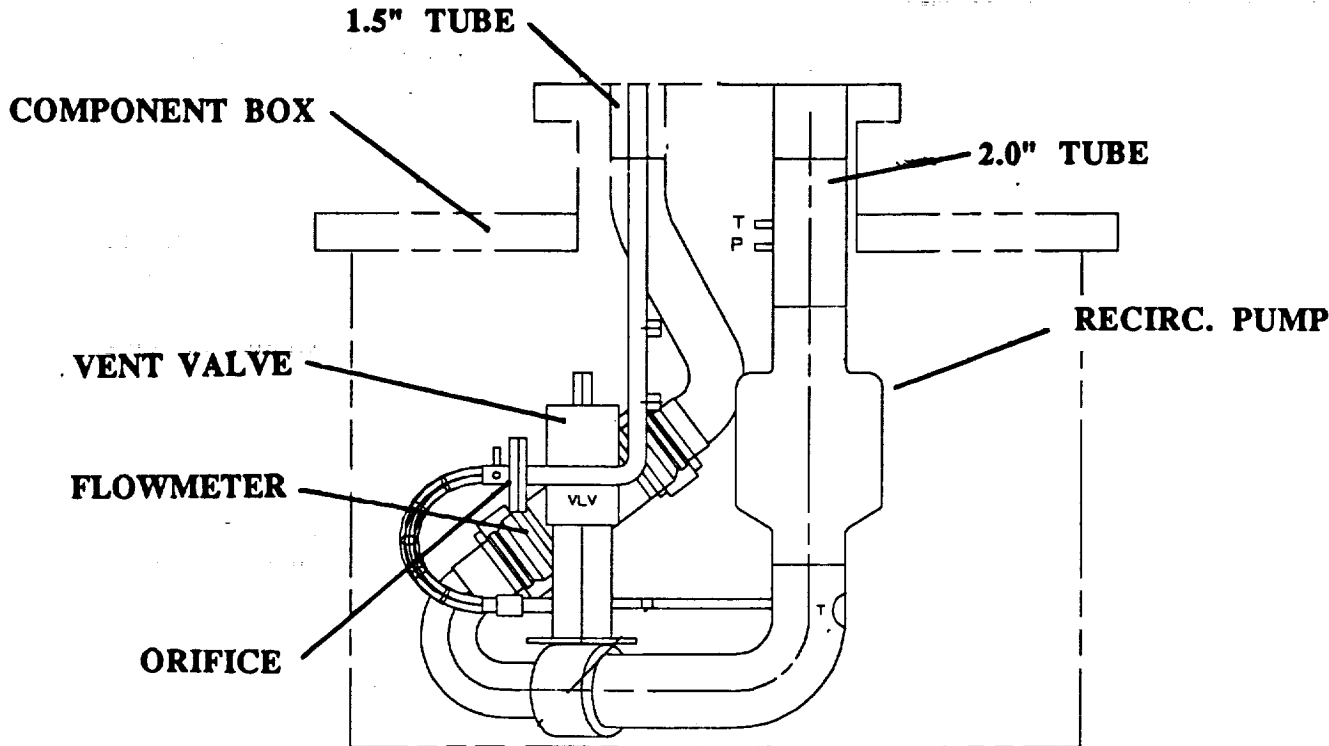


Figure 47 Recirculation pump and vent system assembly

5.3 Component Box Assembly

The function of the component box is to enclose the components, and fluid lines which are outside of the tank, and thereby preventing hydrogen leakage into the vacuum chamber. Leakage is minimized by the use of a Conflat flange and seal between the tank and component box flange (8 in.). Indium wire (1/16") is used between the component box top and bottom sections. All other joints are welded, including the connectors (two Deutsch connectors for pressure, flowmeter, and silicone diode transducers, and two wire pass through for the thermocouples). The component box also has a 1.5 inch vent line which is connected to a facility overboard vent system to relieve pressure in case of internal leakage. The component box will be insulated with foam and MLI by MSFC personnel in order to minimize the environmental heat leakage.

The component box, shown in Figure 48, is a 22 inch diameter by 18 inch cylindrical design. Electrical power connection, AC power for the pump, and DC power for the valve, is routed through the component box vent line. The component box is made out of stainless steel material. The cylindrical wall thickness is 0.125 inches, with the top flange 1.0 inch thick, and bottom plate 0.25 inches. The component box has been designed to withstand 40 psig burst and 15 psig crushing pressure.

5.4. Support Ring Assembly

A support ring assembly, shown in Figure 49, is provided for horizontal support and alignment of the spray injection and heat exchanger assembly at the upper end. The design consists of a support ring with three adjustable set screws, three struts and a strut bracket. The support ring assembly is attached to the three brackets on the top of the tank.

5.5 TVS Stress Analysis Results

All the components in the Zero g TVS have been analyzed for pressure loading of 40 psig maximum operating pressure, 60 psig proof pressure, and 160 psig burst pressure. The majority of the components have large factors of safety for both yield and ultimate stress. Some of the components have been evaluated to be safe by engineering judgement since they are obviously massive and the stresses would be low.

The component box bottom plate has a F.S. (ultimate) of 0.8 for the burst pressure of 160 psig and the component box container top plate has a F.S. (yield of 0.62 for the operating pressure of 40 psig. However, since the box has a large open vent line the pressure inside the component box will be low at all times. The fluid lines in the component box all have F.S. of much greater than 1 for pressure loads.

6.0 Subsystem Testing

Acceptance testing of the TVS hardware was performed to verify the functionality and integrity of the TVS elements prior to delivery, and to update the analytical model based on measured performance parameters. The subsystem tests which were originally planned had to be reduced in order to re-allocate funds to procure the new liquid hydrogen recirculation pump.

6.1 LH₂ recirculation Pump Tests

The hydrogen recirculation pump tests were performed at Barber-Nichols. The tests included definition of the pump head rise vs. flow characteristics as a function of operating speed. The performance tests were conducted with Methanol to simulate the low density of liquid hydrogen. The pump head and flow coefficients were derived from flow and delta p measurements. These coefficients were subsequently used to predict pump performance. Figure 40 presents the results

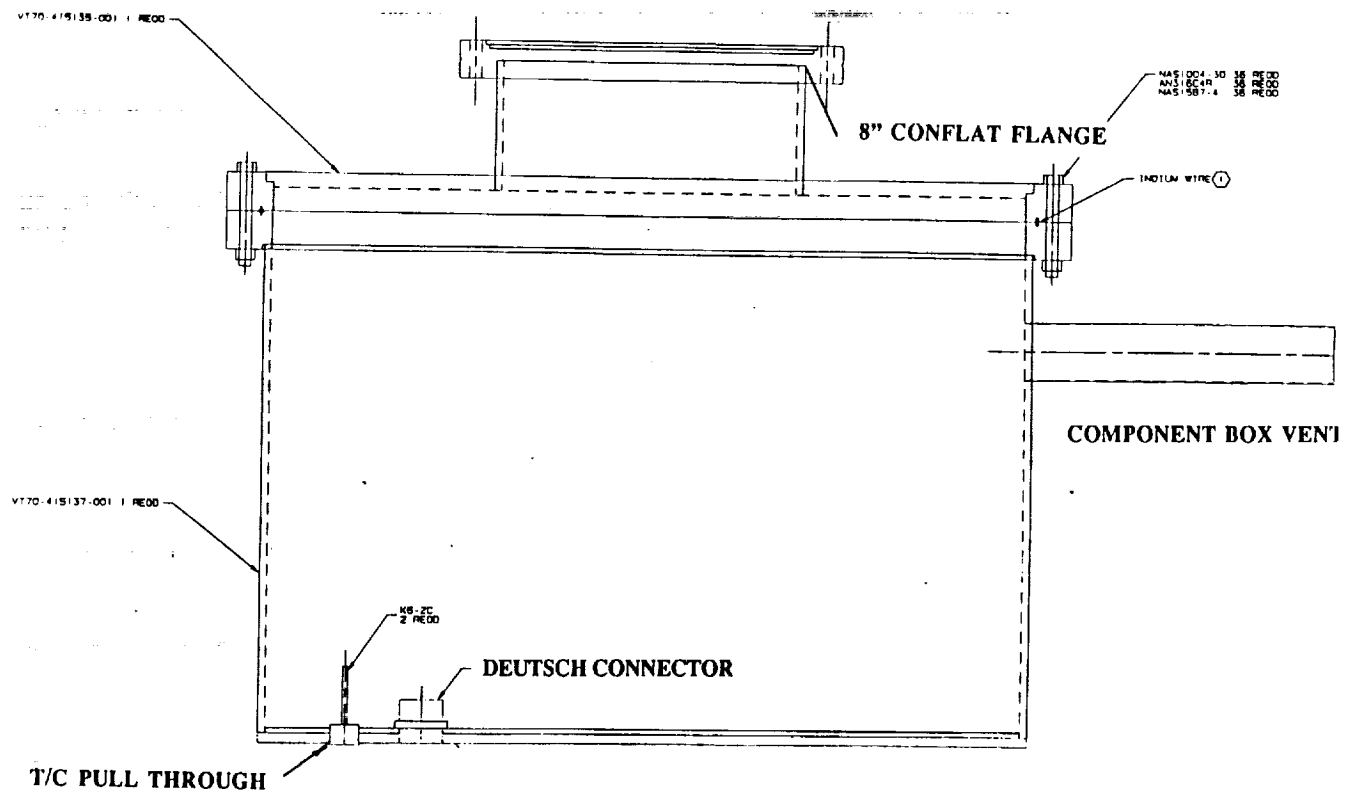


Figure 48 Component box design

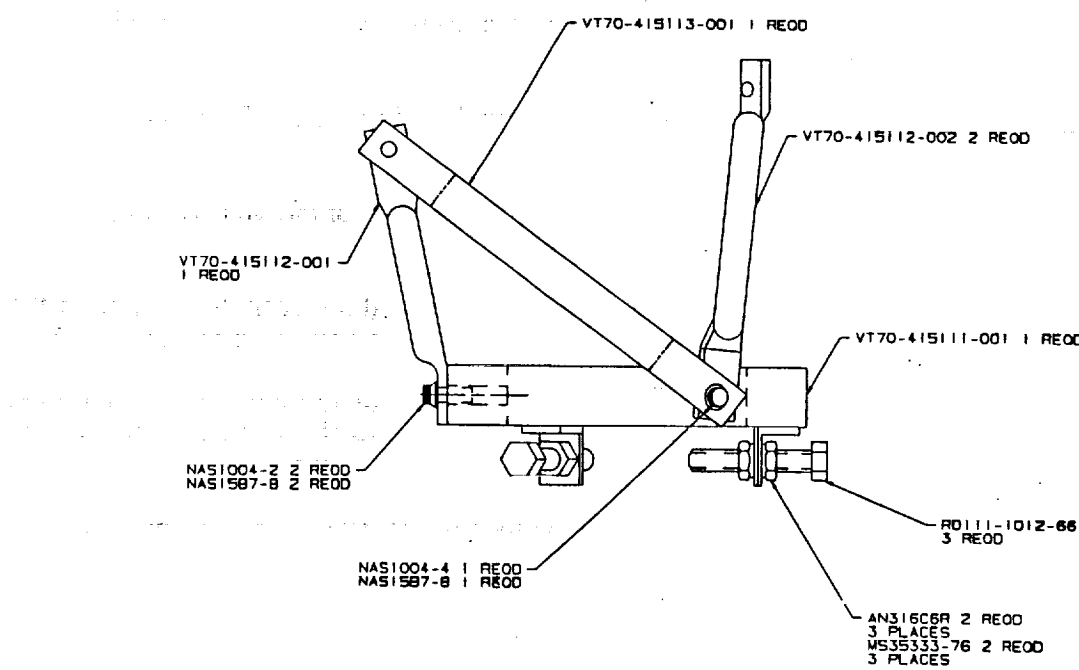


Figure 49 Support Ring Assembly

of the measured performance. As can be seen the pump performance compared very well to the original (proposal) predicted level.

The recirculation pump was also tested in liquid nitrogen at the supplier. The LN2 tests at Barber-Nichols included operating the pump submerged for 5 minutes at reduced speed (1000 to 2000 RPM). The objective of the test was to verify functionality test at cryogenic temperature (electrical continuity, clearance, and fluid pumping). After the pump was received at Rockwell the pump was again submerged in LN2 and spun up to approximately 1000 RPM at ambient temperature (for less than 5 seconds) to insure that no damage had occurred during shipment of the pump.

6.2 TVS Component Testing

The TVS component test were performed at Rockwell Downey. The tests included system pressure drop, flowmeter calibration test, cryogenic shock test with liquid nitrogen, proof pressure, and leakage test with helium

The spray injection tubes were individually flow tested in the horizontal position with water to measure the pressure drop across the spray orifices. A venturi flowmeter measured the flow rate, and a gage pressure measured the inlet pressure to the tube. The test derived pressure loss coefficients were compared to each other in order to verify that the orifices have been properly drilled and de burred. Figure 50 and 51 presents the measure delta pressure and derived loss coefficients as a function of flowrate. The results indicated that the loss coefficients were within 10 percent of each other, insuring that uniform flow will result.

The spray tubes and heat exchanger assembly was also tested vertically with water Figure 52 shows the schematic of the test setup. The pressure drop of the integrated spray bar and liquid heat exchanger was defined, minus the hydrostatic pressure. The total pressure drop was higher than the individual tube pressure losses, as expected, due to the effect of the manifold losses. The results are shown in Figure 53, and compared to the individual spray tube losses. The pressure loss of the total spray tube and heat exchanger (hot side), when compared to the analytical prediction, was generally less than anticipated. (See Figure 54). This lower pressure loss characteristic will result in improved TVS performance both from a spray recirculation effect and power consumption point of view.

Still photos and video tape recordings were also taken in addition to flow and pressure measurements to characterize the external spray penetration, distance and spray angle. The flow tests indicated that the spray penetration was well in excess of 10 ft. Therefor, the TVS spray injection flow will be more than capable of penetrating the ullage mass of the MHTB tank.

The pressure drop test of the cold side of the heat exchanger was also tested. This test was performed in conjunction with the cryogenic shock test using liquid nitrogen. Schematic of the test configuration is shown in Figure 55. Flowing liquid nitrogen was used to chill the heat exchanger and spray injection system. Simultaneously, helium gas was flow through the cold (vent) side of the heat exchanger to measure the pressure drop of the cold side of the heat exchanger. The pressure loss coefficient of the cold side of the heat exchanger was defined from flow and delta pressure measurements. The result was compared to the analytical prediction. The results compared favorably, as shown in Figure 56. The test results indicated slightly higher pressure loss characteristics than anticipated. The reason for the difference is considered to be due to higher heat exchanger entrance and exit losses.

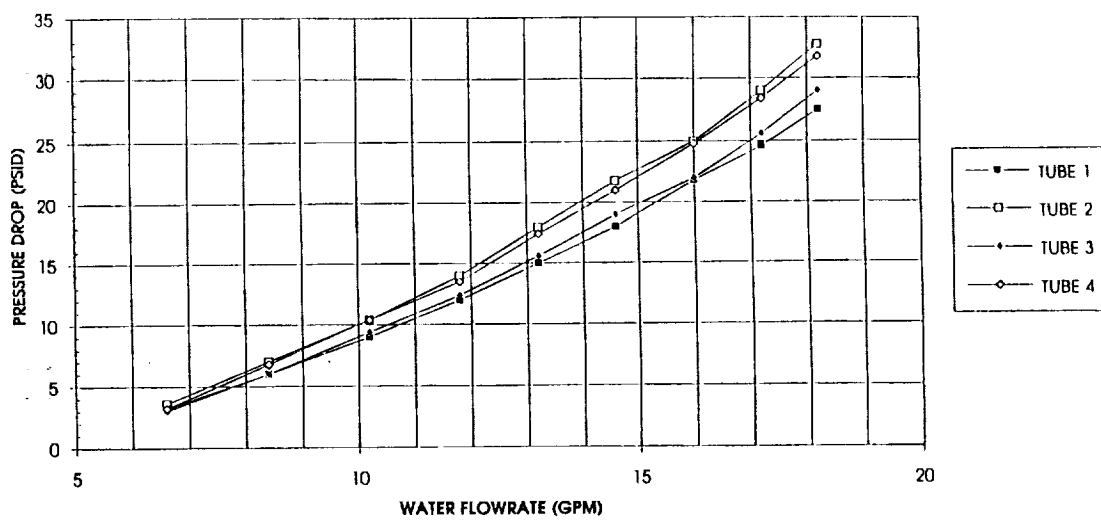


Figure 50 Pressure drop through spray injection tubes (Water flow test results)

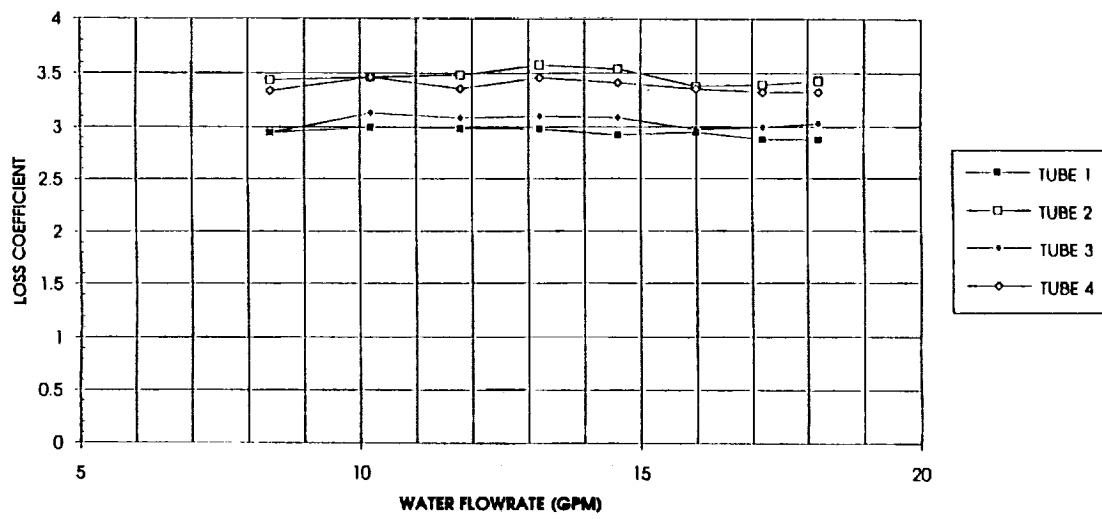


Figure 51 Loss coefficients of spray injection tubes (Water flow test results)

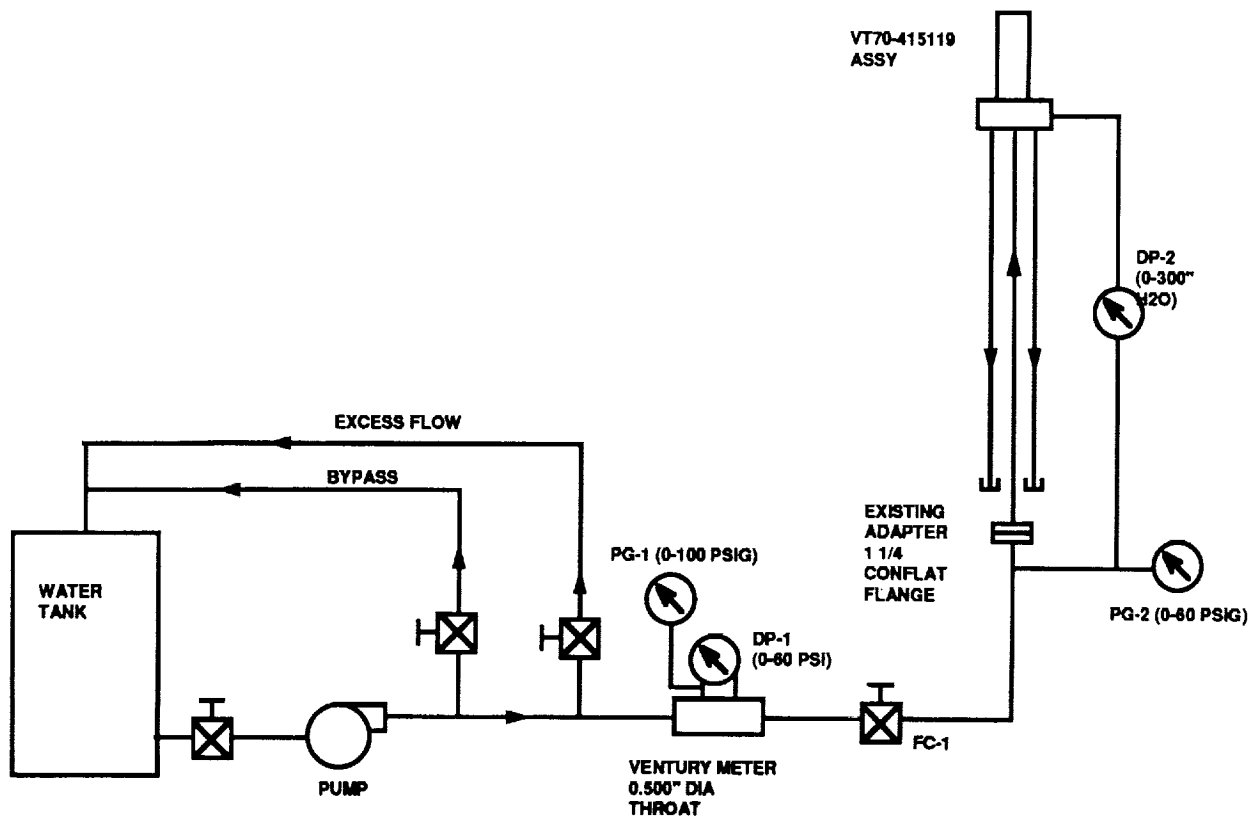


Figure 52 Schematic of Rockwell spray injection water flow test

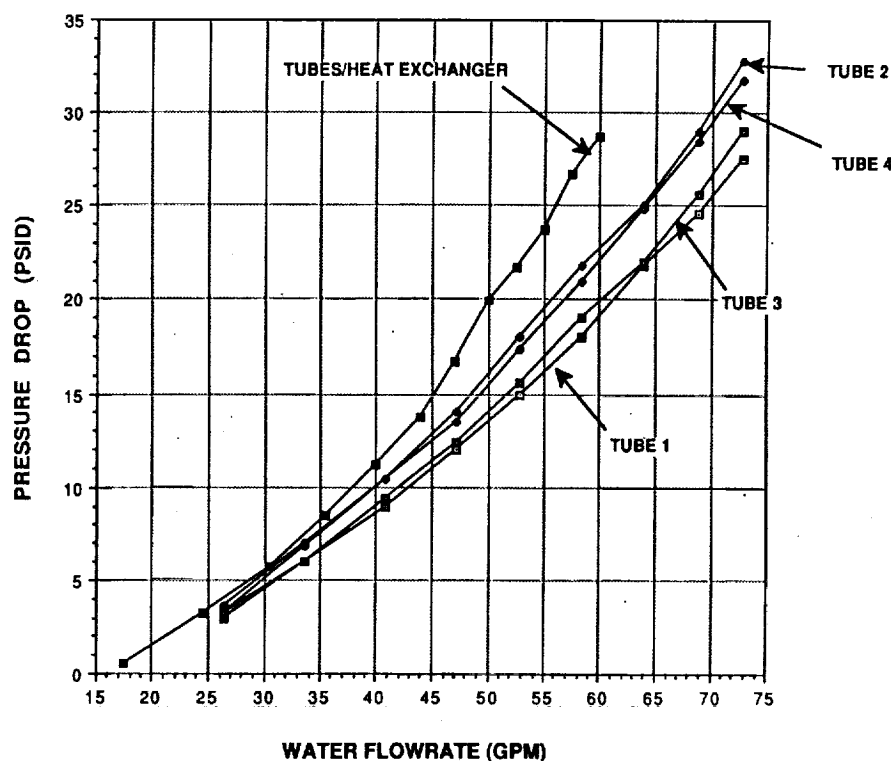


Figure 53 Pressure drop in the spray tubes and heat exchanger assembly (Water flow tests)

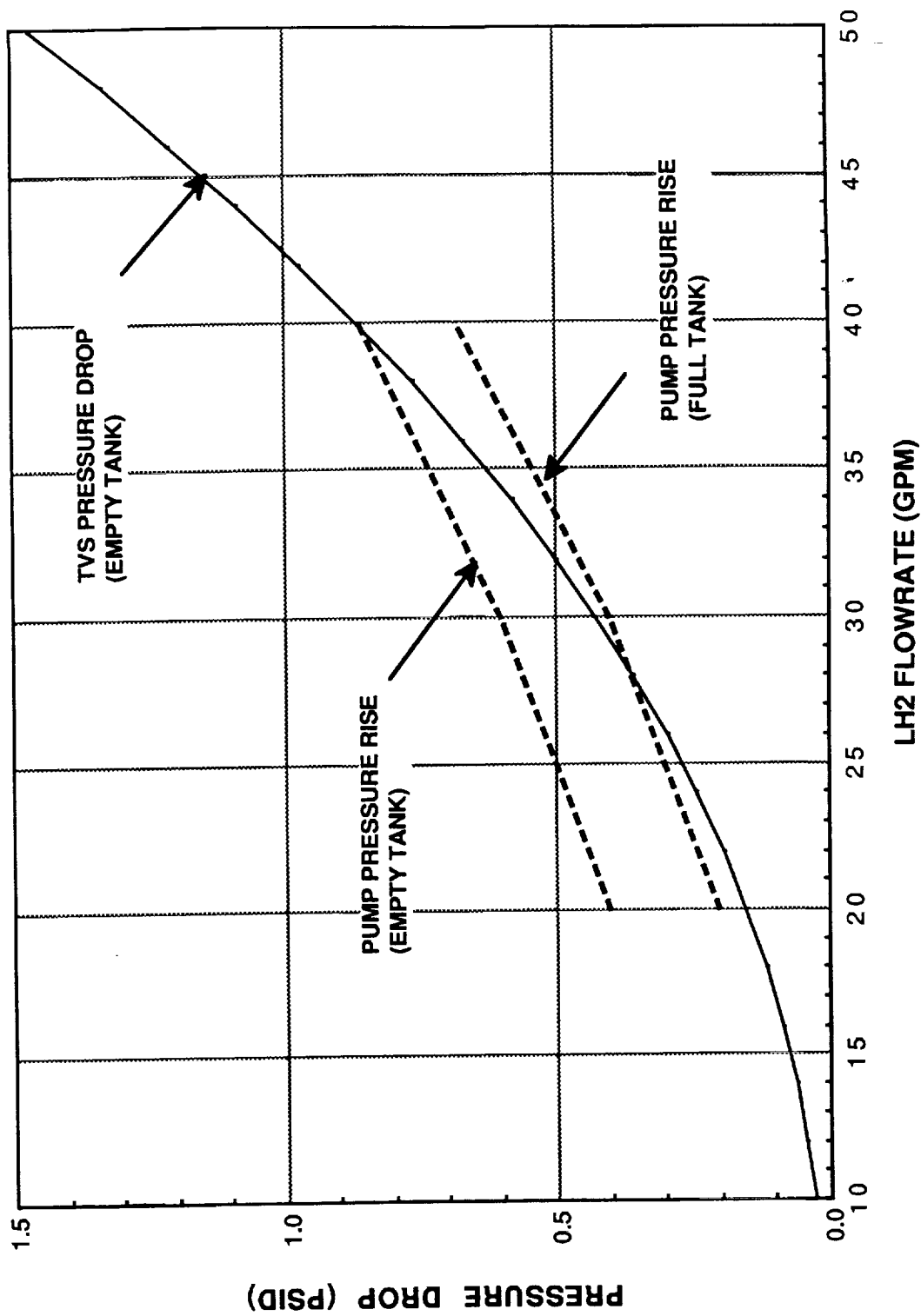


Figure 54 Comparison of predicted and measured spray injection system pressure loss (Water flow test)

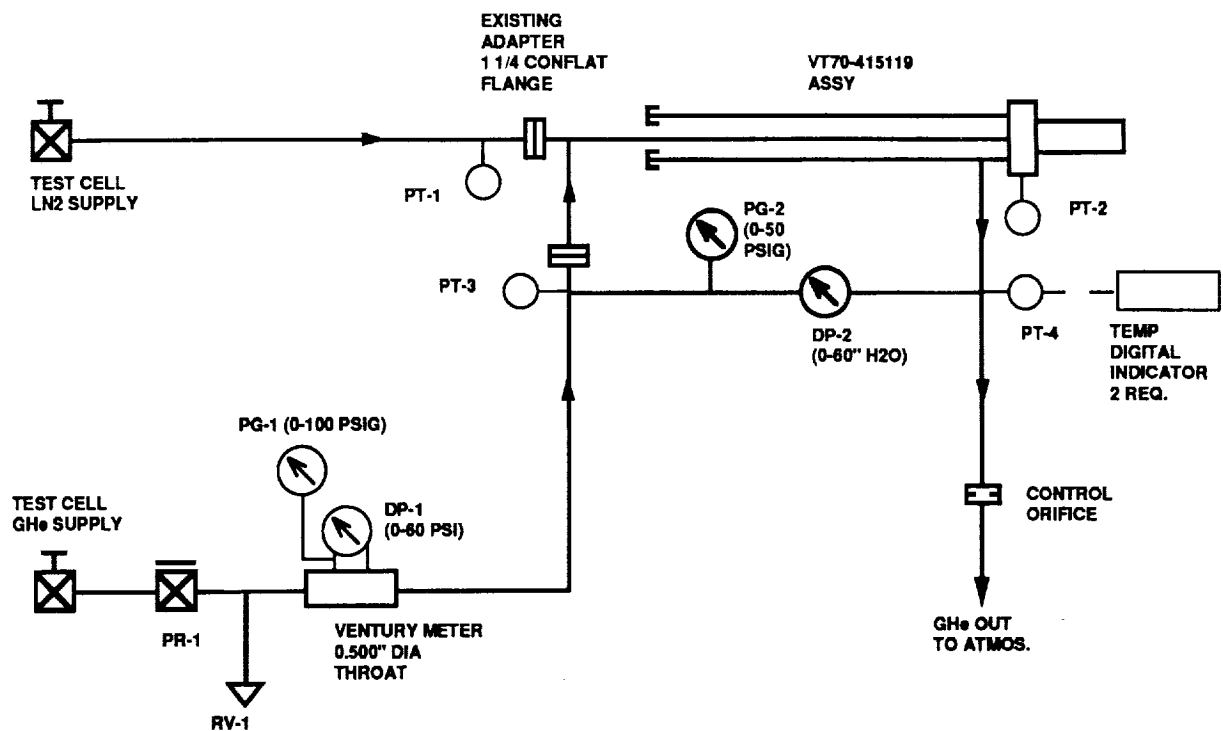


Figure 55 Schematic of Rockwell spray injection liquid nitrogen flow test

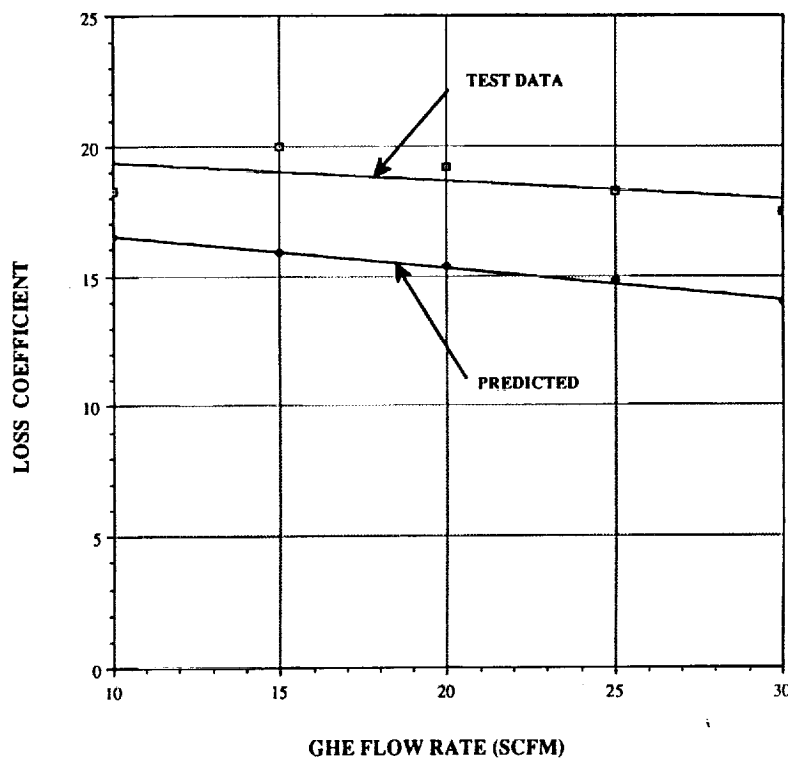


Figure 56 Vent tube loss coefficient (Test vs predicted)

Visual observation of the heat exchanger and spray injection tubes was made to see if there was any evidence of leakage at cryogenic temperature. No evidence of leakage was seen. Following warm up, visual inspection indicated that the spray tubes were displaced from the original position. The tubes were subsequently spot welded to existing metal retainer straps to prevent further motion.

Instrumentation calibration tests were limited to the turbine flowmeter calibration test with water. The temperature and pressure transducer calibration tests will be performed at MSFC after installation into the MHTB, since end to end effects (measurement to recording device), and test at liquid hydrogen temperature can be accomplished in a more cost effective way. The flowmeter calibration test included the actual line inlet and outlet geometries (diameter, bend radii, and angle). The tests were performed by the Rockwell Physical calibration laboratory with water. The results are presented in Figure 57.

Cryogenic shock and leak tests were performed for the component box assembly. The schematic of the test setup is shown in Figure 58. The component box was filled with liquid nitrogen to chill the weld, and connector seals. (The support ring assembly was placed inside the component box to also cryo. shock the components.) The box was pressurized to 60 psig proof pressure. Following proof pressure test the liquid nitrogen was drained and the box was allowed to warm to ambient temperature. Subsequently, the component box was pressurized to 40 psig with helium to measure external leakage across the welds, Deutsch connectors, pipe plugs, and flange seals. The test results were positive. There was no indication of helium leak as detected by the mass spectrometer leak detector. Also, internal pressure decay monitoring (for one hour) also showed no helium leakage. After the internal pressure leak test the box pressure was reduced to approximately 0.02 psia, to measure the leakage from ambient to the box. The internal box pressure measurement also indicated no leakage across the weld, seals and connector.

A special thermocouple feed thru cryo. shock and leak test was performed. The thermocouple feed thru was installed in a special liquid nitrogen test set up. The tube was pressurized to 40 psig with helium and submerged in liquid nitrogen, as shown. the test results showed no helium leakage ($< 10 \text{ exp } -7 \text{ cc/sec}$, lower mass spec limit) from the wire, or wire sheath.

7.0 TVS Performance Characterization

A transient thermo-physical model of the TVS and the MHTB liquid hydrogen tank was formulated in order to define the integrated TVS performance characteristics. The program was written in FORTRAN 77 language on the HP-9000 and IBM PC computers. It can be run on various platforms with a FORTRAN compiler. The analytical model and computer program listing with users guide has been documented separately and is provided as part of the contract deliverable. The analytical model includes the results of the component tests characterizing subsystem performance. The model will be further updated by MSFC personnel following liquid hydrogen tests at MSFC. The final verified model will serve as the basis for future vehicle design definition and performance characterization.

7.1 Heat Exchanger Performance

A two-phase flow heat transfer analysis of the single tube heat exchanger was performed for the design condition of 20 psia saturated liquid at the vent valve inlet, and 0.3 lb/sec (30 GPM) liquid recirculation flowrate. The analysis included the effect of the vent valve pressure loss, and heat exchanger back pressure orifice (0.300 inch diameter) that will be installed in the MHTB. (The analytical assumption and heat exchanger model is described in the TVS computer model documentation). The objective of the analysis was to define the two-phase flow portion of the heat exchanger, and the degree of vapor superheating. The result of the two-phase flow analysis,

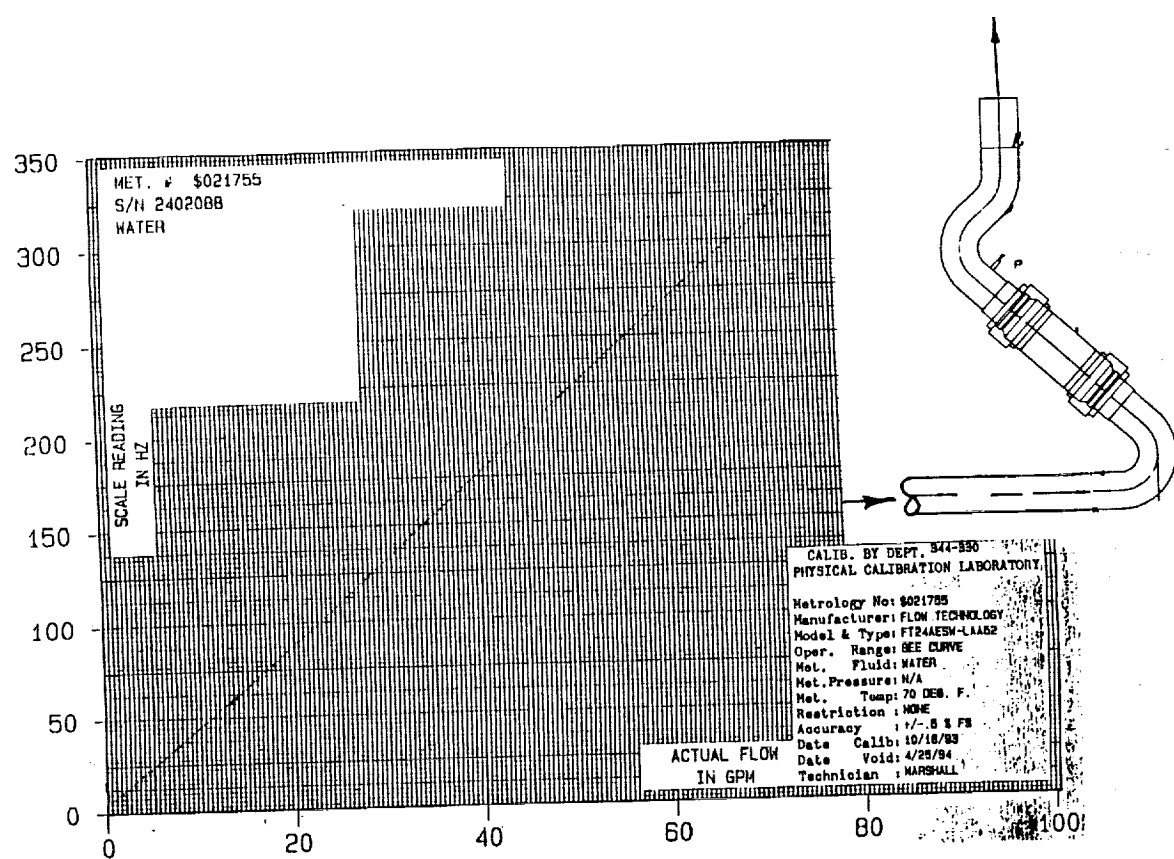


Figure 57 Flowmeter water flow calibration tests results

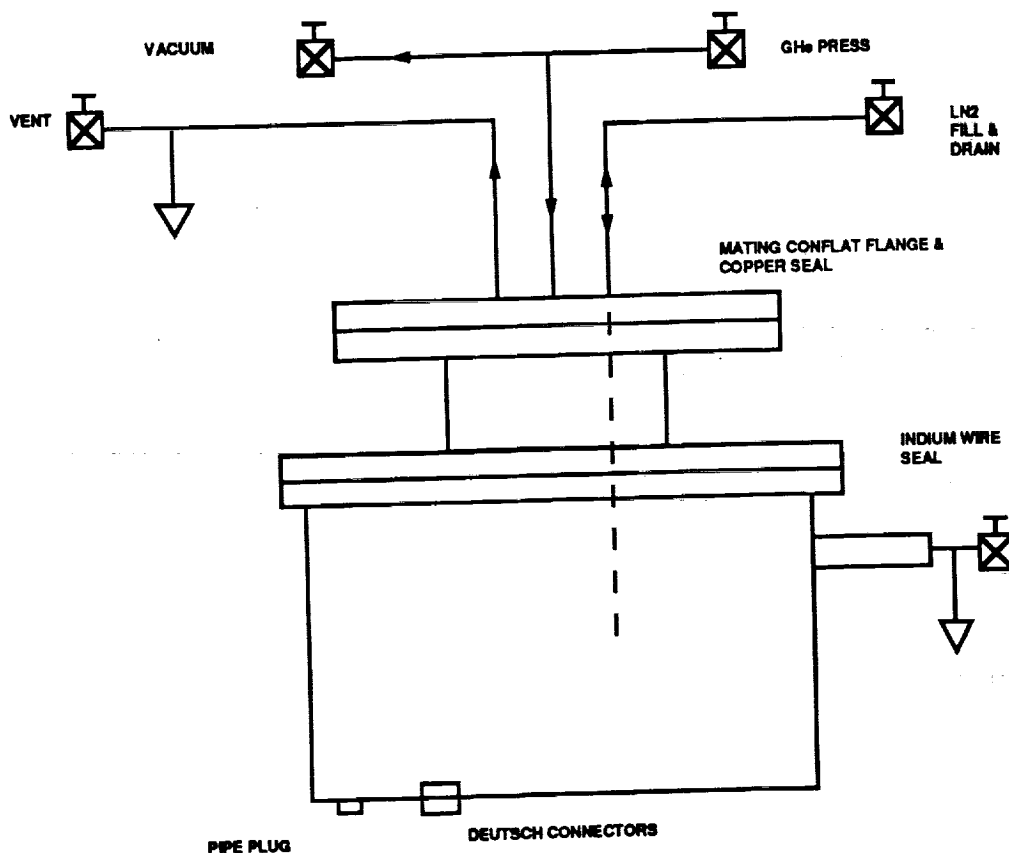


Figure 58 Schematic of component box test set-up

presented in Figure 59, indicated that two-phase flow heat transfer occurs in approximately the first third of the heat exchanger length. The subsequent two thirds is used to super heat the vent flow near the liquid bulk temperature. Since vaporization of the vent flow occurs in a relatively short distance (~ 3.5 ft) the analysis verified the heat exchanger design parameters (tube diameter, radial gap, length, surface area), and assures that superheated gas will be vented.

Because the multi node two-phase flow heat exchanger model is relatively complex, requiring iterating solution, the model was not directly included in the integrated TVS model. Instead, the heat exchanger characteristics were summarized through a series of performance curves. These performance curves, shown in Figure 60, 61, and 62 represent the vent flowrate, total energy absorption potential, and operating pressure level of the vented fluid as a function of tank pressure level and liquid temperature (vapor pressure). The performance curves allow simulation of TVS operation for a range of tank pressure and liquid temperature conditions without increasing the computational time. The results indicate that the vent flowrate increases significantly with both liquid subcooling and liquid vapor pressure (Figure 60). Also, the heat absorption capacity of the vent flow is relatively high. In fact, the heat absorption of the vent flow at low subcooling (less than 2 psi) is approximately 193 Btu/lb which is slightly better than the heat of evaporation at one atmosphere. (See Figure 61). These heat exchanger performance curves will be verified and updated by MSFC following system level tests and TVS model verification. Since the heat exchanger model did not consider heat transfer between the bulk liquid in the tank and the outer surface of the heat exchanger, the actual performance of the TVS is expected to be higher than that shown in Figure 61)

7.2 TVS Vent Valve and Recirculation Pump Operation

The integrated TVS model has been used to verify the control logic, and also to define the key performance parameters, such as TVS ON and OFF time, and cycling frequency. The simulation analysis assumed an ullage pressure control band of 20.5 +/- 0.5 psia, 0.25 Btu/hr-sq ft heat flux, and liquid vapor pressure control of 20 psia (delta P of 0 psi). Sensitivity analysis was made to define the time between venting cycles and duration of the recirculation pump and vent valve operation as a function of liquid quantity. Figure 63 presents the ullage and liquid vapor pressure history for a full cycle with 90 percent liquid quantity. As can be seen the ullage pressure rises more rapidly than the liquid bulk. Because of the large liquid mass the vapor pressure increase is less than 0.1 psia. Once the tank pressure level reaches the maximum control limit (21 psia in 1.2 hours) the recirculation pump is turned ON. Because the liquid vapor pressure is above the minimum control limit (20 psia) the vent valve is also opened to begin heat rejection through venting. Liquid spray injection cools the ullage gas and wall temperature resulting in a rapid tank pressure decay. The tank pressure decays rapidly in approximately 100 seconds, until the ullage pressure equals the liquid vapor pressure. (Figure 64 shows an expanded plot of the ullage and liquid vapor pressure decay). The tank pressure decay subsequently is much slower since it is controlled by the liquid bulk temperature cooling. The recirculation pump and vent valve operation therefore continues for an additional 70 seconds until the liquid vapor pressure is reduced to the minimum control level of 20 psia. When the tank and liquid vapor pressure reaches the minimum control limit of 20 psia the recirculation pump and vent valve are turned OFF. (See Figure 65 for the recirculation and vent flow transients).

The simulation results shown for a 25 percent liquid quantity are presented in Figures 66 through 68. Because the ullage volume is larger at 25 percent liquid quantity the time required to reach the maximum pressure limit is approximately 2.5 hours. Also, because of the smaller liquid level the degree of liquid bulk heating is much more significant. The liquid vapor pressure is approximately 20.5 psia when the ullage pressure reaches the maximum controller level. As in the 90 percent liquid quantity case both the recirculation pump and the vent valve are turned ON at 21 psia,

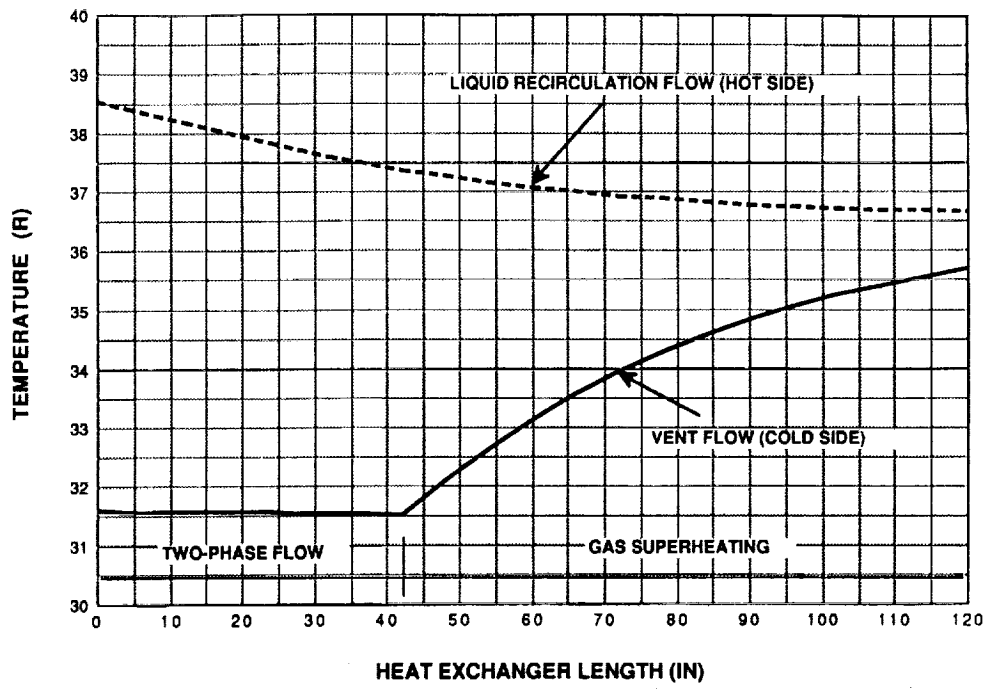


Figure 59 Predicted TVS heat exchanger performance

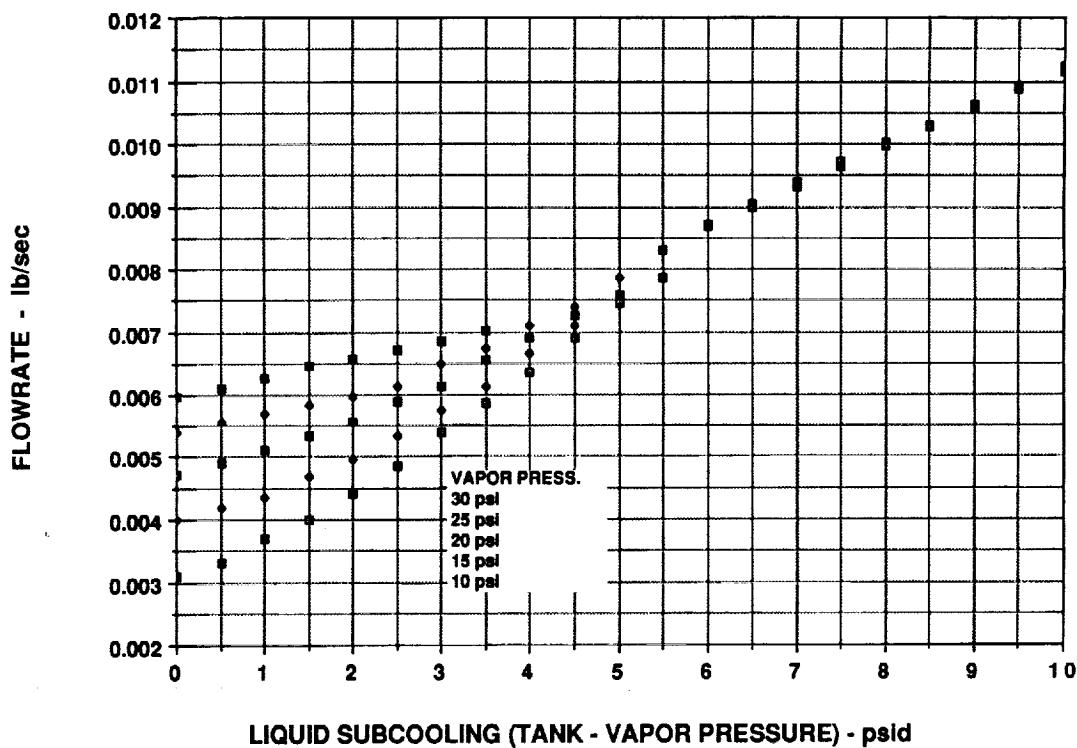


Figure 60 TVS vent flowrate as a function of liquid subcooling

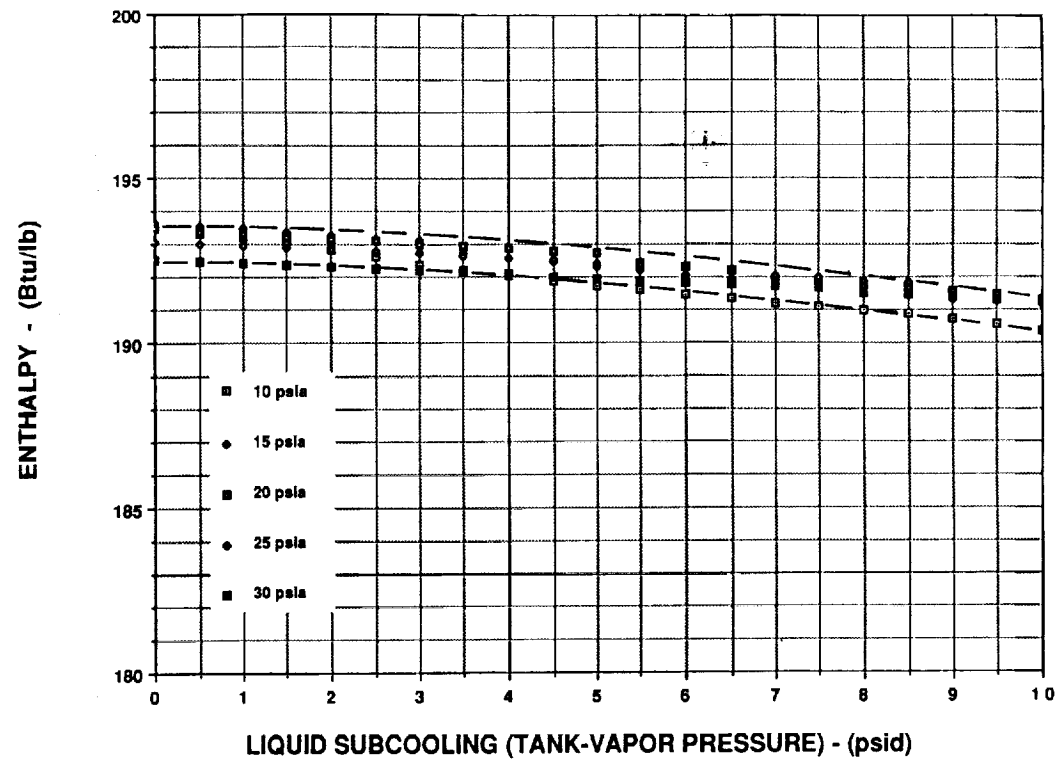


Figure 61 Heat absorption potential of vent flow as a function of liquid subcooling

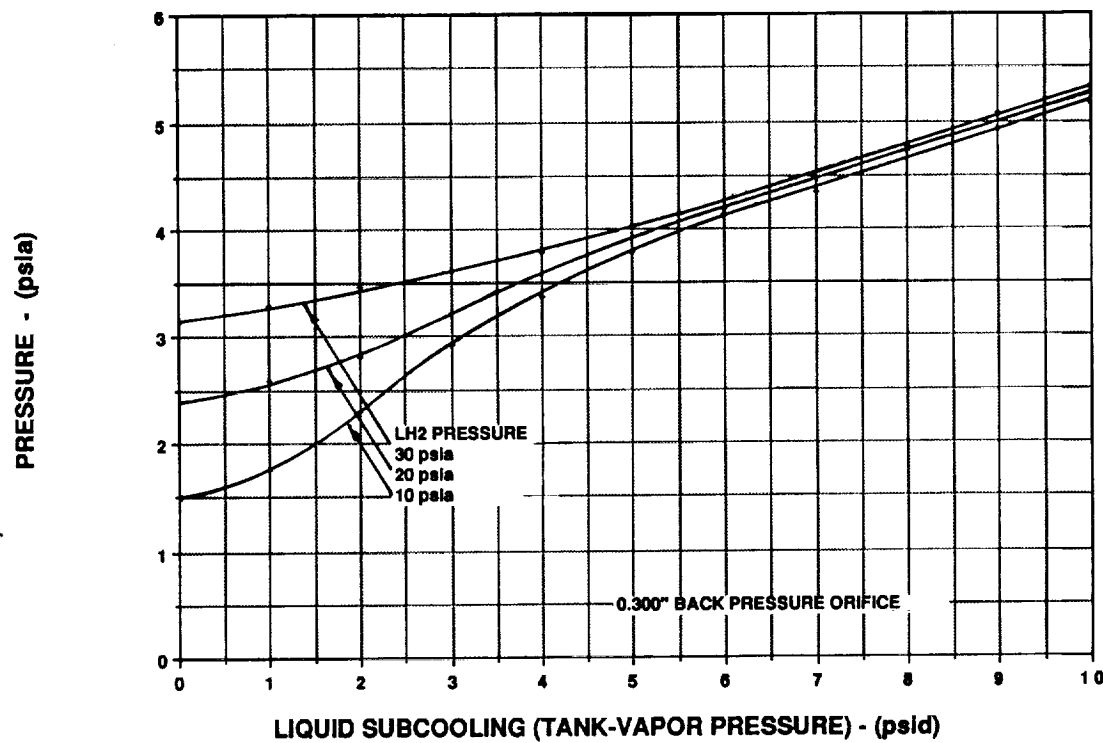


Figure 62 Heat exchanger operating pressure (cold side) as a function of liquid subcooling

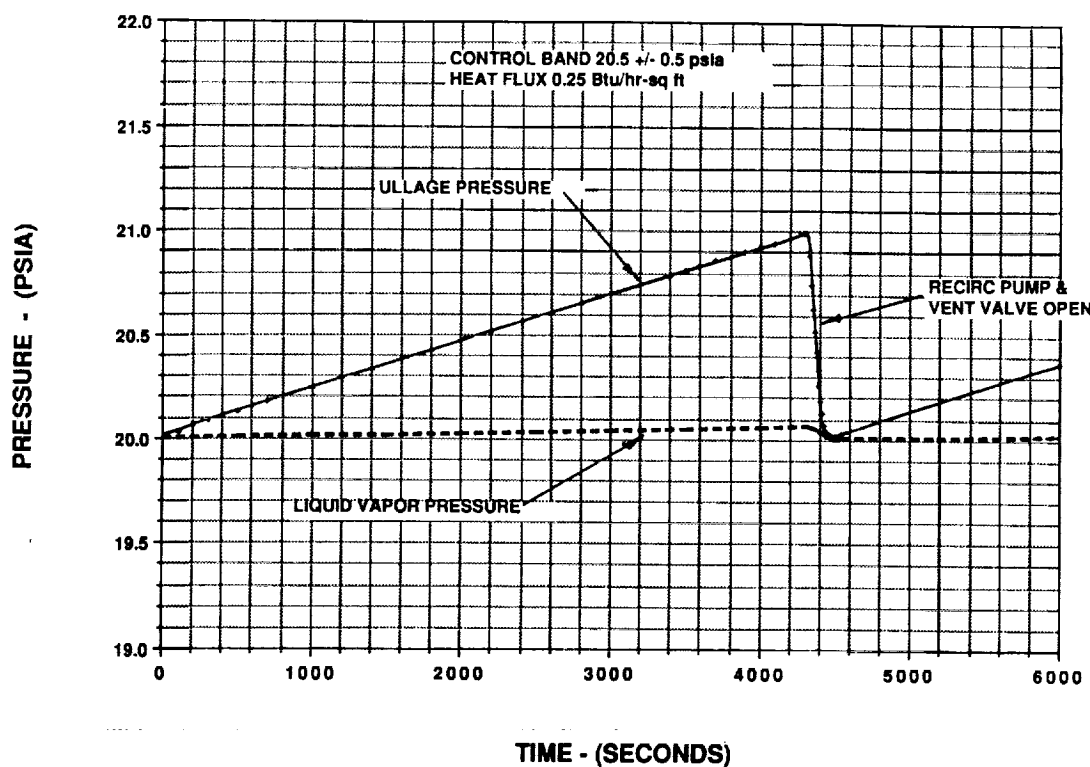


Figure 63 TVS performance simulation at 90 percent liquid quantity (Full scale)

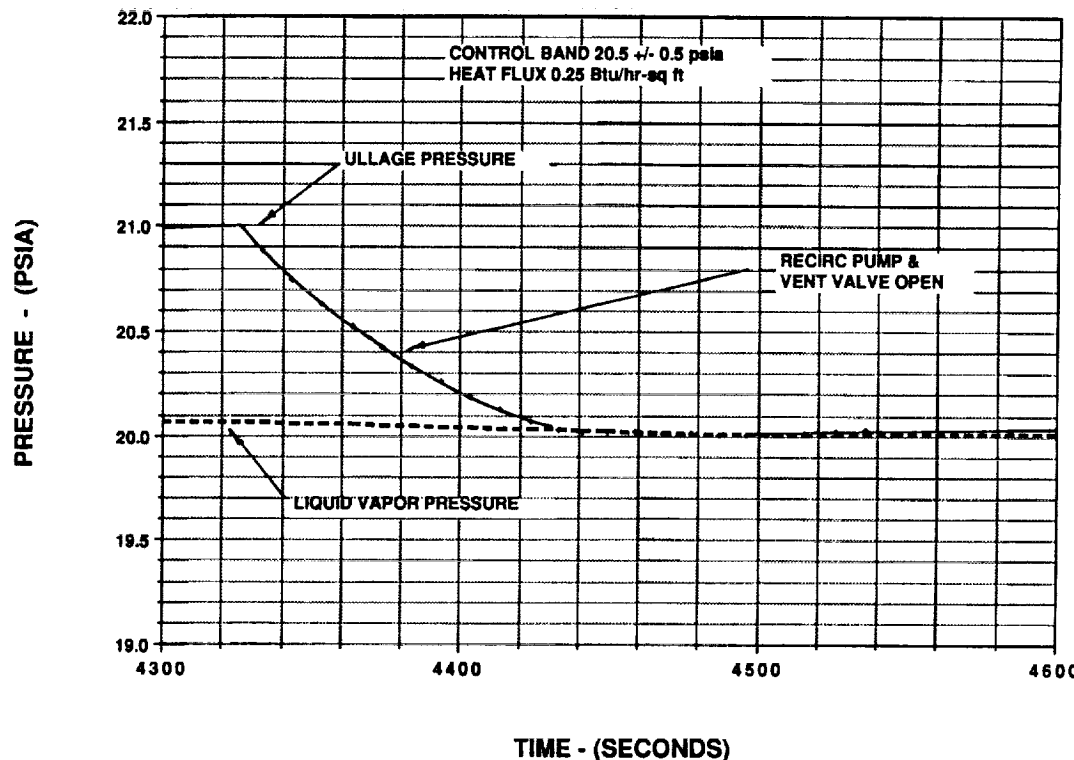


Figure 64 TVS performance simulation at 90 percent liquid quantity (Expanded scale)

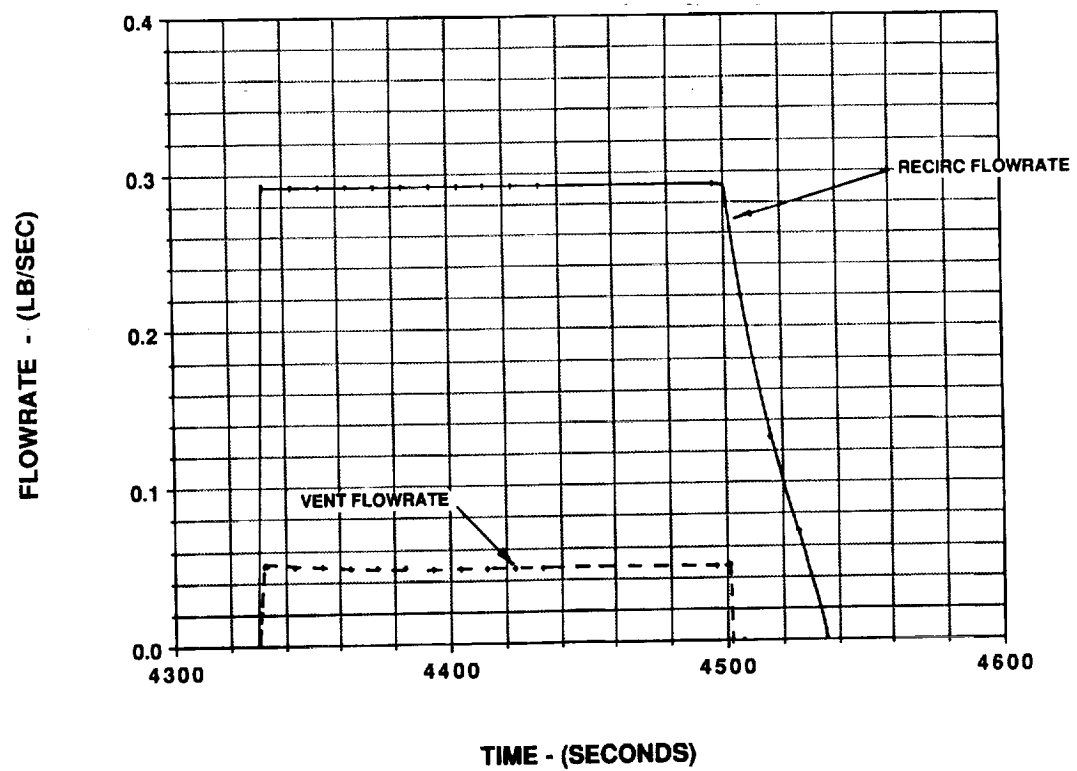


Figure 65 TVS recirculation pump and vent flowrate transient during pressure control at 90 percent liquid quantity

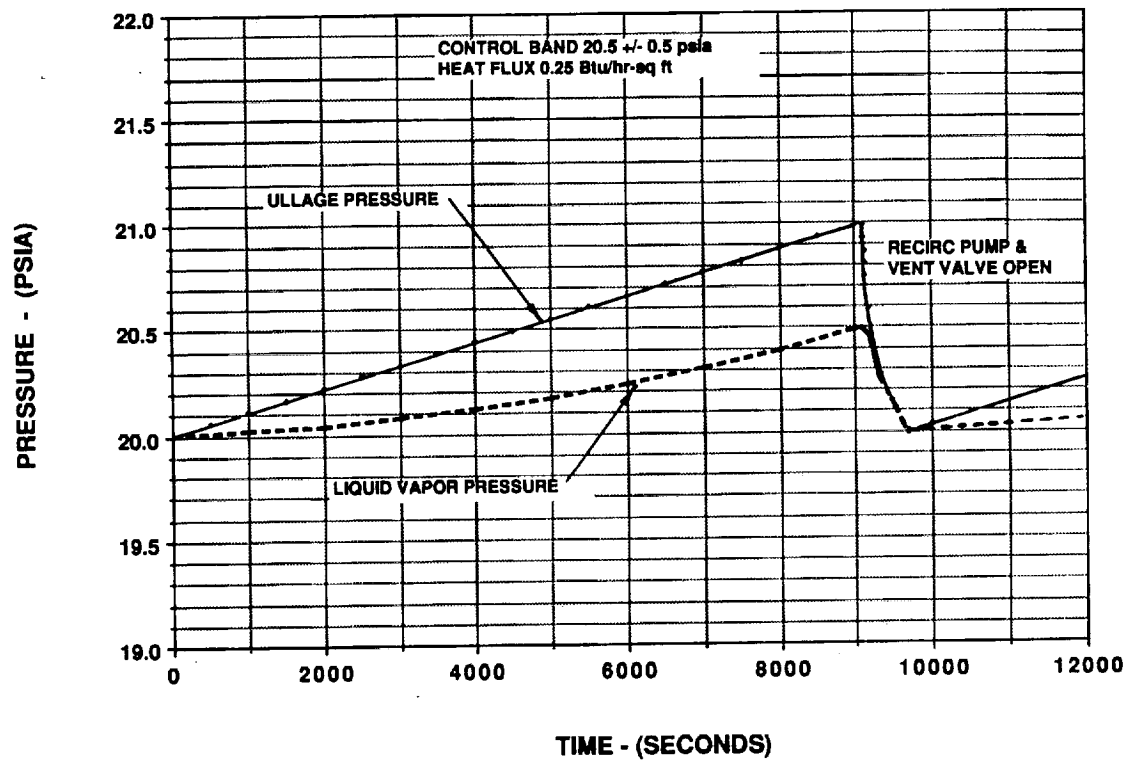


Figure 66 TVS performance simulation at 25 percent liquid quantity (Full scale)

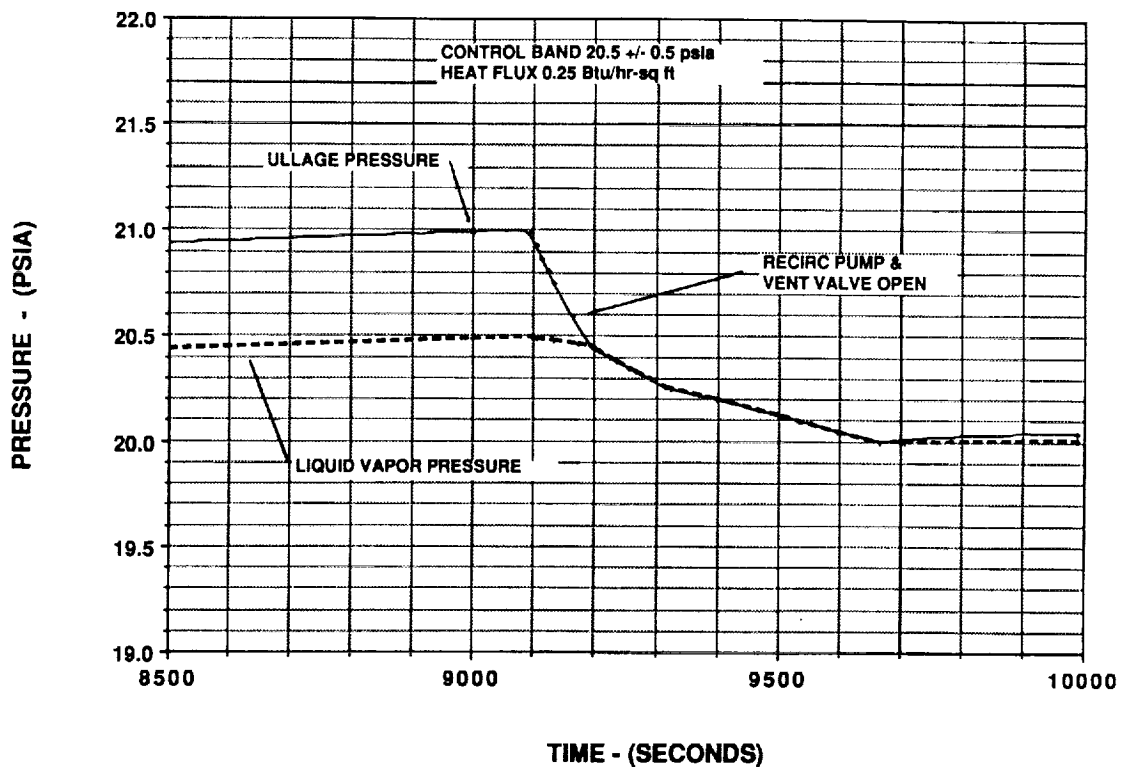


Figure 67 TVS performance simulation at 25 percent liquid quantity
(Expanded scale)

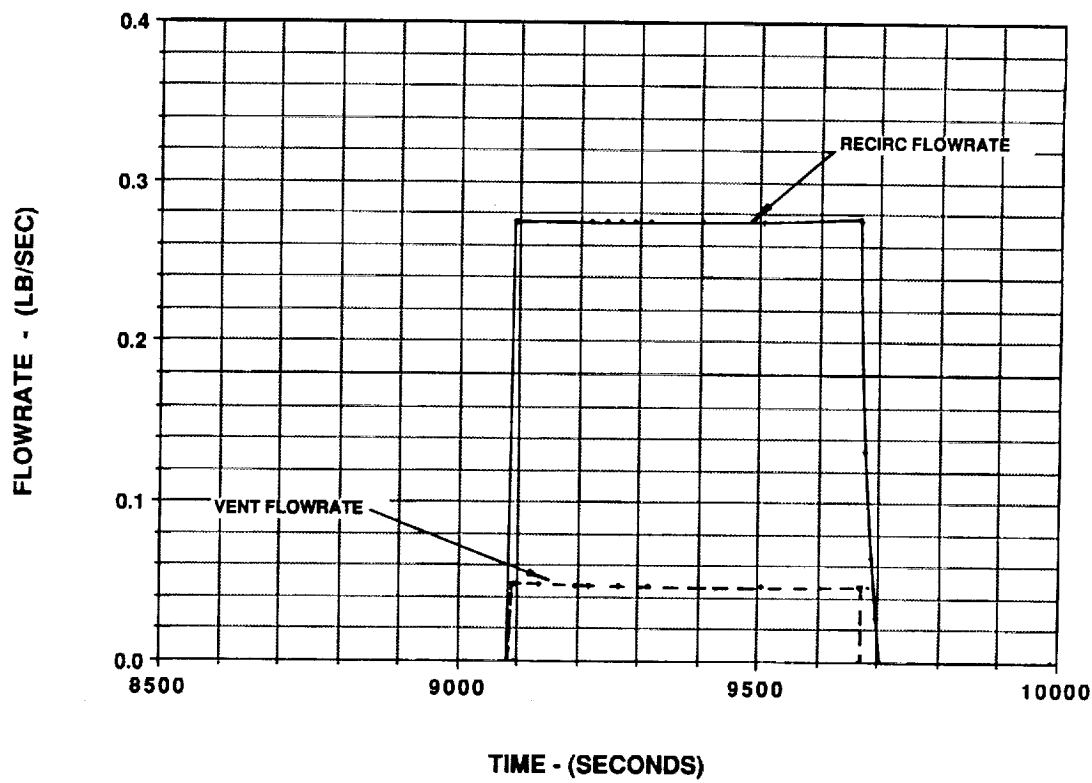


Figure 68 TVS recirculation pump and vent flowrate transient during pressure control at 25 percent liquid quantity

initiating the ullage pressure collapse. Because the liquid vapor pressure is higher, the rapid ullage pressure collapse is halted at 20.5 psia and followed by a slower pressure decay which is controlled by the liquid bulk temperature cooling.

The time between TVS operation, recirculation pump/vent valve operation, and cycling frequency, as a function of liquid quantity, are summarized in Figures 69 through 71. The TVS cycling frequency defined above verified the initial design goal of recirculation pump and venting operation below 10 percent duty cycle. The operating times and frequency will vary with heat flux, tank pressure level, and liquid vapor pressure. The results presented above are given to illustrate the integrated system operation, and should be updated following math model verification with ground test data.

8.0 TVS Design Guidelines for Future Vehicles

The function of the zero g TVS is to control tank pressure through liquid and ullage gas destratification and to reject the environmental heat leakage through gaseous venting. The two elements of a TVS are therefore, the heat exchanger, and the spray injection system. The following section will discuss the design guidelines in sizing the TVS heat exchanger and spray injection system for future flight vehicles.

The heat exchanger must be designed in order to reject the environmental heat leakage that results from the thermal environment and the insulation system performance of the storage system. It is recommended that the heat exchanger be sized to reject at least ten times the average heat leakage rate of the storage system. The reason for the increase in heat exchanger capacity is to allow intermittent operation of the TVS at relatively small duty cycles (less than 10 percent ON time), and also to compensate for heat exchanger design uncertainties associated with two-phase flow heat transfer characteristics. Intermittent operation of the TVS may also be desirable in order to minimize the gaseous venting thrust disturbances. The heat exchanger configuration, whether single or multi tube heat exchanger, will depend on the maximum heat rejection requirement of the storage and feed system. (The coil heat exchanger configuration is not recommended since it is the heaviest, least reliable, has the largest pressure drop of the heat exchanger configurations evaluated for the equivalent heat rejection capacity).

Based on the sensitivity analysis, the cold or vent side of the heat exchanger, should be designed to operate above the fluid triple point in order to take advantage of the maximum change in fluid enthalpy, and also to result in the maximum temperature delta between the vent and the liquid recirculation flow. The back pressure orifice, which regulates the heat exchanger vent pressure level, should be selected to insure that the solid phase is avoided at the minimum vent flow condition. For hydrogen the design vent pressure level of 3 psia is recommended. This level will result in good vent flow heat capacity (greater than 190 Btu/lb) and is significantly above the triple point pressure of 1.02 psia, to prevent solid hydrogen formation within the heat exchanger. To further improve the heat exchanger efficiency, the vent and liquid flow should be counter flowing. A counter-flow heat exchanger will result in maximum vent temperature and therefore maximum heat rejection capability.

The spray injection system should be designed to provide uniform liquid spray injection throughout the length of the storage tank. It is recommended that the spray bar be installed as close to the center of the tank as possible. Radial spray injection should be provided in four orthogonal directions as a minimum. For larger storage tanks the radial injection should be increased from the four orthogonal directions, or installing multiple spray bars adjacent to the tank wall, in order to more efficiently destratify the ullage gas and liquid mass. As a design goal the liquid spray should be near "atomized flow". This requires that the Weber and Reynolds number be approximately 300, and 10,000, respectively. The requirement to have atomized flow will be demonstrated by MSFC during TVS performance characterization. Lewis Research test results,

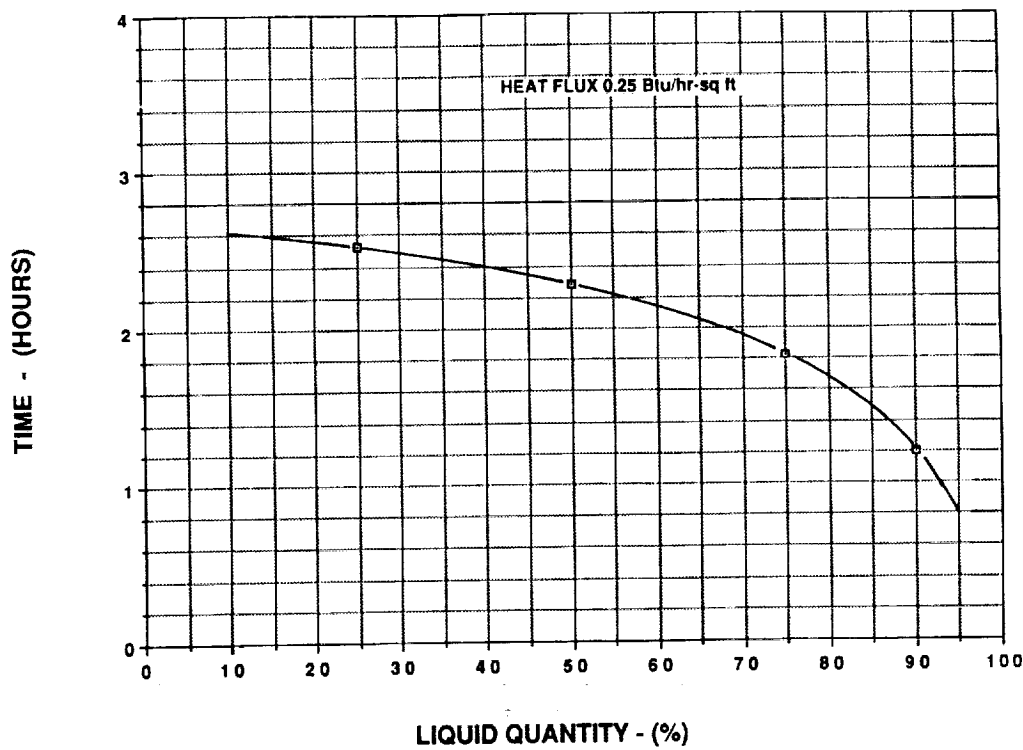


Figure 69 Time between destratification and venting operation as a function of liquid quantity

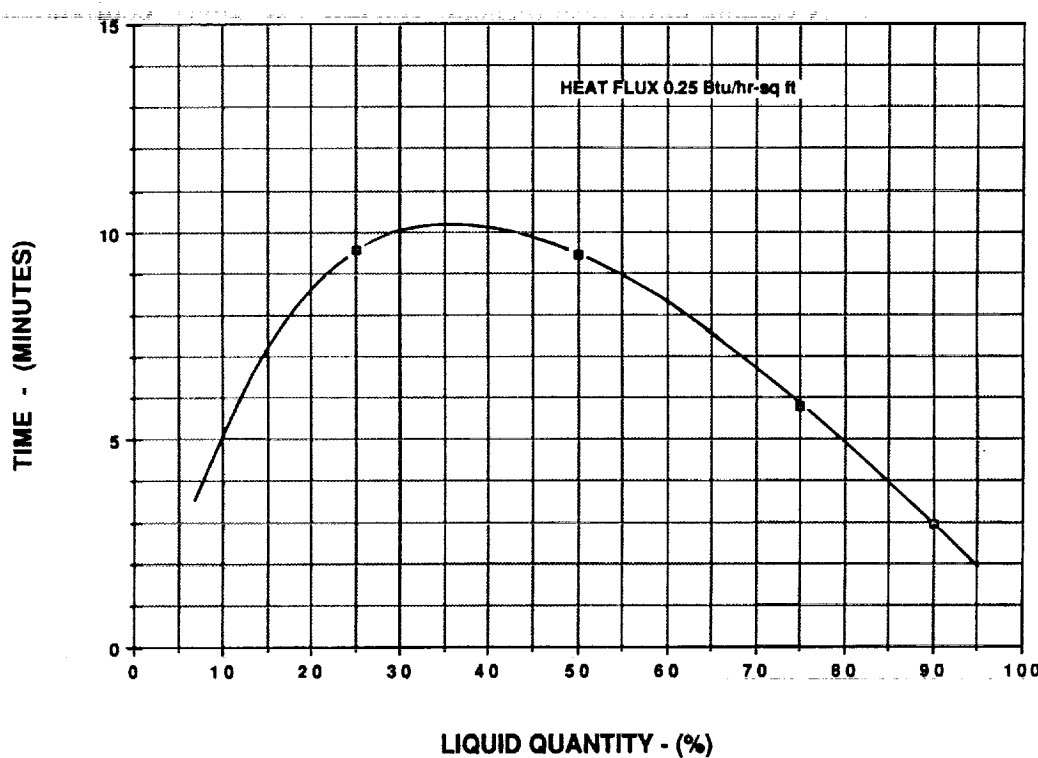


Figure 70 TVS destratification time (recirc. pump and venting operation) as a function of liquid quantity

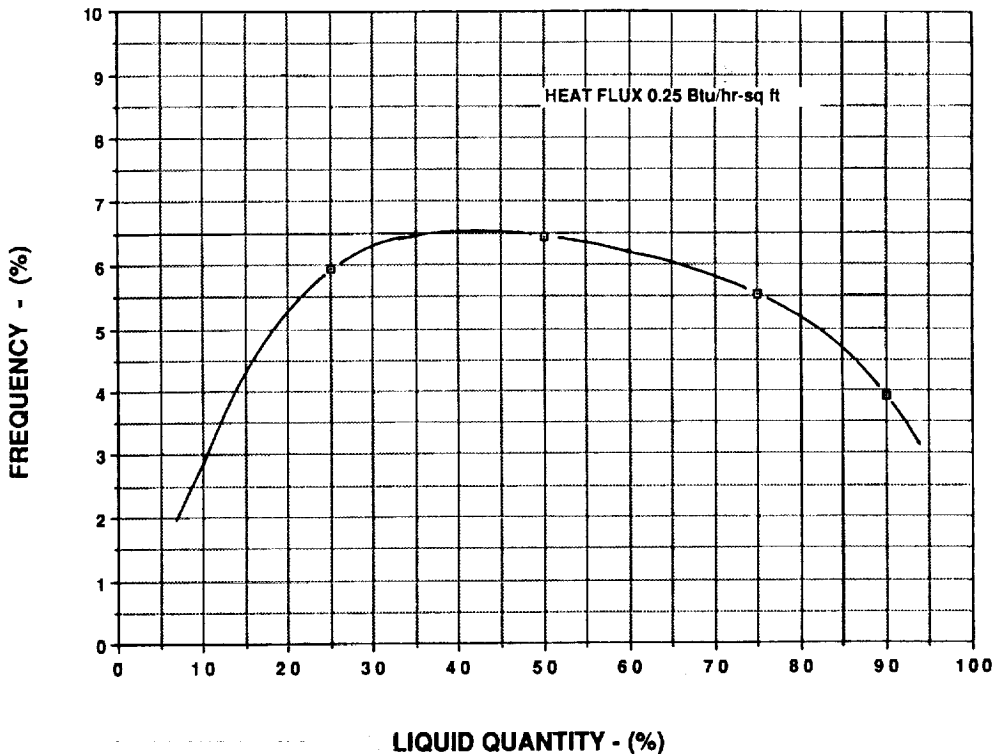


Figure 71 TVS operation frequency (percent) as a function of liquid quantity

however indicated that atomized flow is not a hard requirement since "wavy" flow provided good ullage gas mixing and resultant ullage pressure decay. Once the orifice diameter has been defined from the spray jet requirement (atomized or wavy) the number of orifices and spacing of the orifices can be determined from the total recirculation flowrate. The total recirculation flowrate is defined from both the heat exchanger requirement and also from a system pressure drop sensitivity analysis.

A TVS component box is not required for flight vehicles. The reason for including a component box for the MHTB design was to protect the vacuum chamber from potential component leakage levels which would contaminate the vacuum chamber, and also represents a hydrogen safety hazard.

9.0 Conclusion

The thermodynamic vent system (TVS) design being jointly developed by the Marshall Space Flight Center and Rockwell International Space Division represents a state-of-the-art improvement in zero-g cryogenic venting systems. A patent disclosure describing the innovative features of the zero g TVS has been submitted to the U. S. Department of Commerce Patent and Trademark Office (Docket No. 93ST07, Serial No. 08/064326, "Fluid Management System For A Zero Gravity Cryogenic Storage System"). In addition to efficiently controlling cryogenic storage system pressures in a zero g environment, the TVS design developed and built also provides additional cryogenic fluid management features, such as feedline and engine thermal conditioning, tank chill-down, no vent fill operation, emergency venting, and simple zero g propellant gaging capability, that will be required for future space based storage and propulsion system designs. The contract which was initiated in November 1991, has been successfully completed within cost

and on time with hardware delivery completed in March 1994. In addition to designing and building the TVS hardware, development of a new liquid hydrogen recirculation pump by Barber Nichols Inc. was accomplished within the contract period and original contract budget allocation. The TVS design has been fully characterized through the definition of a transient thermodynamic-fluid system analytical model. The computer model of the TVS operation has been documented and delivered to NASA MSFC which will serve as the basis for system testing and future vehicle design definition. In addition to developing the zero g TVS design, a Safety Program Plan for the MHTB/TVS Test Program was generated. The purpose of the Safety Program Plan was to insure that safety planning precedence is maintained and implemented in the MHTB/TVS Test Program such that potentially hazardous situations attributable to the Rockwell TVS are identified to Program Management for necessary control and corrective action implementation.

The delivered TVS hardware, shown installed in the MSFC MHTB facility on Figure 72, is ready for testing at the Marshall Hydrogen Test Bed facility, which is planned to begin in FY 1995.

10.0 Acknowledgments

Special thanks are extended to Mr. Michel Fazah of NASA MSFC (COTR) for his continued valuable technical support and guidance throughout the TVS contract. The technical comments provided by Mr. Leon Hastings, Dr. George Schmidt, Mr. Jim Martin, Mr. Mark Fisher, and Mr. Kevin Pederson of NASA MSFC in support of the various design reviews are greatly appreciated. Special thanks are extended to Mr. Ted Nyland of the NASA Lewis Research Center for performing the subscale LH₂ spray injection tests, which allowed early verification of spray injection system design performance. The development of a new "zero net positive suction pressure" liquid hydrogen pump by Barber-Nichols within cost and ahead of schedule under the leaderships Mr. Jim Dillard and Mr. John Wehrman of Barber-Nichols resulted in the on time delivery of the TVS hardware to MSFC. The technical expertise, dedication and tireless efforts of the Rockwell TVS team; Mr. Han Nguyen (Analyst), Mr. David Soo Hoo (Analyst), Mr. Lee Durham (Designer), Mr. Tony Liu (Hardware Procurement), Mr. Mario Marchisio (Testing), Mr. Todd Jensen (Safety and Reliability), Mr Gordon Jones (Quality Assurance), and Mr. Ashutosh Bhowmick (Stress) is recognized and greatly appreciated.

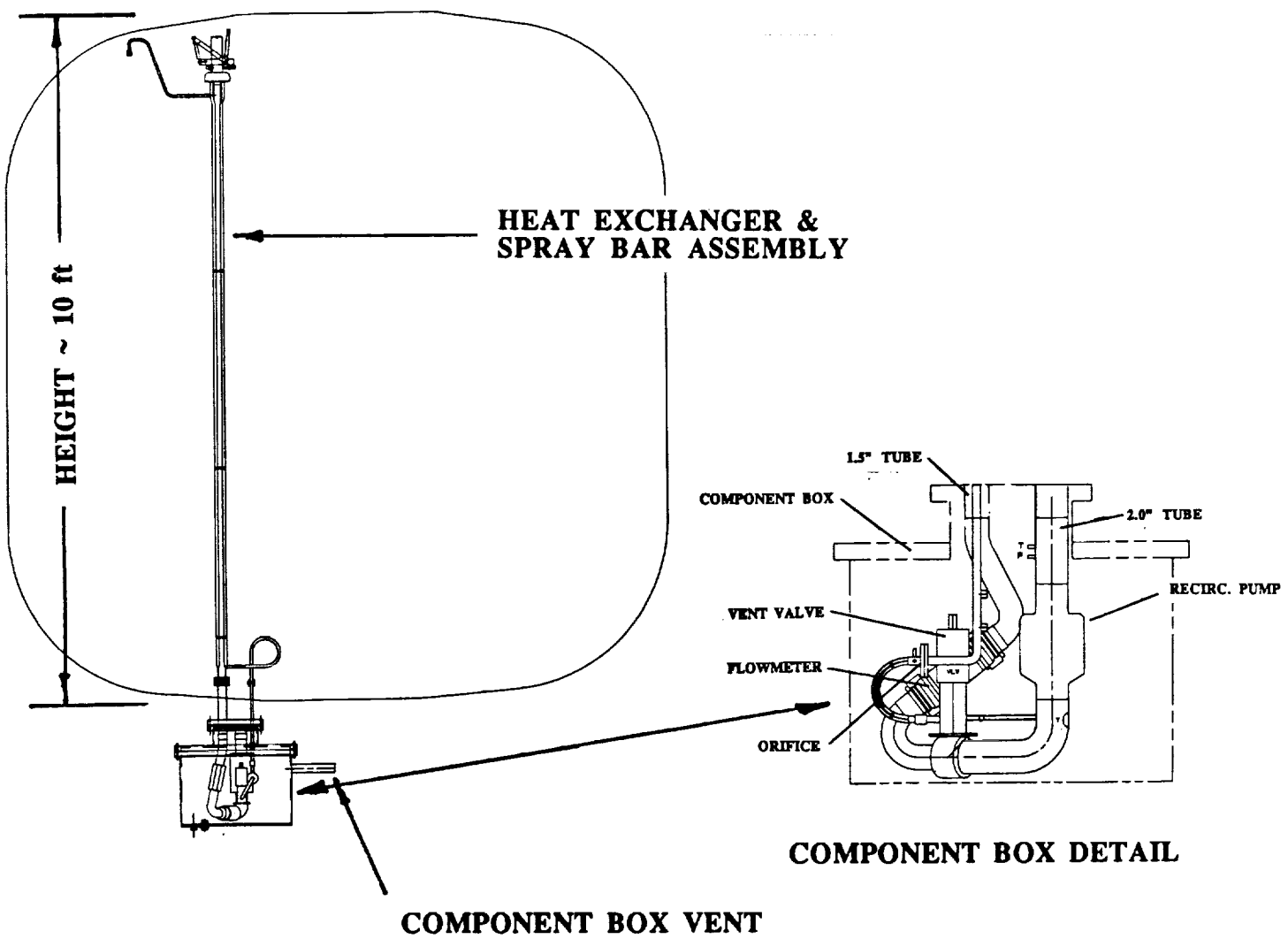
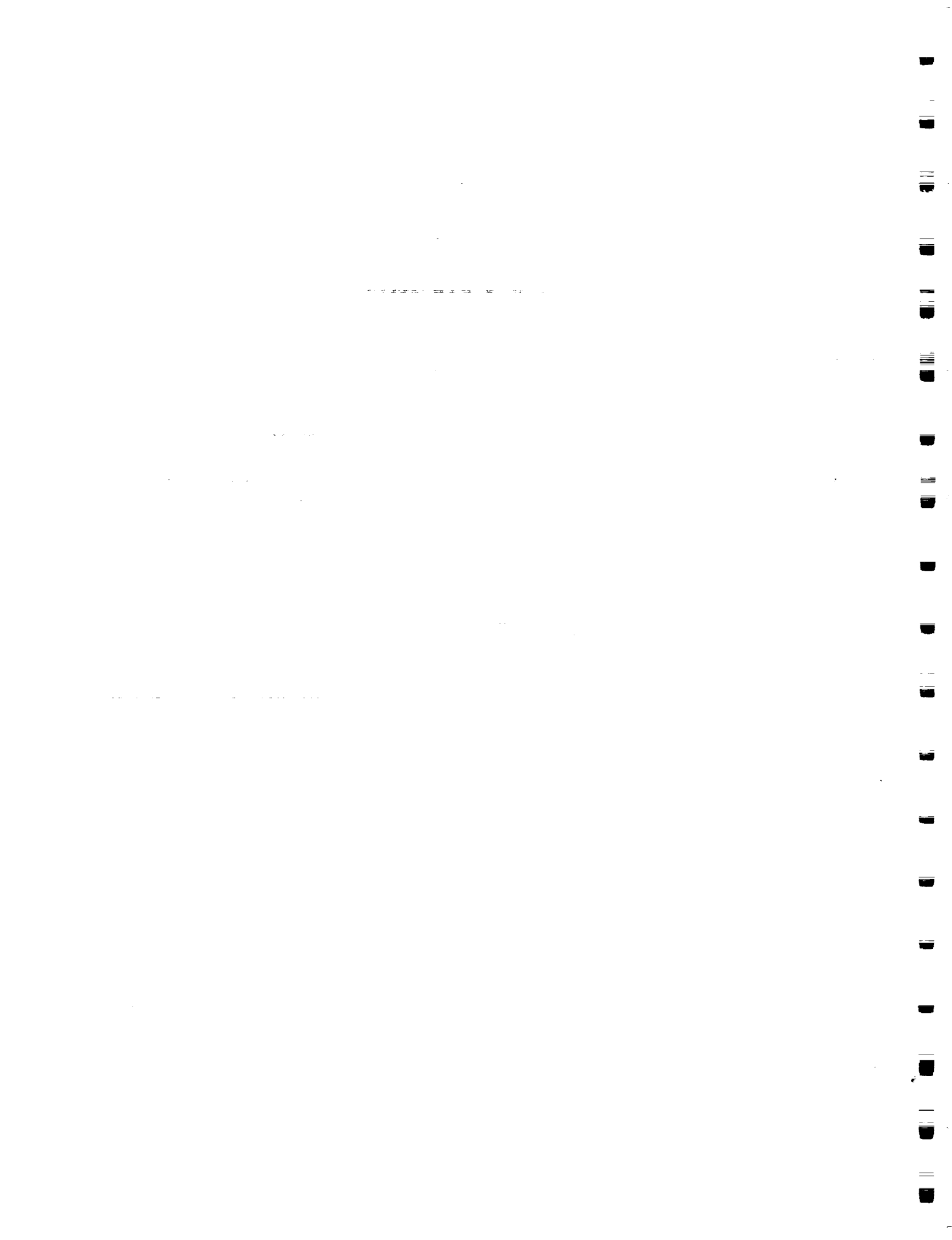


Figure 72 TVS design installed in NASA MHTB tank



NASA SCIENTIFIC AND TECHNICAL AVAILABILITY AUTHORIZATION (DAA)

6-17

To be initialed by the responsible NASA Project Officer, Technical Monitor, or other appropriate NASA official for all presentations, reports, papers, and proceedings that contain scientific and technical information. Explanations are on the back of this form and are presented in greater detail in NHB 2200.2, "NASA Scientific and Technical Information Handbook."

(CASI Use Only)

Control No. 6-8-94

Date

I. DOCUMENT/PROJECT IDENTIFICATION (Information contained on report documentation page should not be repeated except title, date and contract number)
Title: Cryogenic Fluid Management Technologies for Space Transportation: Zero G Thermodynamic Vent System Final Report

Author(s): MSFC**Originating NASA Organization:** Rockwell Aerospace**Performing Organization (if different)** NAS8-39202**Contract/Grant/Interagency/Project Number(s)** SSD 94M0038 NASA CR - 193981**Document Date:**

(For presentations or externally published documents, enter appropriate information on the intended publication such as name, place, and date of conference, periodical or journal title,

or book title and publisher:

These documents must be routed to NASA Headquarters, International Affairs Division for approval. (See Section VII))

II. AVAILABILITY CATEGORY

Check the appropriate category(ies):

Security Classification: Secret Secret RD Confidential Confidential RD Unclassified

Export Controlled Document - Documents marked in this block must be routed to NASA Headquarters International Affairs Division for approval.

 ITAR EAR

NASA Restricted Distribution Document

 FEDD Limited Distribution Special Conditions-See Section III

Document disclosing an invention

 Documents marked in this block must be withheld from release until six months have elapsed after submission of this form, unless a different release date is established by the appropriate counsel. (See Section IX).

Publicly Available Document

 Publicly available documents must be unclassified and may not be export-controlled or restricted distribution documents. Copyrighted Not copyrightedConc: EP01/John P. McCarty *John McCarty*

IN-29

16040

P-64

III. SPECIAL CONDITIONS

Check one or more of the applicable boxes in each of (a) and (b) as the basis for special restricted distribution if the "Special Conditions" box under NASA Restricted Distribution Document in Section II is checked. Guidelines are provided on reverse side of form.

a. This document contains:

 Foreign government information Commercial product test or evaluation results Preliminary information Information subject to special contract provision
 Other-Specify _____b. Check one of the following limitations as appropriate:
 U.S. Government agencies and U.S. Government agency contractors only NASA contractors and U.S. Government agencies only U.S. Government agencies only
 NASA personnel and NASA contractors only NASA personnel only Available only with approval of issuing office: _____

IV. BLANKET RELEASE (OPTIONAL)

All documents issued under the following contract/grant/project number _____ may be processed as checked in Sections II and III.

The blanket release authorization granted _____ is: _____

 Rescinded - Future documents must have individual availability authorizations. Modified - Limitations for all documents processed in the STI system under the blanket release should be changed to conform to blocks as checked in Section II.

V. PROJECT OFFICER/TECHNICAL MONITOR

Michel Fazah

Typed Name of Project Officer/Technical Monitor

EP53

Office Code

*Michel M. Fazah*6/10/94

Date

VI. PROGRAM OFFICE REVIEW

 Approved Not ApprovedB MBlanket authorization - NASA Hdqrs.
Letter dated 06-14-94.

Typed Name of Program Office Representative

Program Office and Code

Signature

Date

VII. INTERNATIONAL AFFAIRS DIVISION REVIEW

Open, domestic conference presentation approved. Export controlled limitation is not applicable.
 Foreign publication/presentation approved. The following Export controlled limitation (ITAR/EAR) is assigned to this document: _____
 Export controlled limitation is approved.

International Affairs Div. Representative

Title

Date

VIII. EXPIRATION OF REVIEW TIME

The document is being released in accordance with the availability category and limitation checked in Section II since no objection was received from the Program Office within 20 days of submission, as specified by NHB 2200.2, and approval by the International Affairs Division is not required.

Name & Title _____ Office Code _____ Date _____

Note: This release procedure cannot be used with documents designated as Export Controlled Documents, conference presentations or foreign publications.

IX. DOCUMENTS DISCLOSING AN INVENTION

a. This document may be released on _____ Installation Patent or Intellectual Property Counsel _____ Date _____
 b. The document was processed on _____ In accordance with Sections II and III as applicable. NASA CASI _____ Date _____

